



THE UNIVERSITY OF
WAIKATO
Te Whare Wānanga o Waikato

Research Commons

<http://waikato.researchgateway.ac.nz/>

Research Commons at the University of Waikato

Copyright Statement:

The digital copy of this thesis is protected by the Copyright Act 1994 (New Zealand).

The thesis may be consulted by you, provided you comply with the provisions of the Act and the following conditions of use:

- Any use you make of these documents or images must be for research or private study purposes only, and you may not make them available to any other person.
- Authors control the copyright of their thesis. You will recognise the author's right to be identified as the author of the thesis, and due acknowledgement will be made to the author where appropriate.
- You will obtain the author's permission before publishing any material from the thesis.

**MICROSTRUCTURE AND MECHANICAL
PROPERTIES OF Ti-6Al-4V PRODUCED BY
SELECTIVE LASER SINTERING OF PRE-
ALLOYED POWDERS**



THE UNIVERSITY OF
WAIKATO
Te Whare Wānanga o Waikato

A report submitted in fulfilment of the requirements of a degree in

Master of Engineering

at the University of Waikato by :

Izhar Abd Aziz

The University of Waikato

Hamilton, New Zealand

14th May 2010

Abstract

The successful development of these cutting edge Rapid Prototyping systems is important for the future progress of Rapid Manufacturing. The purpose of this research is to investigate the microstructure and mechanical properties of Ti6Al4V pre-alloyed powders producing by direct metal laser sintering technique. Traditionally, Ti6Al4V bio-material products were produced through hot working or machining of wrought semi products. A change in the production route of Ti6Al4V from the traditional method needs a lot of verification and thorough studies because the technological properties of this alloy are strongly influenced by the production route. Through this research, the direct fabrication of Ti6Al4V metal parts by selective laser sintering machine has been carried out using EOS GmbH M270 equipment. Employing intricate thermo-mechanical interaction between the laser beam and the metallic powders, the machine consolidates predefined cross sections and binds the particles together to form solid parts which correspond to CAD data. The successive layers are then withdrawn to a certain height followed with the deposition of a new thin layer of powder. This process is repeated and finally by adopting EOS standard process parameters, each layer is bonded to create 3D solid parts. The laser sintered parts were mechanically tested and samples were also heat treated at the microstructural evolution focussed. The geometrical feasibility of the parts, including process accuracy were statistically analysed by simple benchmark studies. The intricate correlation between powder materials and process parameters were thoroughly investigated via fractography, metallography and standard physical testing. It was found that, SLS technologies are capable of directly producing near to full density metal parts with good mechanical properties. Ti6Al4V produced by laser sintering has very fine $\alpha+\beta$ microstructure. This fine and stable microstructure demonstrated a high yield stress and UTS with low elongation at break. The fracture surface has a dimple features typical of a ductile structure. Dimensional analyses were performed on the customised benchmark showing process accuracy below 50 μm . Designated heat treatments modified the microstructure which influences the mechanical behaviour of the parts.

Acknowledgments

I would like to thank my Associate Professor Brian Gabbitas who gave me such a significant assistance throughout the research periods. With his radiant efforts, excellent suggestions and continuous support, the collaboration took place accordingly and the samples' fabrication went smoothly. It is an honour for me to be able to work with him and looking forward for further research works under his brilliant supervision.

For the research and the completion of my writing, I feel a deep sense of gratitude:

To Mark Stanford and Ian Lyall from the University of Wolverhampton. They provided the laser sintering specimens and relevant information pertaining to the process parameters;

To Stella Raynova for her consistent technical support, insights and prompt feedback. Yuanji for all the equipments and training provided. Indar Singh for his commitment in laboratory work especially during XRD training. Helen Turner for her skill and sense of quality during SEM and TEM;

To my wife, Hanna Zulika and kids, Aisya Arianna and Adam Qalifh for their prayers, constant love and for supporting my many involvement outside the home;

I am also grateful to my friends Saiful Riza, Rashid Shamsuddin, Raja Ehsan, Hazwan, Zul Zulkepli, Lim, Jeevan, Aron, Vijay, Amir, Amro and Asma for their encouragement, suggestions and motivation;

Finally, I would like to thank to my parents, sisters and brothers for their constant demonstration of love.

CONTENT

	Abstract	i
	Acknowledgment	ii
	Table of Contents	iii
	List of Figures	vii
	List of Table	x
	Glossary	xi
1.0	Chapter 1 : Introduction	1
2.0	Chapter 2 : Literature Review	4
2.1	Additive Manufacturing	4
2.1.1	Additive Manufacturing	4
2.1.2	Rapid Prototyping	5
2.1.3	Rapid Manufacturing	9
2.1.4	RM Framework	10
2.1.5	Issues and Advantages	12
2.1.6	RM Characteristics	13
2.2	SLS Technologies	14
2.2.1	Solid State Sintering	14
2.2.2	Liquid Phase Sintering	15
2.2.3	Chemical Induced	17
2.2.4	Full Melting	17
2.2.5	Problems in SLS	18
2.3	Titanium Alloys : Theory & Practice	20
2.3.1	Production of Titanium	20

2.3.2	Powder Metallurgy	22
2.3.3	Crystallographic Structure	23
2.3.4	Influence of Alloying elements	24
2.3.5	Classification of Titanium alloys	25
2.3.6	Ti6Al4V microstructure	25
2.3.7	The Advantages of Titanium Alloys	26
2.3.8	Basic Principle of Heat Treatment	27
3.0	Chapter 3 : Direct Laser Metal Sintering	30
3.1.0	Introduction of DMLS	30
3.2.0	Classification of RM systems	32
3.3.0	Laser Technology	40
3.4.0	Fundamental Setup: EOS M270	43
3.5.0	Technical Specification	44
4.0	Chapter 4 : Material and Method	
4.1.0	Specimen Preparation	49
4.1.1	Specimen Record	50
4.1.2	Specimen Cutting	50
4.1.3	Epoxy Resin mounting	51
4.1.4	Grinding and Polishing	52
4.1.5	Kroll's Etching Solution	53
4.2.0	Fabrication Process	54
4.2.1	CAD Design	54
4.2.2	Specimens Fabrication	54
4.2.3	Machine Parameter	55

4.2.4	Energy Density Calculation	57
4.2.5	Processing Environment	57
4.2.6	Scanning Strategy	58
4.2.7	Orientation and Scanning Layout	59
4.3.0	Powder Particles Characterization	60
4.3.1	Particle Size & Distribution	60
4.3.2	Particle Shape Characterisation	62
4.3.3	Morphology and Chemical Compounds	63
4.3.4	Powder Density	64
4.4.0	Mechanical Behaviour	
4.4.1	Tensile Testing	65
4.4.2	Fracture Surface	66
4.4.3	Hardness Test	67
4.4.4	Part Density	68
4.5.0	Heat Treatment	
4.5.1	Experimental Procedures	70
4.5.2	Designated Heat Treatment	71
4.6.0	Metallographic Analysis	72
4.6.1	Optical Microscopy	72
4.6.2	X-Rays Diffraction Analysis	72
4.6.3	Scanning Electron Microscopy	72
4.6.4	Transmission Electron Microscopy	72
4.7.0	Process Accuracy and Feasibility	74

5.0	Chapter 5: Results	
5.1.0	Visual Observation	75
5.2.0	Ti6Al4V Powder	
5.2.1	Particles Size, Shape & Distribution	76
5.2.2	Morphology	77
5.2.3	Chemical Compounds	77
5.2.4	Powder Density	79
5.3.0	Mechanical Behaviour	
5.3.1	Tensile Testing	80
5.3.2	Vickers Hardness	83
5.3.3	Fracture Surface	84
5.3.4	Part Density	85
5.4.0	Metallographic Analysis	
5.4.1	As built specimen	86
5.4.2	Heat Treated ABST - Q	87
5.4.3	Heat Treated BST - AC	88
5.4.4	Heat Treated BST – AC- Ageing	89
5.4.5	XRD pattern and d- spacing value	90
5.4.6	TEM Micrograph	94
5.5.0	Process Accuracy	95
6.0	Chapter 6 : Discussion & Conclusion	97
7.0	Chapter 7 : Future Recommendation	102
9.0	References	104

List of Figures

Figure 2.1: The Applications of RP Technologies [www.wohlersassociates.com]	6
Figure 2.2: The Transformation of RP to RM based on Applications	8
Figure 2.3: Application of RM Technologies in 2008 compared to Wohlers's Report 2006 [25]	10
Figure 2.4: Basic RM Framework	11
Figure 2.5 RM systems based on binding mechanism[46]	13
Figure 2.6: Laser based powder consolidation mechanism [9]	14
Figure 2.7: Liquid Phase Sintering Mechanism [8]	15
Figure 2.8: Different combinations of the powder particles [52]	16
Figure 2.9: Flow Chart and mass balance sheet for titanium product fabrication from ore [44]	20
Figure 3.1: Classification of DMLF [13]	33
Figure 3.2: Schematic representation of DMLS processes	34
Figure 3.3: Schematic Illustration of SLS [13]	35
Figure 3.4: Schematic Illustration of SLM [13]	37
Figure 3.5: Schematic Illustration of 3D cladding [27]	39
Figure 3.6: Influence of the laser parameters [28]	42
Figure 3.7: EOS GmbH M270 Machine[www.eos.info]	45
Figure 3.8: M270 machine: Technical data [www.eos.info]	47
Figure 3.9: EOS range of materials [www.eos.info]	48
Figure 4.1: Schematic Representation of cutting machine procedure	51
Figure 4.2: Preparation of Epoxy resin mounting	52
Figure 4.3: Steps for grinding and polishing	53
Figure 4.4: Data Transfer Platforms	54
Figure 4.5: EOS GmbH Standard Parameters for M270 machine	55
Figure 4.6: Schematic representation of SLM processes [13]	56
Figure 4.7 : Type of Scanning Strategy [63]	58

Figure 4.8:	Scanning layout for specimens fabrication	59
Figure 4.9:	Malvern Mastersizer Machine	60
Figure 4.10:	SEM specimen preparation procedure	63
Figure 4.11:	Gas Pcnometry Instruments	64
Figure 4.12:	Tensile Specimens, Tensile machine and Fractured specimen	66
Figure 4.13:	Fractured surface specimens for SEM	66
Figure 4.14:	Indenter for Vicker's Microhardness Test [www.wikipedia.com]	68
Figure 4.15a:	Disc shaped specimen for Part's Density	68
Figure 4.16:	Fluid displacement technique based on Archimedes's principle	69
Figure 4.17:	Tubular Vacuum Furnace	70
Figure 4.18a:	Specimen Preparation for TEM	72
Figure 4.18b:	TEM preparation instrument	73
Figure 4.19:	Benchmark for Process Accuracy and Feasibility Study	74
Figure 5.1:	Beam shaped, Disc Shaped and A Block specimen	75
Figure 5.1:	Graph of the Particle Size Distributions	76
Figure 5.2:	Ti6Al4V powder particles via SEM	77
Figure 5.3:	EDX of the Ti6Al4V powder particles	78
Figure 5.4a:	Load – displacement Graphs for Tensile Test 1	81
Figure 5.4b:	Stress-Strain Graphs for Tensile Test 1	81
Figure 5.4c:	Load – displacement Graphs for Tensile Test 2	82
Figure 5.4d:	Stress-Strain Graphs for Tensile Test 2	82
Figure 5.5 (a-f):	SEM for Fracture Surface Analysis	84
Figure 5.6 (a-f):	Optical Micrograph Images as built specimens	86
Figure 5.7 (a-f):	Optical Micrograph Images of the ABST-Q	87
Figure 5.8 (a-f):	Optical Micrograph Images of the BST-AC	88
Figure 5.9 (a-f):	Optical Micrograph Images of the BST-AC-Ageing	89
Figure 5.10a:	Diffraction Pattern of Ti6Al4V powder	90

Figure 5.10b: d-spacing of Ti6Al4V powder	90
Figure 5.11a: Diffraction Pattern of Laser Sintered specimen	91
Figure 5.11b: d-spacing value of Laser Sintered specimen	91
Figure 5.13a: Diffraction Pattern of BST-AC-Ageing specimen	92
Figure 5.13b: d-spacing value of BST-AC-Ageing specimen	92
Figure 5.14: TEM Micrograph with corresponding SAD	94
Figure 5.15: Indexing Diffraction pattern based on the SAD	95
Figure 6.1: XRD Diffraction Pattern Comparison	101

List of Tables

Table 2.1:	RP Systems Development Years [18]	5
Table 2.2:	Heat Treatment of Titanium Alloys and microstructure [44]	28
Table 3.1:	Commercially available RM system for DMLF [13]	32
Table 3.2:	The Benefits and Drawbacks of SLM process	38
Table 3.3:	Asorptance of single powder with two different lasers [50]	41
Table 4.1:	Type and Quantity of fabricated specimen	49
Table 4.2:	Specimen labelling and corresponding analysis	50
Table 4.3:	Tensile Testing Machine's Parameter	66
Table 4.4:	Designated Heat Treatment	71
Table 5.1:	Visual Observation and Evaluation Results	75
Table 5.2:	Particle Size Distribution Table	76
Table 5.3:	Compositional Analysis of Ti6Al4V powder	77
Table 5.4:	EDS compositional test results compare to ISO and ASTM	78
Table 5.5:	Ti6Al4V powder density via gas pycnometry	79
Table 5.6:	Results recorded form Tensile's machine	80
Table 5.7:	Tensile Testing Results	83
Table 5.8:	Microhardness Results	83
Table 5.9:	Part Density Results using gas pyncnometry	83
Table 5.10:	XRD and d-spacing analysis	93
Table 5.11:	Dimension tolerances for customised benchmark	95
Table 5.12:	Measurement results for customized benchmark	96
Table 6.1:	Mechanical Properties of Ti6Al4V metal parts	98

Glossary

3DPM	3D Printing Manufacturing
AF	Additive Fabrication
AFF	Additive Freeform Fabrication
AT	Additive Technology
CAD	Computer Aided Design
DLMS	Direct Metal Laser Sintering
DMLF	Direct Metal Laser Fabrication
EDS	Electron Diffraction Spectrometer
FDM	Fused Deposition Modelling
LOM	Laminated Object Manufacturing
OM	Optical Microscopy
PREP	Plasma Rotating Electrode Process
RE	Reverse Engineering
RM	Rapid Manufacturing
RP	Rapid Prototyping
RPM	Rapid Prototyping and Manufacturing
RPT	Rapid Prototyping Technology
RT	Rapid Tooling
SEM	Scanning Electron Microscopy
SFF	Solid Freeform Fabrication
SLA	Stereolithography Apparatus
SLS	Selective Laser Sintering
TEM	Transmission Electron Microscopy
T_{β}	Beta Transus Temperature
UTS	Ultimate Tensile Stress
XRD	X-Ray Diffraction

Introduction

The first commercially available Rapid prototyping system was introduced in the late 1980's. This new technique of producing customised 3D part in one step has evolved rapidly towards the realization of rapid manufacturing processes. There are numerous Rapid Prototyping systems; Stereolithography (SLA), Selective laser sintering (SLS), Fused deposition modelling (Anna Belini & Selcuk Guceri, 2003), 3D printing (Levy et al, 2003), Laminated object manufacturing (Brian et al, 2001), Laser Engineered Net Shaping (J. Zhoa et al, 2009). Early findings have shown that, RP systems significantly reduce the lead time by 54% in producing appearance models (M.Evans et al, 2003). The success of the Rapid Prototyping process marked a revolution in product development and manufacturing. Fundamentally, RP systems as their name suggests used for producing prototype models. It is evolving rapidly from prototyping towards the manufacturing of end user functional products. With the absence of tooling and moulding thus giving the optimum design freedom to the designers as undercuts and draft angle are not longer be the constraints. On the contrarily, compared with the subtractive processes such as high speed machining, RP systems adopt the additive principle. The parts are built additively, layer by layer, according to CAD data. This layer manufacturing or Solid Freeform Fabrication is capable of building parts from various materials such as polymers, hard metals and ceramics to full density (J.H Liu et al, 2009).

The Selective laser sintering technique is the leading RM system due to its capability to sinter a huge spectrum of materials. The interaction between the laser beam and the powder particles through an intricate thermo-mechanical process fusing the selected powders at the powder bed layer by layer until a 2D solid pattern is created. The sintered layer is lowered to a certain height and then a thin layer of new powder is then deposited. Extensive research has been carried out in order to investigate the influence of the fabrication parameters with the corresponding microstructure and the mechanical properties compared with bulk material. Studies show that a profound implication of this technique is successful production of fully dense metal parts in one step. The capability of

producing metal parts up to 99.8% density with fine microstructure and excellent mechanical properties are the main reason behind it. With full part densities achieved, the fabricated parts will have good mechanical properties such as tensile and high fatigue strength. Therefore, a greater details understanding of this process is required to control the specific process parameters in order to get a desired microstructure and good mechanical properties. This includes the effects of laser energy, laser beam spot size, scan speed, scan spacing and layer thickness (J.D Williams & Deckard, 1998).

The literature indicates the rapid growth of RM system but there has not been much works done to thoroughly investigate the process feasibility, repeatability and capability. RM machines are relatively expensive and the unstable economic conditions would not stimulate sales. Industries still need to be convinced that RM machines can reduce their manufacturing cost. M.Ruffo and R.Hague (2007), studied the simultaneous production of mixed components using Selective Laser Sintering to highlight the potential of cost reduction. A comparative study was mentioned elsewhere (J.C Ferriera et al, 2006; Abdel Ghany & Moustafa, 2006). Attempts have also been made to integrate RM with other techniques in order to reduce manufacturing cost and time (G.D Kim & Y.T Oh, 2008; M. Ruffo et al, 2007). Farid Fouchal and Phil Dickens, (2007) demonstrated the feasibility of RM system for high volumes production. For some, RM is more suited for low volume production and for a few this technology is capable of producing mass customisation of high end products. Besides time and cost, the accuracy and repeatability of RM systems have also been heavily investigated (G.D Kim & Y.T Oh, 2008; M.V Elsen et al, 2008).

Light alloys such as aluminium and titanium are widely used in various industries. Compared to aluminium, titanium alloys are more difficult to cast and to machine. Therefore, conventional methods such as investment casting, forging and machining will definitely remain the best method as far as cost is concerned. The EOS GmbH M270 Direct laser sintering machine provides an alternative way to fabricate titanium pre-alloyed powder through a laser sintering process. The parts are proven to have good mechanical properties i.e strength and hardness

compared with forged parts but with slightly lower elongation (M.Shellabear & Nyrhila, 2007). The Ti6Al4V light alloy is ideal for biomedical applications because of its biocompatibility and high strength to weight ratio. In addition, this alloy shows good corrosion resistance which is a crucial requirement for bio-medical applications. Several studies show the use of electron beam melting to fabricate Ti6Al4V implants (Luca fachine,2009; Xiang Li et al, 2009). As expected, there are obvious differences in microstructure as a result of different manufacturing methods e.g the cast Ti6Al4V alloy will have different properties compared with wrought Ti6Al4V. Perhaps this electron or laser sintering technique may produce a unique microstructure due to rapid melting and solidification process.

The microstructure of titanium alloys is described according on the size and arrangement of the two phases α and β (C. Leyens, 2003; I.J Palmer, 1995) Microstructural features are described as fine or coarse and the arrangement of features as lamellar or equiaxed. These sizes and arrangements have a huge effect on some crucial selected mechanical properties. A fine scale microstructure increases the strength as well as ductility, retards crack propagation and is a prerequisite for super-plastic deformation. A coarser structure on the other hand, is more resistant to creep. A lamellar microstructure has high fracture toughness and superior resistance to creep and fatigue crack growth. An equiaxed structure which results from re-crystallization process offers high ductility and increased fatigue strength. Various microstructures were obtained through different thermo-mechanical treatments. One of the crucial factors was the β -transus temperature which defined the single β phase field and the $\alpha+\beta$ field. As an example, slow cooling from above T_{β} will result in a pure lamellar microstructure with the lamellae becoming coarser with reduced cooling rate. Therefore, a comprehensive understanding of the intricate process of laser-powder interaction is a prerequisite in order to have parts with specific microstructure and sound mechanical behaviour. Process parameters, powder technology properties and the designated heat treatments are a few of the variables to be highlighted as the main focus in this study.

2.1.1 Additive Manufacturing

Additive manufacturing is defined as a process of joining materials to fabricate solid parts from digital data or CAD data, usually layer upon layer as opposed to subtractive manufacturing processes (Prashant et al, 2000). This process is also known as layered manufacturing, additive technology, additive fabrication, additive process and solid freeform fabrication (E.C Santos et al, 2006). Notably, this system includes all applications of the technology, modelling, pattern making, tools and mould making, and the production of end use products regardless of the volume of production. It is not all about prototyping.

Generally, all additive manufacturing systems employ the same fabrication technique; driven by digital CAD data, the data is sliced horizontally to create a 2D layered cross section. Due to the intricate interaction between the powder and the heat source, all the layers are combined to create a solid part which corresponds to the CAD data. The earliest technology use this additive method is Rapid Prototyping (N. Hopkinson & P. Dickens, 2001). RP has experienced exponential growth during the 1990's as the platform to produce or 'print' parts quickly and inexpensively for design verification and validation in the early stage of the product development cycle. The physical model of RP has significantly reduced the design error and increases the manufacturability of parts and assemblies. The application of RP has expanded, not just for prototyping purposes but to overcome billions of dollars spent on tooling and mould fabrication (A.Simchi, 2006). For some this is known as '*Rapid Tooling*' which uses the RP system to create core and cavity mould inserts for injection moulding (Maria et al, 2007). Others believe RP can and will evolve to successfully produce functional end parts in one step (P.Mognol et al, 2006). Dimov et al, (2001) applied an SLS technique to build tooling inserts in copper polyamide that can be used for fabrication of final products and used the RT solution for fabrication of injection moulding tools. Due to its capability in creating solid parts upon layer by layer, RP is predicted to produce any part in any geometry of the highest complexity. This has lead to the '*Rapid Manufacturing*' terminology.

However, these additive technologies are still in a premature phase. Much research and developments has been undertaken in order to justify the use of this technology in terms of cost, materials and mechanical characteristics. The systems are relatively expensive and still have limitations on materials that can be processed. Neil Hopkinson and Phil Dickens (2001) have stated that, small parts with geometric complexity in relatively small volumes are the most suitable candidate for this technology.

2.1.2 Rapid Prototyping Technology

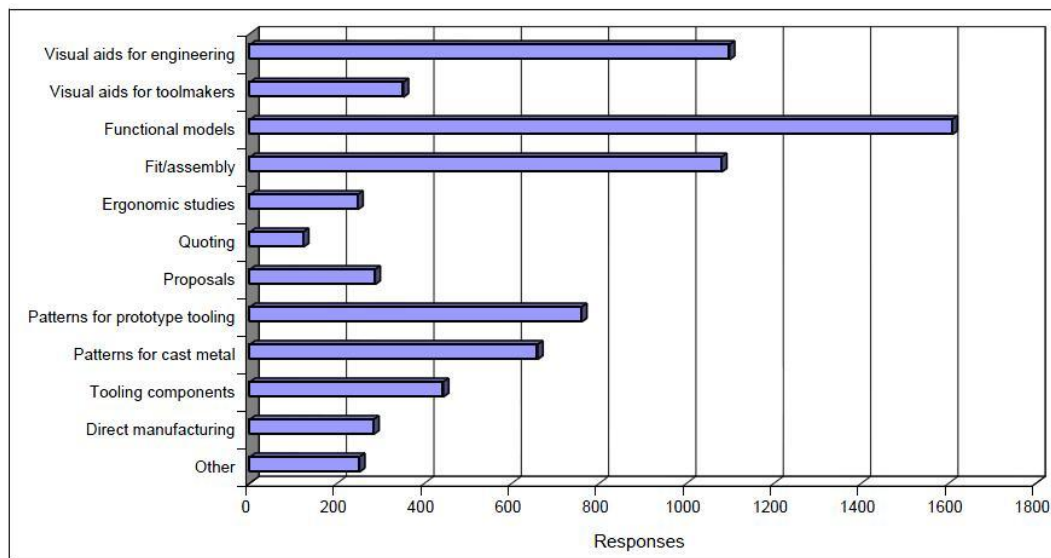
Rapid Prototyping which is also known as Additive Freeform Fabrication was introduced in the late 80's with the SLA machine. Since then, there are tremendously various machines using similar concepts which have been deposited and patented (G.N Levy et al, 2003). LM technologies at this time are often known as Rapid Prototyping technologies due to their main objective of having a design prototype. Indeed, RP refers to the physical modelling of a design using digitally driven, additive processes. RP systems quickly produce models and prototype parts from 3D computer aided design (CAD) data or data from 3D digitizing systems. Via this additive process, RP technology joins liquid powder or sheet materials to form physical objects, layer by layer. RP machines are able to process plastics, ceramics, metals and composites from thin, horizontal cross sections of a computer model (I.Gibsons et al, 2006; J.P Kruth et al, 2007)

Name	Acronyms	Development years
Stereolithography	SLA	1986-1988
Solid Ground Curing	SGC	1986-1988
Laminated Object Manufacturing	LOM	1985-1991
Fused Deposition modelling	FDM	1988-1992
Selective laser Sintering	SLS	1987-1992
3D Printing (Drop on Bed)	3DP	1985-1997

Table 2.1: RP systems development years, source: Gideon N. Levy, et al (2003)

According to Todd Grimm, founder and president of the society of Manufacturing Engineering, "RP is a digital tool that grows parts on a layer by

layer basis without machining, molding or casting. Rapid prototyping can reproduce (quickly and accurately) designs that are impractical or impossible to create by other method” (Todd Grimm, 2004). The introduction of this technology in the area of manufacturing has changed the engineering design and the manufacturing process as RP provides full design freedom. There is no need to wait a few weeks for the tooling to be fabricated, instead the result of the design modification can be seen within one day.



Source: Wohlers Report 2003

Figure 2.1: The Applications of RP Technologies, source; (www.wohlersassociates.com)

Rapid Prototyping technology has vast applications at the beginning of a product development cycle. As shown on the responses graph above in the figure 2.1, the prototype was used as visual aids for engineering, functional models for testing, fit/assembly and also as master patterns for tool making. Prototype models assist in the early development phase for design validation so that the modification can be done during the design stage before it reaches the production phase. This reduces the production cost since no modification needed to the tooling and mould is needed as design errors are detected at an early stage. In addition, any modifications are done via digital data only. According to Wohler’s Report (www.wohlersassociates.com), Rapid prototyping is nearly a billion dollar a year industry and involves more than 30 system vendors. In 2002, 22.4% of RP models were used for functional models, 19.2% as

patterns for prototype tooling, 15.3% for visual aids for engineering and 15% for fit/assembly. 28% of Rapid Prototype models were utilized for patterns cast metal, tooling components and direct manufacturing. Remarkably, the report also mentioned that rapid prototyping has already been used to generate time and cost savings in fighter aircraft and the space shuttle [www.wohlersassociation.com].

For the last twenty years, this technology has spread widely not specifically in the manufacturing area but largely for medical components. For instance in 2001, the physical anatomical model of the Egyptian twins was fabricated in order to assist surgeons to have better surgical planning. Nowadays, lot of works has been done in utilizing the RP technology for the medical purposes such as for craniofacial plates, artificial limbs and crowns and bridges in dentistry. Recently, Giannatsis and V Dedaussis (2009) discussed the utilization of RP technology in medical and health industries. I.Gibson et al (2006) also studied the use of RP technology for medical applications.

In England, a company known as 3T RPD supplied RP parts to the Jordan-Honda F1 team. More than 20 different parts were produced as the prototypes but many were built to directly install into the F1 car. Specific Surface of Franklin, Massachusetts, is manufacturing highly complex ceramic filters that are applied to everything from making soy sauce to filtering diesel emissions. Ongoing research work led by Bill Rogers from Texas University is looking at the capability of the SLS process to fabricate high demand customized artificial limbs [www.manufacturingtalk.com].

Evidently, RP technology can spark innovation. As customer demand becomes more complex and diversified, the manufacturers have to work toward mass customization and individualization. It means creating product variety within a product family in low volumes. This will definitely stimulate the evolution of Rapid Prototyping towards Rapid Manufacturing. Perhaps Rapid Manufacturing will be the next frontier of this technology (Anna Kochan, 2002).

The transformation of RP systems towards RM is also influenced by unique customer requirements. It leads to customization and rapid production. This is the advantage of RP systems which can speed up processes and produce good quality products. However, the realization of this transformation still has its limitations. Expensive machine and materials, overall cost and production volumes are amongst the issues that need to be considered before fully utilising this technology.

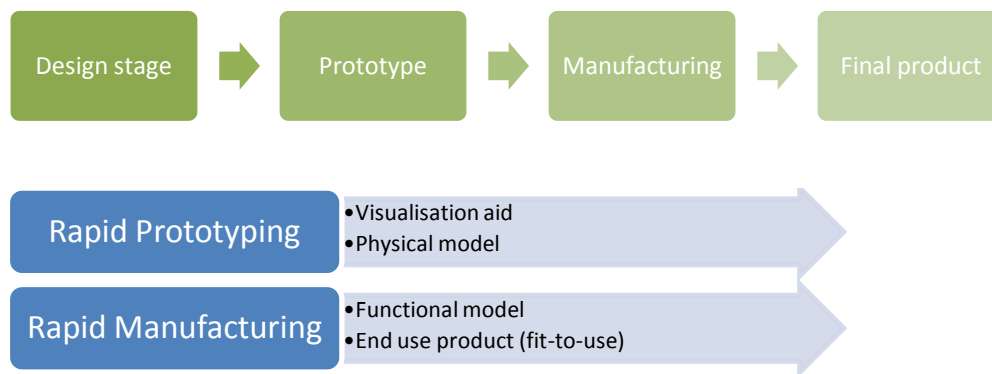


Fig 2.2: The transformation of RP to RM based on the applications; *source N.Hopkinson and P.Dickens (2001)*

The above diagram shows the transition of the physical model produced by RP technologies. The diagram clearly depicts that the optimum objective of the transformation is to have functional end use products with Rapid Manufacturing Systems. There is currently much research and developments underway to achieve this aim. A reasonable machine price and the huge spectrum of available materials are two factors which can stimulate this transformation.

The EOS technology has successfully built metal parts directly from steel, cobalt and titanium alloys [www.eos.info]. Pogson et al, (2003) investigated the major processing factors that influence the production of copper parts through the SLS process. Kruth et al (2003) carried out intensive experimental and numerical simulation in producing metal parts via SLS. Suman Das et al (1998), produced high performance metal components by SLS. P.Fischer et al (2003) successfully sintered commercially available pure titanium powders using an Nd:YAG laser source. This research has proved the use of this advanced technique for direct metal fabrication via a laser sintering process.

2.1.3 Rapid Manufacturing

Rapid Manufacturing has emerged from the advent of rapid prototyping in order to produce models and prototypes through a concept of additive manufacturing. This is in contrast to traditional cutting, forming or casting methods. It belongs to the Rapid Prototyping systems, which is used for various kinds of applications during early product development in order to verify design and manufacturability, through concept evaluation, prototype models for presentation, as well as functional testing. The continuous improvement of RP in the area of powder materials and the sintering/melting technologies, pushed the limit of this system towards direct fabrication of functional parts in a small batch, which is known as Rapid Manufacturing and Rapid tooling (for tooling and mould fabrication).

For clarification, the simple definition of Rapid Prototyping and Rapid Manufacturing is given below (N.Hopkinson & P.Dickens, 2001):

- a. **Rapid Prototyping** – refers to a group of commercially available process which are used to create solid 3D parts from CAD through a technique known as a Layer Manufacturing technique or Additive Fabrication
- b. **Rapid Manufacturing** – uses this Layer manufacturing technique or additive fabrication to directly manufacture solid 3D parts for the end user either as parts of assemblies or as standalone products
- c. **Rapid Tooling** – uses this layer manufacturing technique to directly fabricate tooling and moulds without the aid of any machining processes

There are still arguments regarding the definition of RP and RM. for some, RM means quick direct production of end-use parts by any manufacturing method and for many, it requires the use of layer manufacturing techniques somewhere along the production chain. However Terry Wohlers, a prominent additive manufacturing industry consultant defined RM as a direct manufacturing of finished products through an RP device [www.wohlersassociates.com]. This technique uses additive processes to deliver finished products from digital data which eliminates all tooling. Annon et al (2001) state that, RM is still an emerging set of technologies that have been gradually evolving from mere prototyping

tasks to the final and fully functional manufacture of parts and products. In a regional context, RM is defined as a set of techniques, technologies and methods that provide rapid and flexible manufacturing for a variety of applications: prototypes, moulds, dies, general tooling and final product (www.rmplatform.com).

The Applications of RM technologies

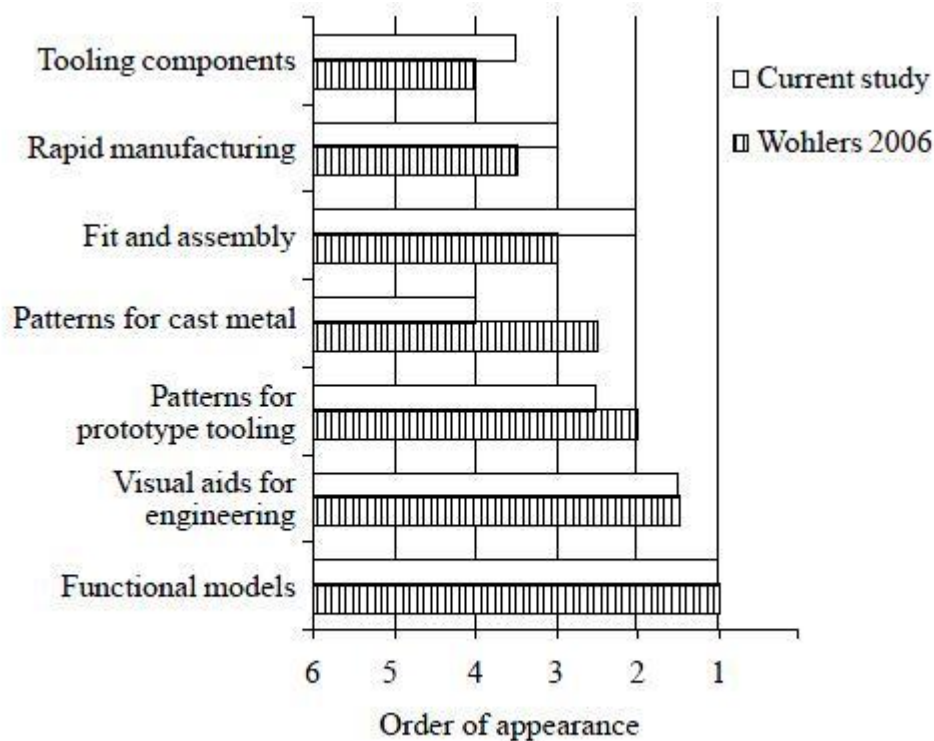


Figure 2.3: Applications of RM technologies in 2008 compared to Wohlers Report 2006;source Javier Munguia et al (2008).

As shown in figure 2.3, a survey was done to investigate the extensive use of RM equipment in Northern Spain. The result was compared to the Wohlers Report in 2006. The application for functional models is still provides the main purpose for having RM equipment and Rapid Manufacturing was ranked sixth on the list. A Comparative analysis was done to change the appearance model to a fully functional model has significantly reduced production time scales. Maria Grazia Violante et al (2007) reported the use of RM technologies to manufacture fixtures. P. Mognol et al (2006) used SLS as one of the hybrid tooling methods to quickly produce multi component parts for tooling applications.

2.1.4 Rapid Manufacturing Framework

Rapid manufacturing offers the fastest path to bring functional end products to the market. This is because the data is transferred digitally from the design platform to the end of fabrication platform. Evidently, it shortens the product development cycle (Anna Kochan, 2002).

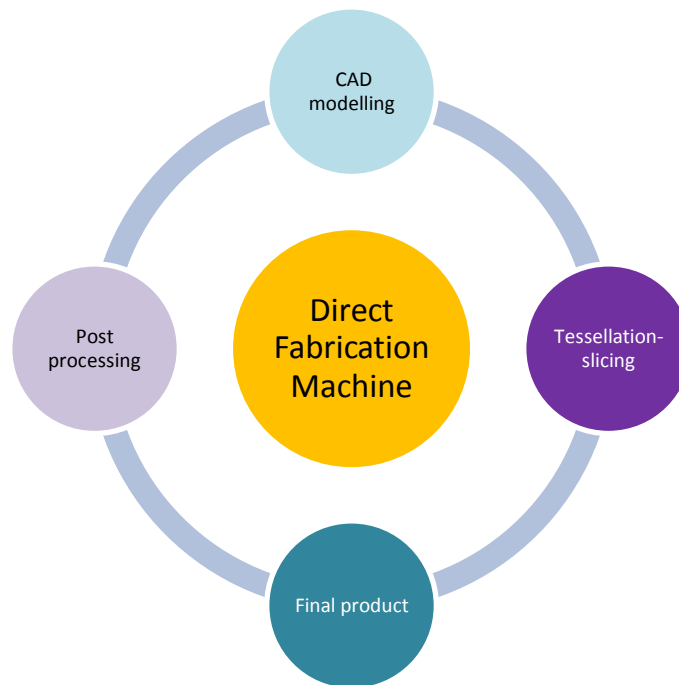


Figure 2-4: Basic Rapid Manufacturing Framework, *source; Prashant Kulkarni et al (2000)*

CAD data is digitally transferred to the RM machine. The machine builds the final product without any tooling or moulding. During intermediate phases, the CAD data is transformed to triangulation data format and then sliced for the 2D scanning path generation. A secondary process such as machining and heat treatment is performed depending on the intended application requirements. With the full melting technique, the parts are fabricated to near full density so that RM systems have the capability of producing parts with good mechanical properties thus eliminating the post processing phase.

2.1.5 Issues and Advantages pertaining to Rapid Manufacturing

Hopkinson and Dickens (2001) highlighted three major issues pertaining to RM. They also concluded that the high cost of RM materials is generally acceptable and it is not the major driver for material's selection. It is satisfying the requirements of a product that is most important. The following issues will affect the growth of Rapid Manufacturing ;

1. Material properties
2. Quality Control
3. Identification of suitable product to be produced by RM technologies

The material properties of parts produced by rapid manufacturing have been compared to those made by injection moulding. It is known that the material properties of RM parts sometimes did not match those of parts made by injection moulding but a lot of research has been carried out to enhance the material properties of RM parts. RM systems also face the issue of quality control as the parts produced by RM normally have high surface roughness and a stair effect on the surface (Kamran & Hopkinson, 2009). This means that post process machining is required which can be costly and time consuming. An extensive analysis was undertaken and a comparison was made to justify the use of RM systems as a new production technique, to replace the conventional method (L. Dong et al, 2009). M.Ruffo et al (2006) studied the feasibility of RM systems. M. Ruffo and R. Hague (2007) confirmed the intuitive concept of producing mixed components in one building space via RM systems to effectively reduce the cost of each component. Although there are quality control issues above, RM has distinct advantages:

- a. Complicated geometries can now be made
- b. A reduce number of parts as assemblies can be made in one piece
- c. The realization of concurrent engineering
- d. High integrity products for low volumes
- e. Reduced cost, lead time and improved quality

2.1.6 Rapid Manufacturing Characteristic

Rapid Manufacturing Systems share a similar procedure for producing 3D parts. This is because the development of this system happened simultaneously. Major differences amongst these sophisticated systems are the type of materials that can be processed and the binding mechanism that fuses the powders on each layer. Basically, RM systems have the following procedure;

- a. They produced fine powders particles
- b. Spread powder in a very thin layer (100um or less)
- c. fuse the powders according to a CAD design by applying thermal energy via a laser or electron beams
- d. Repeat the process to build stacking layers
- e. Post process to increase density

There are numerous RM systems commercially available on the market as mentioned earlier. There are also RM systems which is capable of producing metal parts using powder technologies such as Electron beam melting. The system and mechanism was discussed elsewhere (Luca Facchine, 2009). Kruth et al (2007) highlighted distinct differences between the various RM systems. Prashant et al (2000) in their reviews have categorized the RM systems based on the method of binding.

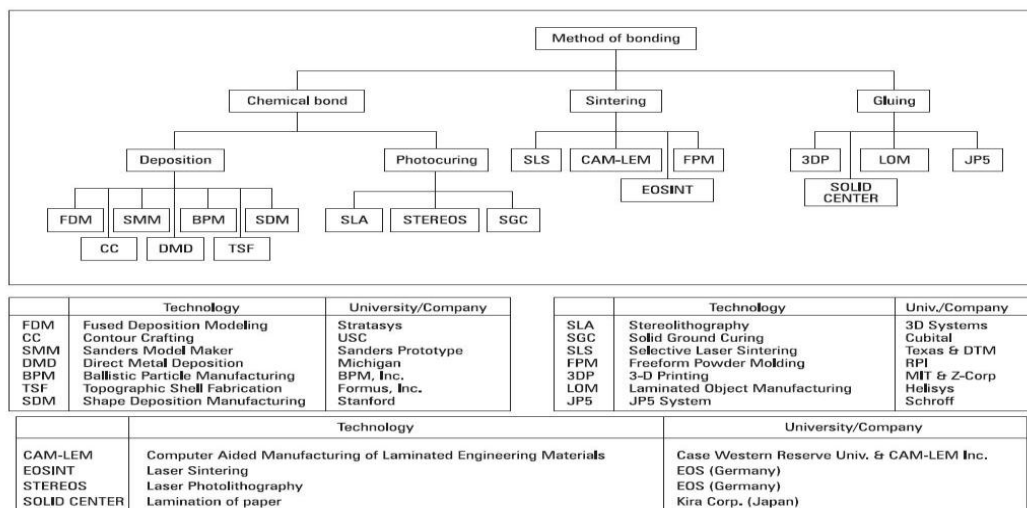


Figure 2.5: The Classification of RM system based on binding mechanism, Source; M. Agarwala et al (1995).

2.2 SLS Technologies

Selective laser sintering technologies can be classified as a different category based on the binding mechanism applied by the machine to form a solid 3D part. Different manufacturers have an identical technique to binds each layer. Generally, SLS can be classified into four categories but this classification is not absolute and the borders are not very clear especially between SLS and SLM.

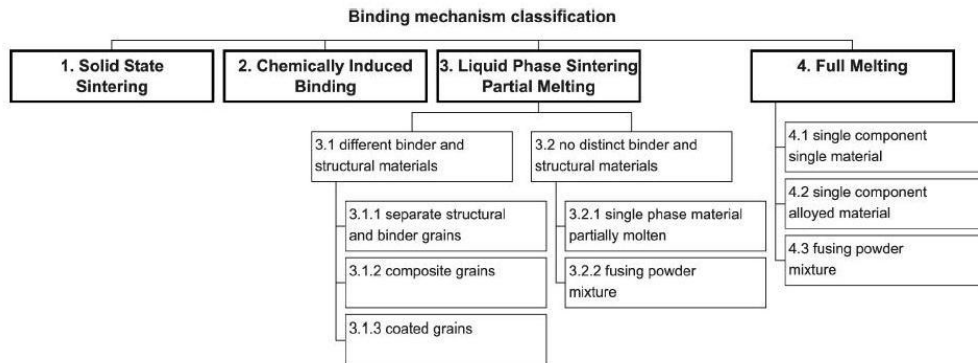


Figure 2.6: Laser based powder consolidation mechanism, *Source; B.V Schueren & J.P Kruth (2007)*

2.2.1 Solid State Sintering

Solid state sintering is a thermal process which fuses the powder particle by creating a neck between the particles. The advantage of this sintering technique is the capability to sinter a broad range of powder materials as long as enough energy is provided to give sufficient heat to bind the particles. All powders are consolidated via diffusion of atoms i.e surface, volume, grain boundary diffusion. The temperature needed to induce sintering between two particles depends on the material and particle shape, size and distribution. For a crystalline material a grain boundary grows at each contact point to replace initial solid-vapour interfaces. Normally, a two spheres model is used to describe the sintering process. During prolonged sintering the grain boundaries migrate and the particles coalesce into a single sphere with final a diameter equal to $2^{1/3}$ times the original diameter. This physical diffusion happened at slightly below the melting temperature (Randall M German, 1996). This binding mechanism is rarely used since the process is slow and not parallel to the high laser scan speed. This will contribute to the higher cost and low productivity. However, this

technique is best suited consolidate ceramics parts and is sometimes applied for post processing after partial laser consolidation of metallic parts of solid state sintering.

2.2.2 Liquid Phase Sintering

Liquid phase sintering reduces of sintering time due to a faster scan speed compared to solid state sintering. However, complication exist with a single component powders since it is necessary to understand the process parameters to ensure sufficient surface melting but avoiding core or structural particles melting. (Nikolay, et al, 2004) states that the 'balling' phenomenon is one of the problems obstructing successful performance of single component laser sintering. In the case of two components, there is a clear distinction between the structural material as the main component with high temperature capability and the binders (Nikolay et al, 2003). The laser irradiation was adjusted to a level that exceeded the binder's melting temperature and the liquid binder wets and binds the structural particles. Normally, the binder components are smaller than the structural particles favouring higher solubility leading to better wetting and spreading for densification. There are three main concerns during the liquid phase sintering process; rearrangement, solution re-precipitation and final phase sintering.

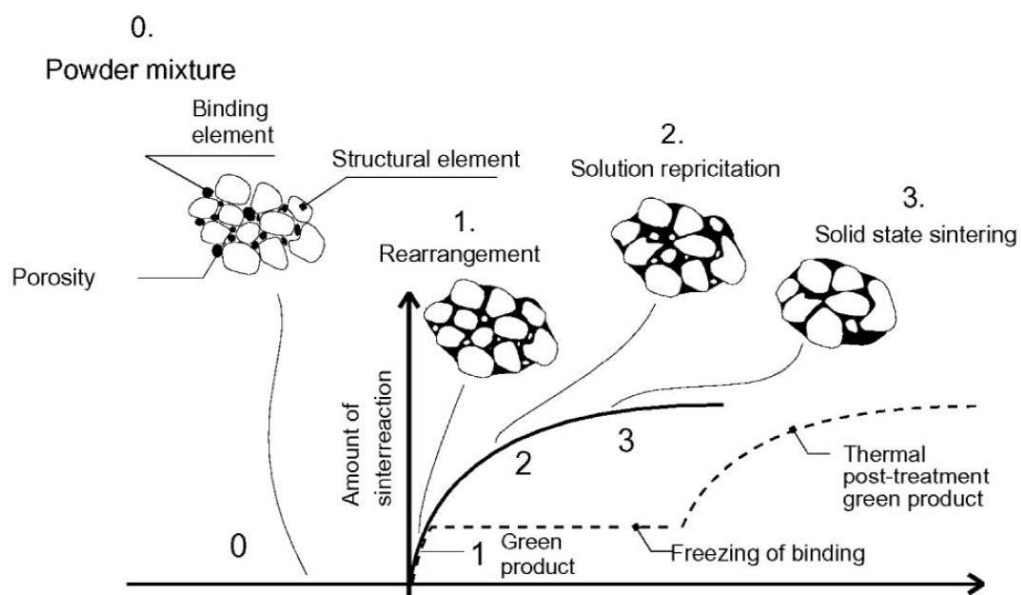


Figure 2.7: Liquid Phase Sintering Mechanism, source; Prashant et al,(2000)

Liquid phase sintering can be simplified into three stages. The first stage is a rearrangement of particle when the liquid forms and wets the solid structure. The second step occurs when solution re-precipitation becomes active leading to pore elimination by grain shape adjustment and the third step is microstructural coarsening, where the mean grain and pore sizes increase continuously. The post processing or debinding process such as furnace treatment, HIP or infiltration are normally required in this process to eliminate the 'green' parts in order to increase density of the parts.

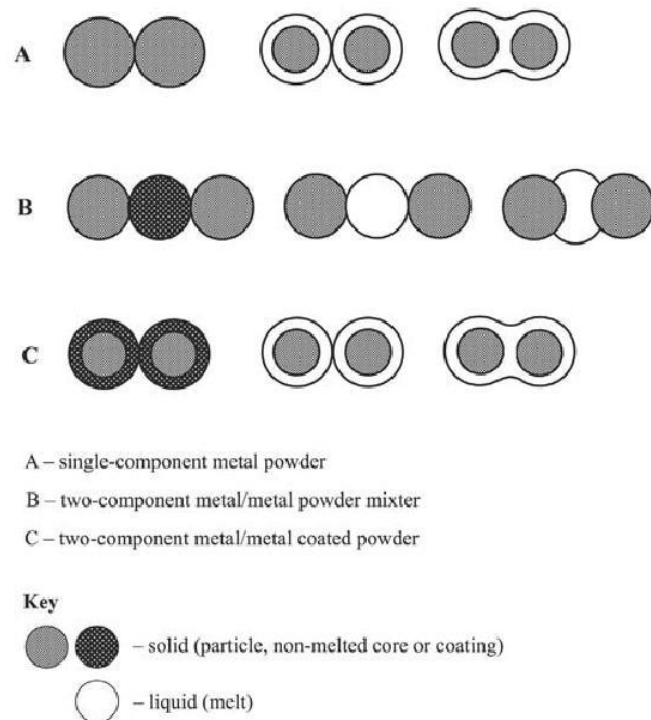


Figure 2.8: Different combinations of the powder particles, *source; Nikolay et al, (2003)*

There are three different combinations of powders that can be used for this technology;

1. *Separate grains* – this technology separated the core and binder components. The binders have a smaller size and lower melting temperature compared to core components with a higher melting temperature. The core can be a ceramic or metal but the binder is mostly metallic.

2. *Composite grains* – through the mechanical alloying process, the powders structural and binders are repeatedly milled, fractured and welded together. In turns, the composite grains constitute of two different powders in one individual powder grain.
3. *Coated grains* – the structural grains are coated with the binder component. The laser irradiation scans and melts the binders first and the structural component remains solid throughout the process.

Partial melting – here there is no distinction between the structural and binder components which mean it can be a single phase component. However, there is a clear distinction between molten and non-molten areas throughout the process. The laser energy input is adjusted to ensure that insufficient energy is supplied and only the outer shell of the particles is melted rather than complete particles melting. The molten materials will act as a binder to join the core particles which remain unaffected.

2.2.3 Chemically induced process

This process is rarely utilized for commercially available sintering machine but has proved to be feasible to sinter ceramics, metals and polymers. IPT Achen, Germany have used this technique to sinter SiC ceramics parts. SiC powders will partially disintegrate into Si and C during heating. A reaction with oxygen will then form SiO which will then act as a binder to fuse the SiC particles. Finally post processing via Si infiltrants is used to achieve fully dense parts (B. Vandenbroucke & J.P Kruth, 2007).

2.2.4 Full melting

The development of full melting processes such as selective laser melting is driven by a requirement to have optimum mechanical properties in bulk material with fully dense parts. The ability to achieve almost 99.8% part density through completely melting the powders has eliminated those lengthy post- processing treatment. Polymers as well as metals can be made fully molten by this process. However there is a limitation on the metallic materials that can be processed by

this technique. This cutting edge process is achievable because of significant improvement of laser energy density. Nowadays, a shorter wavelength laser Nd:YAG (1.06 μ m) is used to provide greater laser energy with a smaller spot size compared to previous CO₂ laser sources (Nikolay et al, 2000). P. Fischer et al (2003) reported the use of a Nd:YAG laser for pure Titanium powder. R Morgan et al (2001) used the nanosecond pulse of Nd:YAG to sinter metallic powders. In addition, the absorbance of laser energy in metallic material is greater in a shorter wavelength laser rather than in a long wavelength CO₂ laser. However, studies have shown drawbacks when using a full melting process, such as part distortion due to internal stresses and high surface roughness caused by a 'balling' phenomenon (Nikolay et al, 2004). Therefore, details which aid our understanding of the process parameters and suitable preheat treatments are mentioned in several research works in order to minimize the effects.

2.2.5 Problems in SLS

SLS technologies offer a promising technique for producing parts that would be difficult and impossible to build using traditional tools. Despite the benefits, there can be problems during material consolidation which needs to be thoroughly understood if quality and accuracy are to be achieved. The consolidation process involves the intricate interactions between the powder and the laser beam. The process environment is also important. Problems during consolidation are summarized below;

- a. A short laser-powder interaction which may lead to short material heating times relative to the time required for fully melting the powder particles. Nikolay Tolockho, et al (2000) mentioned during laser processing, sintered, semi-sintered/semi melted or fully melted material can be formed. Dai and Shaw, (2002) investigated the transient thermal effects on the fabricated parts.
- b. The melt pool must wet the previously processed layer and when it solidifies it must be flat enough to enable the next thin layer to be

deposited. Since the reaction is mainly based on capillary forces, the wetting characteristics of liquid over the solid particles are critical (B. Van der Schueren & J.P Kruth, 2007).

- c. The intermediate handling of the powders, especially during the consolidation process is of prime importance to avoid powder contamination which would be detrimental to laser-powder interaction. Oxide layers, trapped gas and impurities within the powders have been identified as sources of contamination (B. Engel and D.L Bourell, 2000).
- d. Two components SLS processes, requires careful control of process parameter to sufficiently melt the desired powders. Another problem is when a liquid metal wetting its solid forms if the solid has almost the same temperature (Nikolay et al, 2003).
- e. Sung Min Hur et al (2001) studied the effect of different orientation and packing during the SLS process. The build direction and the length ratio of the x to y-axis were highlighted as important factors contributing to better SLS parts.
- f. N. Ragunath et al (2007) studied the effect of shrinkage in selective laser sintering using Taguchi method. P. Mercelis & J.P Kruth, (2006) reported the effect of residual stresses in Selective laser sintering and selective laser melting.

2.3 Titanium : Theory and Practice

2.3.1 Production of Titanium

Titanium is present in several minerals, sand, rocks and is normally found as a rutile (TiO_2) and ilmenite (FeTiO_3). In the 1940's an inexpensive metallurgical process was introduced known as extended 'Kroll process' to reduce TiO_2 to metallic titanium. Via initial enrichments and pre cleaning, ilmenite is processed to give a similar concentration of TiO_2 comparable to rutile. Titanium tetrachloride is formed with the added of Chlorine and then magnesium is used for final reduction. The magnesium chloride formed by this reaction is subsequently electrolysed to reduce it to magnesium and chlorine which is recycled contributes to cost reduction. The final purity of the sponge is determined by the level of magnesium contamination and the reaction with the reactor walls.

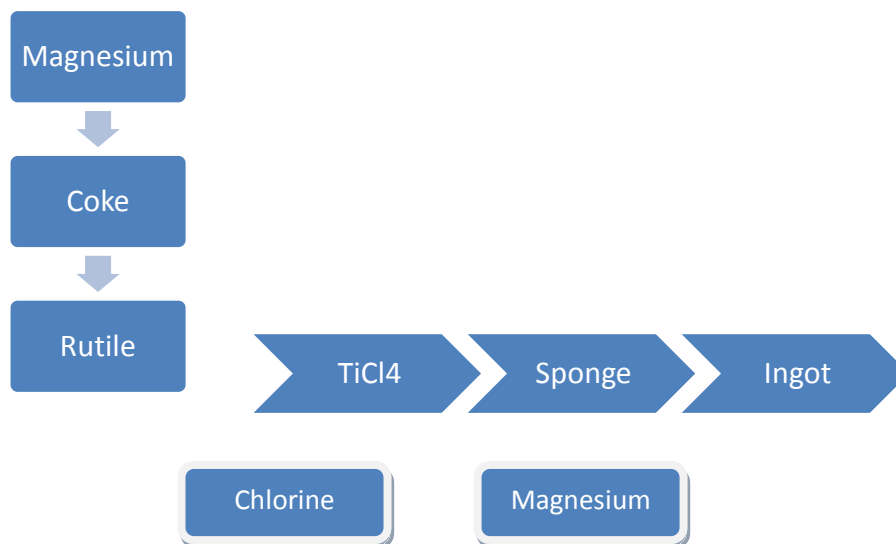


Figure 2.9 : Flow Chart and mass balance sheet for titanium product fabrication from ore, *Source; I.J Palmer, 1995)*

Further processing converts titanium sponge into an ingot. The ingot is formed through multiple re-melting processes. This re-melting is necessary in order to achieve high purity titanium by reducing remaining magnesium and chlorides. However the higher purity titanium has poor strength and is not used for industrial applications. The alloy composition desired is set during the

transformation from titanium sponge to ingot. The titanium sponge is pre-densified in a hydraulic press to form a compact of pure titanium. At this point, the compacts are adequately alloyed. The compacts are then assembled into an electrode for multiple melting processes via vacuum arc melting (VAC). Due to the high oxygen affinity of titanium, the compacts must be welded under argon in a plasma welding to form an electrode. Production of titanium is mostly done through single, double and triple vacuum arc melting in a vacuum chamber, not in an open furnace like other metals.

The self consuming electrode consists of the compact predefined titanium alloys. An arc is formed between the electrode and some swarf placed at the bottom of the water cooled crucible. As a result of a high arc energy, the self consuming electrode is melted and forms an ingot in the crucible. The melting temperature, cooling water and the electrode gaps are essential to for the effective control of the process and production of defect free material.

Plasma Rotating Electrode Process (PREP)

In the Plasma Rotating Electrode Process (PREP), the feedstock, such as Ti Grade 5, is in the form of a rotating bar which is arced with gas plasma. The molten metal is centrifugally flung off the bar, cools down and is collected. The powders produced are spherical; between 100 and 300 μm is size, with good packing and flow characteristics, making the powder ideal for high quality, near net shapes produced by HIP, such as aviation parts and porous coatings on hip prostheses (ASM Metal Handbook, Volume 7).

Gas Atomisation Process

In Gas Atomisation (TGA Process), titanium is vacuum induction skull melted in a water cooled copper crucible, the metal is tapped and the molten metal stream is then atomized with a stream of high pressure inert gas. The tiny droplets are spherical and measure between 50 and 350 μm . The TGA process has been used to produce a wide variety of materials such as CP titanium, conventional alpha-beta and beta alloys (ASM Metal Handbook, Volume 7).

Hydride Dehydride Process

This process is based on a reversible interaction between titanium and hydrogen. Titanium has very high affinity for hydrogen and is easily dehydrogenated by heating titanium in a hydrogen atmosphere. Hydrogenated titanium is very brittle and can be crushed to a fine powder. The hydrogen can then be simply removed by heating the powder in a dynamic vacuum. The minimum hydrogenation temperature is about 400C at 0.007MPa positive hydrogen pressure. Starting stock can be a variety of pure and pre-alloyed titanium materials such as ingot, billet, scrap or machine tunings. The resulting powder is angular and is amenable to cold compaction and subsequent densification by sintering or HIP (ASM Metal Handbook, Volume 7).

Mechanical alloying

Mechanical alloying is a high energy ball milling process, which can be used to produce materials with unique compositions and microstructure. Generally, it involves loading a mix of powders and a grinding medium, usually hardened steel ball into a container under protective argon gas. A small amount of a process control agent is normally added to prevent excessive cold welding of the powder particles during the milling operation. The material is then processed in a high energy ball mill. Alloying occurs as the result of repeating welding, fracturing and re-welding of the powder particles (ASM Metal Handbook, Volume 7).

2.3.2 Powder metallurgy

Clearly, in order to expand the use of titanium alloys in the medical industry or any other industries, production costs must be reduced. Undoubtedly, the production route must be carefully selected to avoid extra costs. The introduction of powder metallurgy offers an alternative production route for titanium fabrication and is considered to be an economic production method for near net shape components. The powder-metallurgical production of titanium parts covers both the powder production with the help of rapid solidification methods and the compaction of these powders to the final component by Hot

Isostatic Pressing (HIP). However, with the full melting of titanium powders via selective laser melting there is no longer a need for HIPing owing to the full density achieved through SLS alone. Consequently, the production of the powder particles is of prime importance since the grain size, morphology and grain size distribution have a large influences on the final part.

Generally, titanium powders can be produced through a Blendend Elemental (BE) technique or by Pre-Alloying technique before the consolidation process takes place. Typical consolidation processes are direct powder forging, rolling metal injection moulding or a layered manufacturing method

The traditional technique of titanium production is via the Kroll Process which involves chlorination of TiO₂ ore in the presence of carbon and reacting the resulting TiCl₄ with magnesium to produce titanium sponge. These processes take place at temperatures as high as 1040 °C. The sponge particles range in size from 45 to 180 µm, with particles ~150 µm termed 'sponge fines'. These fines are irregularly shaped and porous with a sponge like morphology. The fines are then blended with alloy additions; cold compacted into a green compact at up to 415MPa then vacuum sintered at 1260 °C to produce a 99.5% dense component. Hot Isostatically Pressing (HIP) can further increase the density of these parts and produce components more economically than cast or wrought parts, but the porosity present in the material degrades fatigue and fracture properties. More recently, close to 100% dense Ti Grade 5 parts has been achieved using a hydrided powder along with 60:40 Al:V master alloy. The mechanical properties compare well with those exhibited by cast-and-wrought products (www.wikipedia.com)

2.3.3 Crystallographic Forms

Titanium is allotropic and at 825.5°C undergoes a transformation from a low temperature hexagonal packed structure (α) to a body centred cubic (β) phase which remains stable up to the melting point. This transformation in crystal structure means that alloys with α , β or mixed α/β structures are possible and heat treatment can be used to extend the range of phases that can be formed.

2.3.4 Influence of Alloying Elements

Titanium is a transition metal meaning that it has incomplete electronic structure in its outer shell that enables Titanium to form solid solutions of both substitutional and interstitial kinds. The classification of titanium alloys is normally based on the influence of alloying elements. This is because the alloying of titanium is dominated by the ability of elements to stabilize either of the α – or the β - phases (Matthew J Donachie, 2000).

Depending on their influence on the β -transus temperature, the alloying elements of titanium are classified as;

- a. neutral, - Neutral alloying elements have a minor influence on the titanium transformation temperature. Sn and Zr are falls into this category but as far as strength is concerned they are not neutral since they primarily strengthen the α -phase.
- b. α -stabilizers - α -stabilizing elements extend the α phase field to higher temperature and while extending the α phase field, the α -stabilizers develop a two phase $\alpha+\beta$ field. Of these, the α -stabilizing elements are subdivided into β isomorphous and β eutectic elements. Aluminium and the interstitial elements such as oxygen, nitrogen and Carbon belong to this category.
- c. β stabilizers - β - stabilizing elements shift the β phase field to a lower temperature. Fe, Mn, Cr, Co, Ni are among the β stabilizing elements

Aluminium and Oxygen are the most important elements that preferentially will dissolve in the α phase and expand the β transus to higher temperature. The addition of Tin and Zirconium elements do not influence the transus temperatures and are categorised categorize as neutral elements. Vanadium is a common β stabilizing.

2.3.5 Classification of Titanium Alloys

Titanium alloys can be classified according to their microstructure. These are (I.J Palmer, 1995; M. Donachie, 2000);

- **α alloy**
- **near α alloy**
- **$\alpha+\beta$ alloys**
- **near β alloys**
- **metastable β**

α and near α titanium have mainly α structure and depending on the processing condition may have different microstructural grain morphologies, ranging from equiaxed to acicular (martensitic). β titanium alloys contain a balance of β stabilizers to α stabilizers which is sufficient to ensure that fully β phase microstructure can be retained on fast cooling. In contrast, slow cooling in a furnace, for instance, causes β phase decomposition. The microstructure of titanium alloys is mainly dependant on the thermo-mechanical processing and can be manipulated by suitable heat treatment such as a duplex heat treatment, solution treatment and ageing for intended applications. Generally, an $\alpha+\beta$ alloy is preferable due to its attribute of being heat treatable, and formable by forging. $\alpha+\beta$ alloys have higher strength and higher toughness.

2.3.6 Ti-6Al-4V Microstructure

Microstructure refers to the phases and grain structure present in a metallic component. Ti6Al4V is an $\alpha+\beta$ alloy containing 6 wt % of Al and 4 wt % of Vanadium. This titanium alloy is formed when a blend of alpha favouring (*Aluminium*) and beta favouring (*Vanadium*) alloy elements is added to titanium. A wide variety of microstructure can be generated in alpha-beta alloys by adjusting the thermo-mechanical processing parameters. The transformation of an alpha structure to beta structure upon heating is complete if the heating temperature goes above the β -transus temperature. Upon the subsequent cooling, the beta structure will change back to alpha with a small amount of Beta

(depends on the quantity of β -stabilizers elements) as untransformed beta at room temperature. The alpha phase present during cooling, which is primary alpha, can remain relatively globular (equiaxed), however the transformed beta (martensite or alpha) can be very acicular or elongated. The amount of alpha phase and the fineness or coarseness of this final microstructure will affect the behaviour of this titanium alloy (M.Donachie, 2000; W. Sha & S. Malinov, 2009).

2.3.7 The Advantages of Titanium alloys

The application of titanium alloys has expanded from the aerospace industry, automotive to the medical industry. Although the materials themselves are considered to be expensive materials, the physical properties are desirable for high end products and under elevated temperature conditions. The mechanical properties such as strength, ductility, creep resistance, fracture toughness and crack propagation resistance depend essentially on the microstructure, which is formed during thermo-mechanical processing and thermal treatment procedures. The main advantages of titanium alloys are;

1. Higher strength to weight ratios.
2. Low densities, which fall between aluminium and iron and give attractive strength to weight ratios allowing lighter and stronger structure.
3. Superior corrosion and erosion resistance in many environments, in particular to pitting and stress corrosion cracking.
4. High temperature capability in the range of 300-400°C.
5. High toughness, which is useful for making precision mechanism gears, turbine engine components and biomedical prosthesis devices.

2.3.8 Basic Principle of Heat Treatment

Heat treatment of Titanium alloys is designed for many purposes;

- a. Stress relieving – to remove residual stress after a heat treatment process, laser forming or machining process.
- b. Annealing – to produce an acceptable microstructure coupled with desired properties to enhance the manufacturability and service life.
- c. Solution treatment or ageing – to optimize strength, ductility, fracture toughness, fatigue strength, creep resistance for the intended application.

As shown above there are specific reasons for the heat treatment process. Parts are directly heat treated in order to remove the residual stresses after a fabrication process. For titanium alloys, the β transus temperature and the alloying elements are the main consideration for the selection of heat treatment process parameters. Different heat treatment parameters will cause different types of microstructure and cater for different applications. Therefore a detailed understanding of the $\alpha - \beta - \alpha$ transformation during heating and subsequent cooling can lead to optimum microstructures for a given applications.

Heat treatment is the process used to alter an alloy's microstructure. The process aims to control the size and ratio of the α lamellar phase, optimise use the α to β phase ratio and control the morphology of the β phase. Hot deformation of the Ti6Al4V alloy in the β phase field results in relatively large prior β grains. The α phase is formed during cooling and martensite may be formed on rapid quenching. When processing in the $\alpha+\beta$ phase field, a much finer $\alpha+\beta$ structure can be obtained, because the primary α phase limits the growth of the β phase. When processing in the β phase region, the microstructural evolution may include mechanical deformation of the equiaxed β grains and possible dynamic or metadynamic recrystallization during processing and during the β to α phase transformation when cooling after deformation.

Heat treatment designation	Heat treatment cycle	Microstructure
Duplex annealed	Solution treat at 50-75C below T_{β} , air cool and age for 2-8 hours at 540-675C	Primary α plus widmanstatten $\alpha+\beta$ regions
Solution treat and age (STA)	Solution treat at 40C below T_{β} , water quench and age for 2-8hours at 535-675C	Primary α plus tempered α' or a $\alpha+\beta$ mixture
Beta anneal (BA)	Solution treat at 15C above T_{β} , air cool and stabilize at 650C-760C for 2hour	Widmanstatten $\alpha+\beta$ colony microstructure
Beta quench	Solution treat at 15C above T_{β} , water quench and temper at 650-760C for 2hours	Tempered α'
Recrystallization anneal (RA)	925C for 4hours cool at 50C per hour to 760, air cool	Equiaxed α with β at grain boundary triple points
Mill anneal	$\alpha+\beta$ hot work, anneal at 750C for 30min to several hours and air cool	Incomplete recrystallized α with small volume fraction of small β particles

Table 2.2: Heat treatment for Titanium alloys and the microstructure, *source; M.Donachie, (2000)*

Microstructure Evolution

Heat treatment is normally carried out for α/β or β alloys because the α alloys show only little response to heat treatment. Notably, the alloy content of a particular alloy is crucial and reflects the output microstructure and grain morphology. At different temperatures, different amounts of α and β phases are in equilibrium and during slow cooling, the α phase can be precipitated at different stages (temperatures). The α phase precipitated at different temperatures has a different morphology e.g. finer lamellae are attributed to lower temperature of transformation. For Ti6Al4V, the composition after

different heat treatments is mainly α phase with a small amount of β phase in the annealed condition.

The β transus temperature is crucial for heat treatment processes especially when designated heat treatment is slightly below or above the transus temperature. As for the solution treatment of $\alpha+\beta$, it generally involves heating either slightly above or slightly below the β transus temperature. This increases the amount of β phase present in the material, which then transforms back to the α phase on cooling. Notably, the dominant mechanism during the transformation is the cooling rate. At slower cooling rates nucleation and growth occurs via the Widmanstätten process. Rapid cooling rates give a martensitic microstructure. The differences in microstructure are reflected to the mechanical properties of the parts (Tim Sercombe et al, 2008).

Chapter 3: Direct Metal Laser Sintering Machine

Layer manufacturing techniques have evolved from Rapid Prototyping through to Rapid Tooling and Rapid Manufacturing. This transition moves rapidly due to significant improvements in the powder technologies and sophisticated RP systems. Nowadays, SLS is the leading commercial RPM system in the market due to its material's versatility. The introduction of smaller spherical particle size, through gas atomization technique and a higher absorption of laser beam has contributed to a better quality and sound mechanical properties. K. Abdel Ghany & S.F Moustafa (2006), investigated four different RPM systems prior to direct metal fabrication. Suman et al, (1998) reported the use of DMLS coupled with post treatments such as Hot Isostatic Pressing (HIP) and produced material with comparable mechanical properties to Ti6Al4V manufactured conventionally. The feasibility of producing direct metal parts by laser sintering has been demonstrated using various RM systems;

1. A.Simchi et al (2006) investigated densification of the iron powder during the laser sintering process. He reported the influence of specific energy input on the densification mechanism.
2. Jialin Yang et al (2009) successfully developed a low power, direct metal laser sintering machine for Cu-based and 316 metallic powder.
3. H.H Zhu et al (2005) showed the microstructural evolution in direct laser sintering of Cu based powder.

3.1.1 Background of Direct Metal Laser Sintering

A layer manufacturing technique was introduced by Ciroud in 1971. Housholder later described the process of SLS and SLM and patented it in 1977. However, these ideas were not really ready to put into the market due to lack of high end computers and expensive laser systems at that time. In 1992, Deckard from the University of Texas, Austin produced a DTM machine under the principle of SLS. DTM was acquired by 3-D systems in 2001. EOS GmbH Optical system introduced its first direct metal fabrication machine in 1994 in collaboration with Electrolux.

A year after, a company known as MCP Tooling Technologies successfully developed an RP machine called MCP Realizer. This machine used a selective laser melting principle (SLM) in order to directly manufacture metal parts. In 2004, EOS acquired the right of all the patents under DTM, University of Texas and 3-D system on the use of laser sintering.

This additive technology principle has grown rapidly. The manufacturers' are competing to be the first to introduce the highest quality metal parts with attractive mechanical properties using a huge spectrum of process-able materials. Wohlers report in 2001 showed that the RP industry is experiencing unprecedented growth in revenues and unit sales. The reported sale is \$395 millions in USA and \$425 millions in all other countries [www.wohlersassociates.com]. As the demand on RP machines increased, Optomec in partnership with Sandia National Laboratories introduced the laser engineering net shape (LENS) process. This uses the evolving technique of 'powder in bed' principle to powder injection for metal fabrication. This research project earlier developed by Westinghouse Corp in collaboration with Sandia National laboratories filed for a patent application in the 1990s. This system, was further developed by Arcella at the University of Justin allows the fabrication of complex metal parts using titanium alloys and steel. In 2003, TRUMPF introduced two new machines based on SLM and 3D laser cladding. TRUMPF holds the rights for direct laser fabrication of metal (powder in bed) and fully melting of single components [www.trumpf.com]. In this chapter, SLS, SLM and 3D Cladding systems were described for direct metal fabrication. There are other RPM systems that can directly build metal parts which are not discussed in this work;

1. Brian K. Paul et al (2001) reported the use of a Laminated Object Manufacturing technique for direct metal fabrication.
2. Luca Fachini (2009), Ola. LA Harryson et al (2008) investigated the mechanical properties and microstructure of a Ti6Al4V alloy and pure titanium produced by electron beam melting.
3. Thomas Himmer et al (2008) studied the multiple laser processing for the development of direct metal tooling fabrication.

Machines	Company	Process	Laser	Power
Sinterstation 2000/2500	DTM	DMLS	CO ₂	50W
EOSINT 250	EOS	DMLS	CO ₂	200W
EOSINT 270	EOS	DMLS	Ytterbium fibre laser	200W
LUMEX 25C	MATSUURA	SLM	Pulsed CO ₂	500W
TrumaForm LF 250	TRUMPF	SLM	Disc Laser	250W
Realizer	MCP	SLM	Nd:YAG	100W
Lastform	Aeromet	3D Laser Cladding	CO ₂	10-18kW
LENS 850	Optomec	3D Laser Cladding	Nd:YAG	1kW
Trumaform DMD 505	TRUMPF	3D Laser Cladding	CO ₂	2-6kW

Table 3.1: Commercially available RM machines, *source; Edson Costa Santos et al (2006)*

3.2.0 Classification of Direct Metal Laser Sintering Systems

The classification of DMLS systems is based on Levy et al (2003). According to Levy, DMLS can be classified into partially melting and fully melting processes.

The methods are given below;

- a. Selective laser sintering and laser micro sintering (partially melting, powder in bed)
- b. Selective laser melting (full melting, powder in bed)
- c. 3D cladding (full melting, powder injection via nozzles)

There are three types of materials currently used for the DMLS process, such as single component powders, pre-alloyed powders and mixtures of low melting point powder with high melting point powders. For SLS, post treatments such as infiltration or HIP are normally required to further improve the part density. Direct fabrication of metal parts through SLS normally produces part density in a range of 45% to 85% of the theoretical density. In contrast, SLM has been shown to successfully produce nearly 99.8% of metal parts without any post treatments.

This is because the method achieved full melting of powder particles during fabrication.

Direct metal fabrication, through laser sintering, is capable of producing good metal parts if the raw materials, powder characteristics and the process parameters are well selected. The aim is to have the following properties;

- High strength – according to the required application.
- High density (not less than 95%), low porosity.
- Homogenous, coherent and crack free microstructure.
- Controlled low thermal expansion coefficient and low thermal shrinkage during thermal process (<1%).
- Low melting temperature, which is important for saving the laser energy required to melt the metallic powders (most RM systems use compact laser sources between 50 and 300W depending on the application) and also speed up the joining process (reduces time and cost)

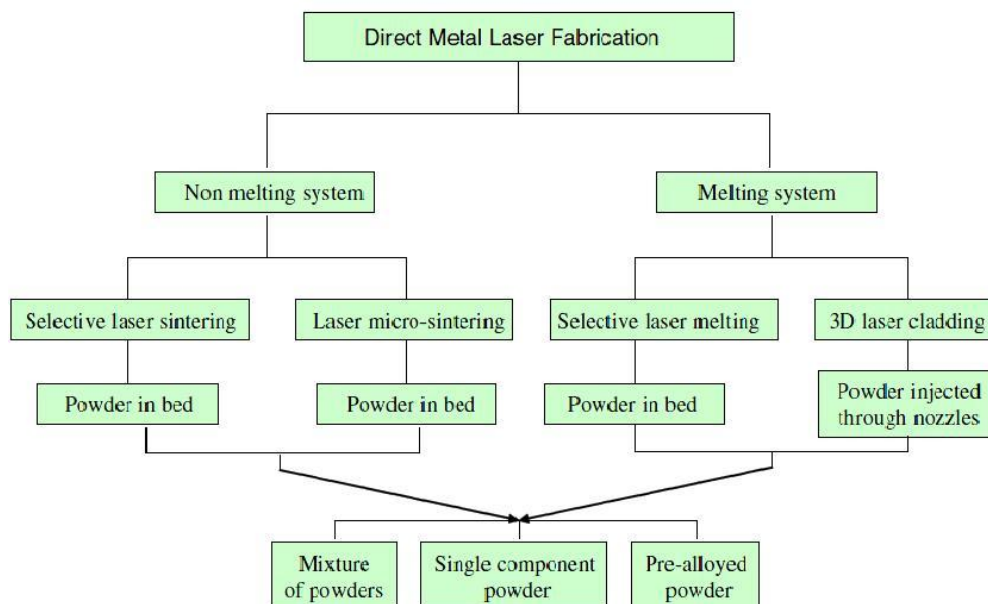


Figure 3.1: The classification of DMLF methods, source; *E.C Santos et al (2006)*

Figure 3.1 shows the classification of direct metal laser fabrication systems based on the binding mechanism. 3D laser cladding uses injected powder instead of a powder deposition technique. All of these techniques are capable of processing elemental, mixtures and pre-alloyed powder.

Direct metal laser fabrication systems can be divided into three main categories as shown below;

1. ***Selective Laser Sintering (partially melting).***
2. ***Selective laser Melting (full melting).***
3. ***3D Cladding (full melting).***

The similarity of the above systems is the use of a laser as the heat source. The systems can be further divided, based on the materials that can be processed (powder, foil or wire). Different manufacturers have come up with different types of sintering or melting systems with various types of materials. Each machine has its own ultimate objective such as process accuracy and processable materials. However, this technology is still new and is rapidly improving in performance (Lino Costa, 2009). For those systems that are not equally advanced, further studies were needed in order to choose a suitable system for an intended application. To cater the requirements of the motor industry, Sebastian Storch, et al (2003), used SLS technology for direct metal parts fabrication. They discovered that the material exhibited brittle behaviour depending on the build direction. Mahesh et al, (2004) proposed a geometric benchmark to further evaluate different RP processes for metal parts. Abdel Ghany & Moustafa (2006) investigated four RPM systems for direct metal fabrication to help users select the appropriate systems for their application.

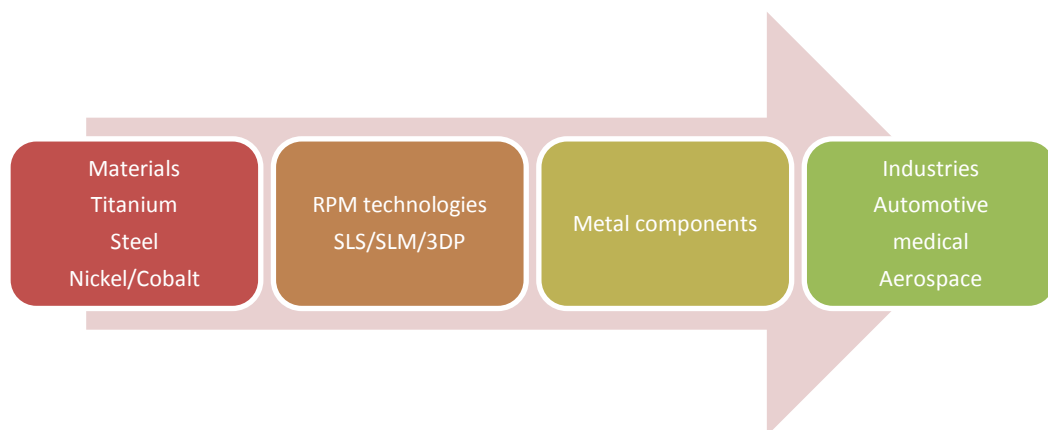


Figure 3.2 Schematic representation of DMLS Processes, source; M.Agarwala et al(1995), P.A Kobryn & S.L Semiatin,(2001), T.Laoui et al (2004)

3.2.1 DMLS based on SLS system

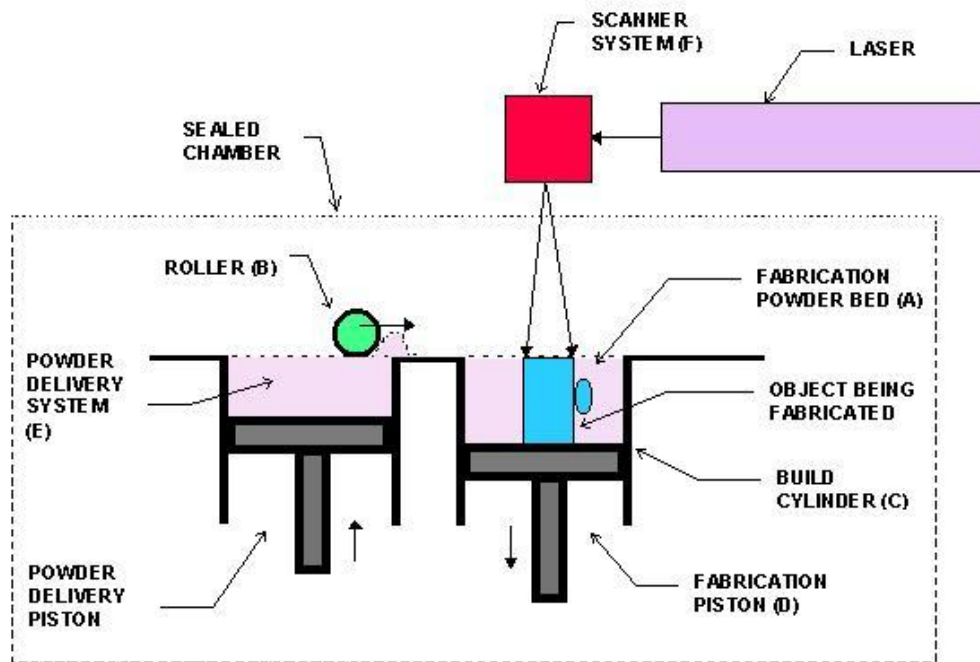


Figure 3.3: Schematic representation of SLS process; *Source E.C Santos et al (2006)*

Figure 3.3 shows a schematic illustration of SLS. A roller type feeding system is used to first place a thin layer of powder onto the part build area. Both the powder delivery system and the powder build area are attached to a piston for height adjustment. The piston is lowered according to the pre-set layer thickness after every successive layers of powder deposition. The scanner system equipped with galvano mirrors produces the laser beam and is scanned onto the powder bed to consolidate the powder layers.

The powder in other areas, which is not sintered, remains loose and acts as a support. Then the building area drops one layer thickness (typically 0.02 – 0.1mm) and another layer of thin powders is deposited. The cycle is repeated until the solid part is completed. The whole process is shielded from oxidation by using an inert gas such as argon or nitrogen. This SLS processes can be further divided into single component and two components' part building.

In the case of a single component, liquid phase sintering happens as a result of surface melting of the particles and liquid flow. For two components or mixed components, the powder with the lower melting point (normally organic) is

melted and acts as the binder. Infiltration is required to achieve full density parts. Suman Das et al (1998) demonstrated the production of metal parts using SLS coupled with Hot Isostatic Pressing (HIP) to improve part densities.

A lot of research has been done to demonstrate the use of SLS for direct metal fabrication.

1. Agarwala et al (1995), discussed the SLS of a bronze-nickel powder mixture in greater detail. They emphasised that SLS is not only capable of producing accurate prototype models from polymers and plastic but can be used to directly produce structurally good metal parts.
2. A. Simchi and H. Pohl, (2003) successfully investigated the SLS processing parameters with iron powder. Simchi in his other works described the liquid phase sintering of multi-component iron based powder for Rapid Tooling applications.
3. T. Traini et al (2008) reported that the direct metal laser sintering technique can efficiently build porous titanium dental implants. He highlighted that DMLS proved to be an efficient means of construction of dental implants with functionally graded material.
4. S.R Pogson et al (2003) demonstrated the SLS process to fuse copper powders with a stainless steel substrate. Processing with a continuous wave laser beam at the maximum power of 76W produced the best results. With a laser in pulsed mode using a low pulse rate, resulted in vaporisation of the powder.
5. P. Fischer et al (2005) described the effect of using a highly pulsed laser beam to sinter pure titanium powders. In this study, the energy exchange in SLS has been described in terms of the coupling between the laser and material. A numerical simulation of the heat flow equation was performed and the process densification corresponding to different energy intensities was mapped.

3.2.2 DMLF based on SLM

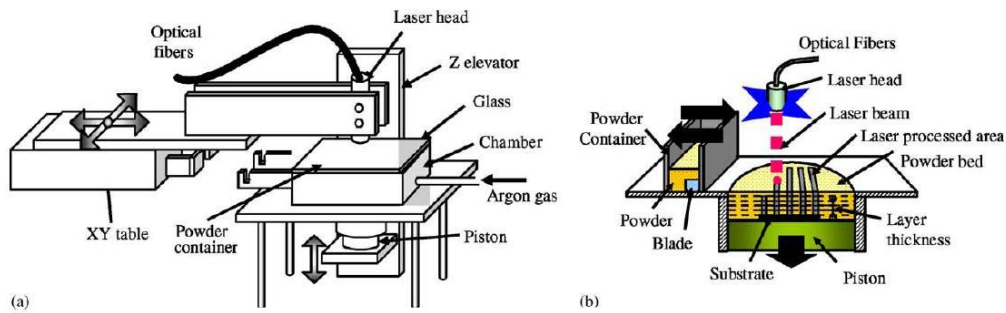


Figure 3.4 Selective Laser Melting, source; E.C Santos et al, (2006)

Obviously SLM is very similar to SLS in terms of equipment but uses a much higher energy density. This is because SLM fully melts the powders to enable higher part densities. A Nd:YAG laser of maximum peak power of 3kW and maximum average power of 50W is used. An optical fibre is used to guide the laser beam. A small and focused laser beam can be produced using this setting (typically 0.8mm beam diameter). A laser head is attached to the x-y table, which is controlled by a high end computer. A steel substrate is attached to a piston, which moves down one layer thickness of 0.05 to 0.1mm in the z direction. The process is carried out in a closed chamber and argon is flushed continuously in order to minimize the level of oxygen and nitrogen.

This system is commercially used for processing aluminium, bronze, steel and pure titanium powders. Vandenbroucke and Kruth (2007) found out that SLM is capable of directly producing metal parts with densities up to 99.98% for titanium using optimised process parameters. Strength, stiffness, corrosion behaviour and process accuracy fulfil the requirements for medical and dental implants. Matthew Wong et al (2007) fabricated the heat sink devices from aluminium via SLM which evidently proved to be more feasible and efficient. A full melting process can be attained by SLM to produce fully dense parts, but without proper process control, the parts will have high internal stresses and poor surface finish. This is due to high temperature gradients during processing. The risk of having 'balling' and dross formation in the melt pool may lead to high surface roughness. The benefits and drawbacks of this system are given in table 3.3.

full melting	Benefits	Drawbacks
<ul style="list-style-type: none"> • Material choice • Production steps (time, cost) • Part Quality 	<ul style="list-style-type: none"> • No distinct binder and melt phases • No post processing for debinding • Capable of directly produce 99.9% part densities 	<ul style="list-style-type: none"> • Not suited for well controlled composite materials • Higher laser processing energy • Melt pool instabilities

Table 3.2: Benefits and drawbacks of SLM process, *source; EC Santos et al (2006)*

Obviously, SLM benefits through having full melting of powder particles. This leads to near full density and eliminates the after processing treatment. However, it requires a highly focussed laser energy to ensure that powder particles melt during fast laser beam scanning. Higher laser processing energy increases the temperature gradient and affects the melt pool stability. Some of the literature is given below;

1. Peter Mercelis and JP Kruth (2006) presented the effect of residual stresses during SLM and SLS. SLM demonstrated higher residual stresses compared to SLS. The crucial factors affecting the magnitude and shape of residual stresses are material properties, laser scanning strategy and heating conditions.
2. Matthew Wong et al (2007) illustrated the heat sink devices produced by the SLM process. Aluminium 6061 was used with the SLM method to fabricate complex fin shapes and sizes for better performance of heat sink devices.
3. Maarten Van Elsen et al (2008) presented a dimensionless parameter to describe the SLM process. This work helped to develop a manageable system to describe the intricate process of SLM and a technique to differentiate the influence of process parameters.

3.2.3 DMLF through 3D Cladding

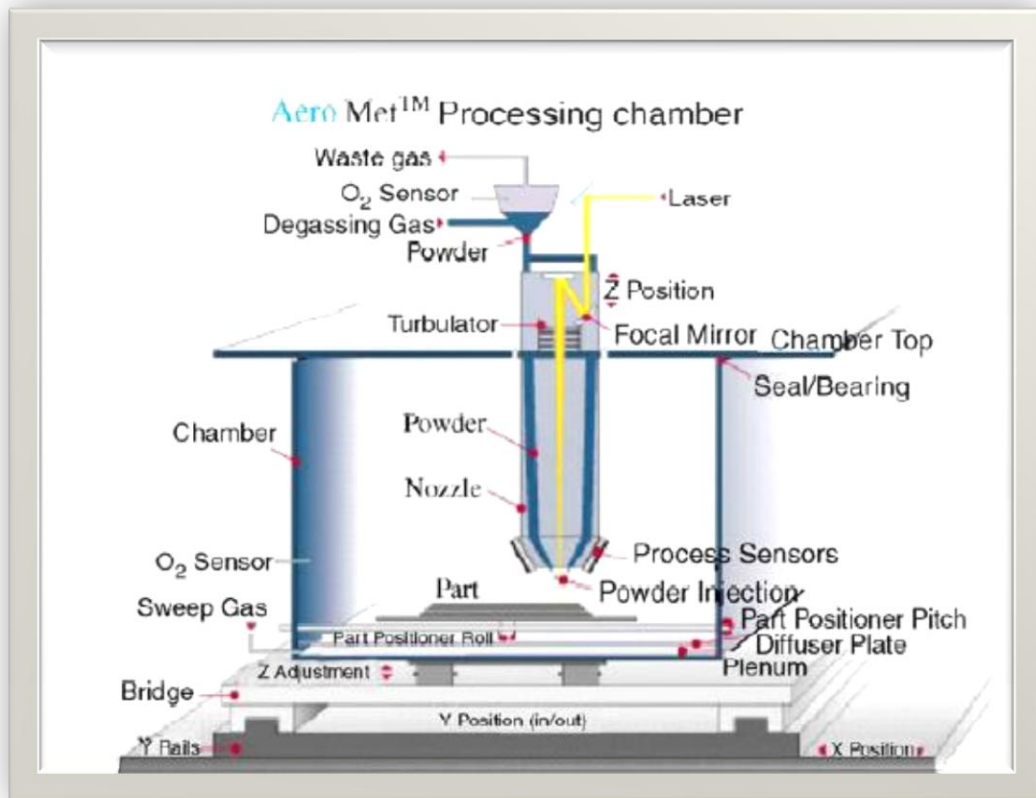


Figure 3.5: Schematic illustration of 3D Cladding mechanism, *source ; J. Zhao et al (2009)*

3D Cladding or Laser Engineered Net Shaping (LENS) was developed at the Sandia National Laboratories and was commercialised by the Optomec Design Company of Albuquerque, New Mexico. The energy source is usually a laser beam with a coaxial or lateral delivery system of metal powders or metal wire. The distinct difference between this system and the system mentioned before is in the powder feeding system. Instead of fusing material in a powder bed, the 3D - Cladding technique jets the powder through nozzles. The powder is usually delivered coaxially with the laser beam which means perpendicular to the substrate. The powder feeder and the laser beam axis may also form an angle between them which is usually from 0 – 45deg.

The metal powder is fused in the focal zone of a high energy laser beam and parts with complex geometries can be formed. The process occurs in closed chambers with controlled inert atmospheres. The advantage of laser cladding

processes is their ability to produce gradient materials by applying different powder delivery nozzles that allow switching from one material to another. Another unique feature is the capability of allowing real time mixing of elemental constituents across the geometry. Research has been undertaken to test this technique, as shown below;

1. Jing Zhao et al (2009) investigated LENS capability by producing metal thick wall parts from nickel based alloy powders. Thick wall metal parts with thickness ranging from 20 to 25mm were successfully fabricated. The laser used in this experiment was a cross-flow CO₂ laser machine. Some limitations of this study were the formation of oxide layers which led to porosity and tearing during the laser sintering process.
2. Fude Wang et al (2006) studied the microstructure of parts fabricated by LENS. Two types of feedstock were fed simultaneously into the laser focal point, a burn resistant (BurTi) alloy powder and Ti-6Al-4V wire. The laser used was a ROFIN SINAR TRIAGON 1750W CO₂ laser. The results presented have shown that the use of wire as one of the feedstock materials is a practical way for the manufacture of functionally graded alloys.

3.3.0 Laser Technology

One of the important parameters in a Direct Metal Laser fabrication machine is the heat source and it is usually a laser beam. A greater understanding of the short interaction of the laser irradiation with the metallic powders will lead to better process optimisation. Different kinds of lasers are applied in laser consolidation systems. The choice of a proper SLS laser might not be independent of the material to be sintered. Process parameters such as laser characteristic (energy, type, speed, focus, and spacing) and powder characteristic (particle size, shape, distribution, powder composition) greatly influence the part properties (J.D Williams & Deckard, 1998). Kruth et al (2003) investigated the influence of laser absorption upon different types of materials. He reported that

SLS process is not only controlled by the amount and speed of energy supply but to a great extent by the basic laser-material selection.

Metallic Powder materials	Nd:YAG $\lambda = 1.06 \mu\text{m}$	CO ₂ $\lambda = 10.6 \mu\text{m}$
<ul style="list-style-type: none"> •Cu (absorption in solid Cu) •Fe (absorption in solid Fe) •Sn •Ti •Pb •Co alloy(1% C, 28%Cr,4% W) •Cu-alloy (10% Al) •Nickel Alloy I (13% Cr,3% B,4% Si, 0.6% C) •Nickel Alloy II (15% Cr,3.1% Si,0.8% C) 	<ul style="list-style-type: none"> •0.59 •0.64 •0.66 •0.77 •0.79 •0.58 •0.63 •0.64 •0.72 	<ul style="list-style-type: none"> •0.26 •0.45 •0.23 •0.59 •0.25 •0.32 •0.42 •0.51

Table 3.3 Absorptance of single component powders measured with two different lasers, *Source; N. Tolockho et al (2000)*

The types of lasers used for consolidation depend on the material being processed. Notably, table 3.3 shows that metals absorb better at shorter wavelength which is Nd:YAG with a wavelength of 1.06 μm . The absorptance measured for the metallic powders shown above at 1.06 μm is 1.5-2.5 times greater than that measured at 10.6 μm .

3.3.1 Laser Influences in processing Parameters

Process parameters are the pre-defined values that control the consolidation of the metallic powders during the SLS process (J.D Williams & Deckard, 1998). The mechanical properties and geometrical output of the laser sintered parts are all influenced by the quantity of energy delivered to the metallic powders. The influence of the laser on the consolidation process is shown below (J.P Kruth et al, 2004; Nikolay et al, 2000);

- a. Laser absorption of various materials greatly depends on the laser wavelength: there is high absorption by metals at the $\pm 1\mu\text{m}$ wavelength of a Nd:YAG fibre and disc laser
- b. The possible consolidation mechanism is highly dependent on features such as energy density : high beam quality and high focus-ability easily achieved by fibre and disc lasers
- c. Laser mode : continuous, pulsed or Q-switched

There are two types of laser used in the direct metal laser fabrication technique: CO₂ and Nd:YAG. The main difference between these two lasers is the wavelength. CO₂ lasers have longer wavelength which is 10.6 μm compared to Nd:YAG lasers which have a wavelength of 1.06 μm . For metals, the absorption of the laser energy is greater at shorter wavelength. Higher absorption leads to greater energy density and lower power requirement, thus the use of Nd:YAG is preferable for metals compared to CO₂. Another advantage of an Nd:YAG laser is the possibility of using an optical fibre to guide the beam.

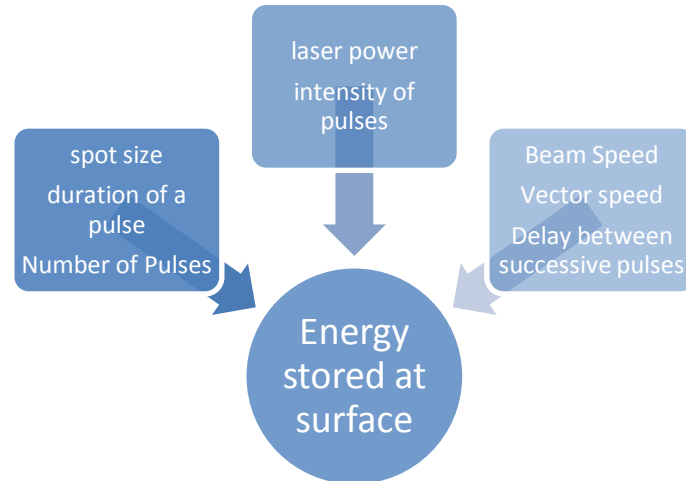


Figure 3.6: Influence of the laser parameters, Source; J.D Williams & Deckard (1995)

Several comparisons have been made in order to justify the advantages of using a Nd:YAG laser compared to CO₂. A research team at the University of Lueven, Belgium used Fe – C and WC powders for laser sintering using both type of laser at the same laser energy. They reported that Nd:YAG resulted in a higher density, a deeper sintering depth and a larger processing window (G.N Levy et al, 2003).

At Osaka University, a pulsed Nd:YAG laser with a maximum peak power of 3kW and maximum average power of 50W was applied for fabrication of metal parts made of nickel, aluminium, steel, bronze and titanium with full success (J.P Kruth et al, 2007). The comparison is not limited to the types of laser but also extent to the laser mode, either pulsed or continuous mode of Nd:YAG lasers. Results showed that by using pulsed lasers, very good metallurgical bonding between the tracks and layers is obtained with a smaller heat-affected zone by the high pulse energy in a short pulsed length (R. Morgan et al, 2001). It was also mentioned that the depth of penetration should be similar to the layer thickness for good inter-layer bonding. The only machine equipped with a milliseconds-pulsed laser in the market is the LUMEX 25C from MATSUURA. Even the Nd:YAG laser shows a significant improvement in producing better interaction with metal powders, most of the commercially available machine are still using a CO₂ laser. This is perhaps because CO₂ lasers have higher efficiency, are cheaper and require lower maintenance compared to Nd:YAG. The future trends of this laser technology are to provide greater beam quality and be more cost effective for metal fabrication process.

The research work carried out to investigate laser process parameters is summarized below;

1. R Morgan et al (2001) described the effects of the major process variables (Q-switch pulse frequency, laser power, scan speed, scan spacing and scan length) on the production of single layer coupons. He reported that greater scan speeds and spacing enabled faster processing times.
2. H.H Zhu et al (2005) identified the effects of laser scan speed and scan spacing on the surface morphology, microstructure and structure evolution in direct laser sintering of Cu-based metal powder. The result showed that a decrease in the scan speed and scan spacing leads to densification due to solute reprecipitation mechanisms. During laser sintering, concentration diffusion acts as the main mechanism at a fast scan speed and a large scan spacing while solute-reprecipitation acts as the main mechanism at a low scan speed and small scan spacing.

3. A. Simchi (2006) investigated the effects of the energy delivered by the laser onto the metallic powders. It was found that as the laser energy input increases (higher laser power, lower scan rate and scan spacing, lower layer thickness) better densification is achieved. Nevertheless, there is a saturation level in the laser energy which prevents a further density increase.

3.3.2 DMLS Crucial Processing parameters

There are four factors in DMLS process parameters that mainly influence the laser-material interaction. These parameters affect the consolidation of object produced by the SLS process. Good pre-defined process parameters lead to good geometrical and mechanical results. The influence of the process parameters on the consolidation process is given below;

- a. Laser power– energy supplied by the laser beam to a volumetric unit of powder materials. Higher energy density will cause a greater temperature gradient and affect the melt pool stability. This will lead to parts with higher residual stresses. Four factors that determine the energy density are laser power, scan speed, scan spacing and layer thickness
- b. Scan speed – the speed by which the laser beam scans over the powder bed during laser sintering. The higher the value of scan speed, the less time the laser beam will get to interact with the powder bed thus causing less heat for melting and subsequently sintering of the powders. At the other extreme, lower values of scan speed will decrease the production speed
- c. Scan spacing – distance between two consecutive laser scan tracks on the powder bed surface. A higher value of scan spacing will not allow all the powder area between the successive scan tracks to be sintered by the laser beam. A narrow value of scan spacing will make some powder areas over exposed to the laser beam.
- d. Layer thickness – the thickness of successive layers of the powder bed. A higher value of layer thickness does not allow enough laser energy to

spread through the top layer and into the supporting under layer, to ensure good bonding between the successive layers. With a small thickness there is concern that the powder layer will not be able to remain uniform during its deposition. Smaller layer thickness also increases the build time significantly and negates the rapidity of Rapid Prototyping.

3.3.2 EOSINT M 270 Machine

Electrical Optical System (EOS) launched EOSINT M250 in 1994 for direct metal fabrication and a year later introduced EOSINT M 270 with a better technical specification. In 1997, EOS sold its Stereos product to 3D systems and in return they acquired an exclusive worldwide license to all patents owned by 3D systems for use in laser sintering application. EOS is one of the icon manufacturers in producing laser sintering machines. The EOSINT M 270 uses a Direct Metal Laser Sintering (DMLS) technique to produce solid metal parts. The technology consolidates the metal powders individually according to the CAD data. The machine is specifically developed to build metal parts additively layer by layer. A fibre type laser with a highly focused beam is used to fully melt the metal powders. EOS also claim that the sintering process is not similar to conventional sintering. Conventional sintering is defines as 'the use of pressure and heat below the melting point to bond and partly fuse masses of metal particles, or to be bonded in this way' (www.eos.info).

The EOS M system uses a laser directed by an f-theta lens based optics system to melt the material particles typically in the order of 0.02mm in size with the focussed laser beam. Depending on the powder material used, either the entire powder is melted and re-solidified, or certain metallic components melt and bond to the others via a liquid phase sintering. The powder deposition system is described as using a single chamber with a rigid re-coater blade. A thin layer typically between 0.02 and 0.1mm thick, depending on the pre-set layer thickness parameter, is deposited on the top of the build area.



Figure 3.7: EOS GmbH M270 Machine, *source; (www.eos.info)*

3.3.3 EOSINT M 270 technical specification

Electrical Optical Systems (EOS) produce two types of direct metal laser fabrication machine. These are EOSINT M250 and EOSINT M270. There are two main differences between these two machines in terms of the type of laser and the way it operates. Generally, EOSINT M 270 has slightly a bigger build chamber which is 250mm x 250mm x 215mm. It uses a solid state fibre laser with a spot size that can be varied between 0.1 and 0.5mm thus providing a controllable scanning strategy. With the variable diameter spot, the M 270 can adjust the scanning according to the details required. The smallest spot setting is used for greater detail and larger spot setting for scanning a large area. In addition, the M 270 has a protective build chamber to give a high purity environment, thereby making it possible to process a wide range of materials including reactive metals [www.mcad.com].

The build speed is one of the important factors that makes the M270 worthwhile. It has a build speed which varies from 2 to 20mm³/s. However, the sintering time still depends on the material being processed and the selected layer

thickness. The type of materials to be sintered, absorptivity, powder particle size and distribution are amongst the critical parameters that contribute to the machine parameter setting. The layer thickness can be varied between 0.02 and 0.1 mm, the smaller layers producing finer surface quality and detail resolution but longer build times.

The M 270 processing software has the advantage of offering a varied scanning strategy. The software provides two types of scanning strategy which are Skin and Core. Skin refers to the outer shell of part while Core refers to the inner part. As the part can be divided into two portions, the set-up software allows a user to define different parameters such as layer thickness and scan speed according to the area. This will speed up the processing time by optimizing the machine's parameters for each region.

Technical Data

<i>Effective building volume (including building platform)</i>	<i>250 mm x 250 mm x 215 mm (9.85 x 9.85 x 8.5 in.)</i>
<i>Building speed (material-dependent)</i>	<i>2 - 20 mm³/s (0.0001 - 0.001 in³/sec.)</i>
<i>Layer thickness (material-dependent)</i>	<i>20 - 100 μm (0.001 - 0.004 in.)</i>
<i>Laser type</i>	<i>Yb-fibre laser, 200 W</i>
<i>Precision optics</i>	<i>F-theta-lens, high-speed scanner</i>
<i>Scan speed</i>	<i>up to 7.0 m/s (23 ft./sec.)</i>
<i>Variable focus diameter</i>	<i>100 - 500 μm (0.004 - 0.02 in.)</i>
<i>Power supply</i>	<i>32 A</i>
<i>Power consumption</i>	<i>maximum 5.5 kW</i>
<i>Nitrogen generator</i>	<i>standard</i>
<i>Compressed air supply</i>	<i>7,000 hPa; 20 m³/h (102 psi; 26.2 yd³/h.)</i>
Dimensions (B x D x H)	
<i>System</i>	<i>2,000 mm x 1,050 mm x 1,940 mm (78.8 x 41.4 x 76.4 in.)</i>
<i>Recommended installation space</i>	<i>approx. 3.5 m x 3.6 m x 2.5 m (137.9 x 141.8 x 100 in.)</i>
<i>Weight</i>	<i>approx. 1,130 kg (2,491 lb.)</i>
Data preparation	
<i>PC</i>	<i>current Windows operating system</i>
<i>Software</i>	<i>EOS RP Tools; Magics RP (Materialise)</i>
<i>CAD interface</i>	<i>STL. Optional: converter for all standard formats</i>
<i>Network</i>	<i>Ethernet</i>
Certification	<i>CE, NFPA</i>

Status 12/05. Technical data subject to change without notice. EOS®, EOSINT®, DMLS®, DirectTool®, DirectPart® and e-Manufacturing™ are registered trademarks of EOS GmbH. Windows is a registered trademark of Microsoft Corporation. EOS is certified according to ISO 9001.

Figure 3.8: Technical data for EOS GmbH M270 Machines, Source; (www.eos.info)

3.3.4 EOS Direct Metal Laser Sintering Materials

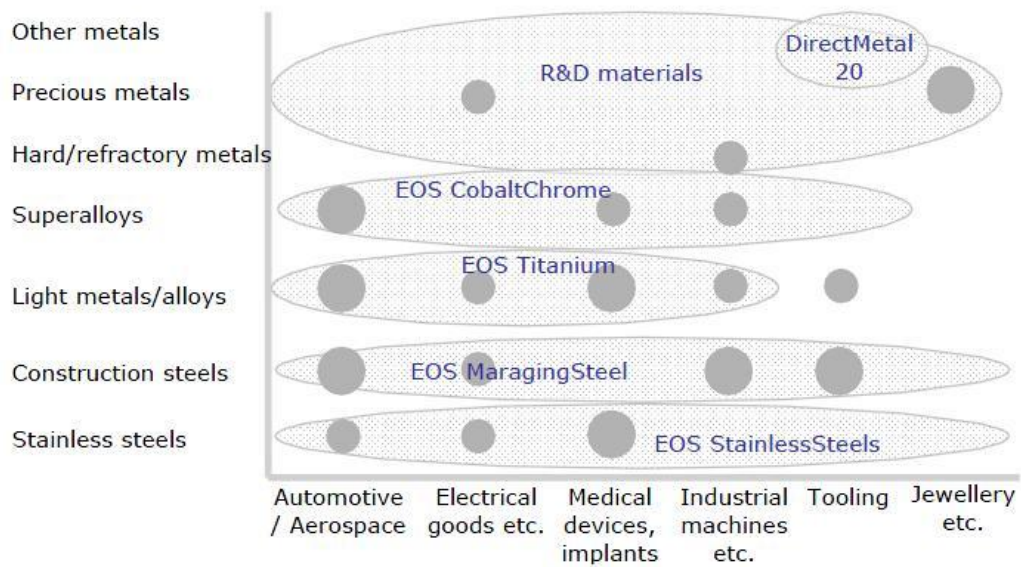


Figure 3.9: EOS Direct Metal Laser Sintering range of materials, *source; (www.eos.info)*

As in figure 3.9, EOS produces a wide range of materials for various applications. The materials are meant for commercial purpose and have been tested extensively. The materials that can be processed are stainless steel, Cobalt Chrome, Maraging steel, titanium and a non standard material developed by EOS. For the medical and aerospace applications, EOS introduced EOS Ti64 for sintering a pre-alloyed Ti6Al4V alloy. The brochure on Direct Metal Laser Sintering parts in Ti64, claims that the strength and hardness of the laser sintered parts exceed that of forged parts but have slightly lower elongation [www.eos.info]. Also available are an ELI (extra-low interstitial) version of Ti6Al4V and commercially pure titanium.

Chapter 4: Material and Experimental Procedure

4.1 Specimen Preparation

Good and careful specimen preparation is important in order to get better metallographic analysis. During sectioning of specimens excessive deformation and overheating was avoided as both can cause changes in microstructure. In particular, deformation can result in mechanical twinning and internal stress and overheating can change the phase distribution or the phases present.

All specimens were prepared using an EOSINT M 270 Direct Metal Laser Sintering machine. There were three types of specimens;


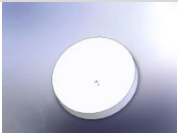
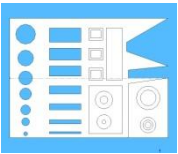
Specimen		Quantity	Experiment
1. Beam Shaped		5	Tensile Testing
2. Disc Shaped		3	Microhardness & Microstructure analysis
3. A block with different CAD features		1	Process Accuracy & Feasibility

Table 4.1: Type and quantity of fabricated specimen

The beam shaped specimens were designed according to the ASTM 8M standards for tensile testing. The beam has an overall length of 200 mm with a reduced section of 50 mm. The disc shaped specimens (25mm x 4mm) were for the microhardness and microstructure analysis. Both disc shaped and beam shaped specimens have a same thickness of 4mm. The third type of specimen was a block with dimensions 30mm x 30mm x 8mm. The block was designed to have different CAD features such as different diameter holes, various sizes of rectangles and sharp angles. This was later used for evaluating process accuracy and a feasibility study.

4.1.1 Specimens Designation

All specimens were given specific label before testing and heat treatment. Photographic images were recorded and specimens were labelled prior to sectioning and designated post heat treatments.

Specimen	Sectioning	Experiment	label	Quantity
Beam Shaped Specimen	As built specimen	Tensile Testing	T1/T2/T3/T4/T 5	5
	T1 tensile specimen used for fracture surface analysis	SEM & EDS	T1FS1 & T1FS2	2
Disc Shaped	As built specimen		D1/D2/D3	3
	D1	OM, SEM	D1CS1/D1SA1	
	D2	Micro-hardness	D2LS	1
	D3	Metallographic analysis -	D3ABST-Q D3BST-AC D3BST-AC - Ageing	1
	D3 3 ultra thin \varnothing 3mm specimens	TEM specimen	D3BST-AC- Ageing -TEM	1
Block		Process Accuracy and feasibility	B1LS	1

Table 4.2: Specimen labelling and corresponding analysis

4.1.2 Specimens Cutting

A sectioning plane was defined prior to metallographic analysis. A cutting machine with a diamond cutter was used for the sectioning. The specimens were then labelled and stored in a plastic container to avoid any contamination.

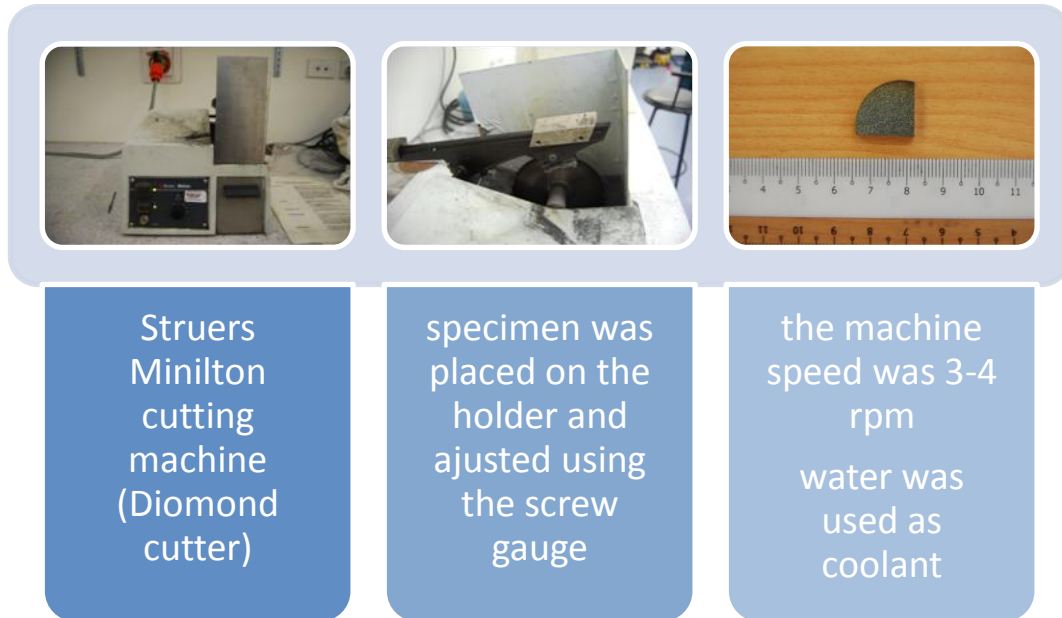


Figure 4.1: Schematic representation of cutting procedure

4.1.3 Specimen mounting

Before polishing for metallographic examination, specimens were mounted as follows:

1. The ratio between the resin and the hardener was 1:4.44. A clean plastic container was used and placed on the digital weight measurement apparatus. The weight of the plastic container was reset as zero
2. Based on the size of the specimens, the height of 15mm was required to fully enclose the specimen. Approximately, 8.88g of resin and 2g of hardener were mixed together for the casting.
3. A specimen was placed on the rubber cup and epoxy resin was poured onto the rubber cup. The specimen was cured overnight.

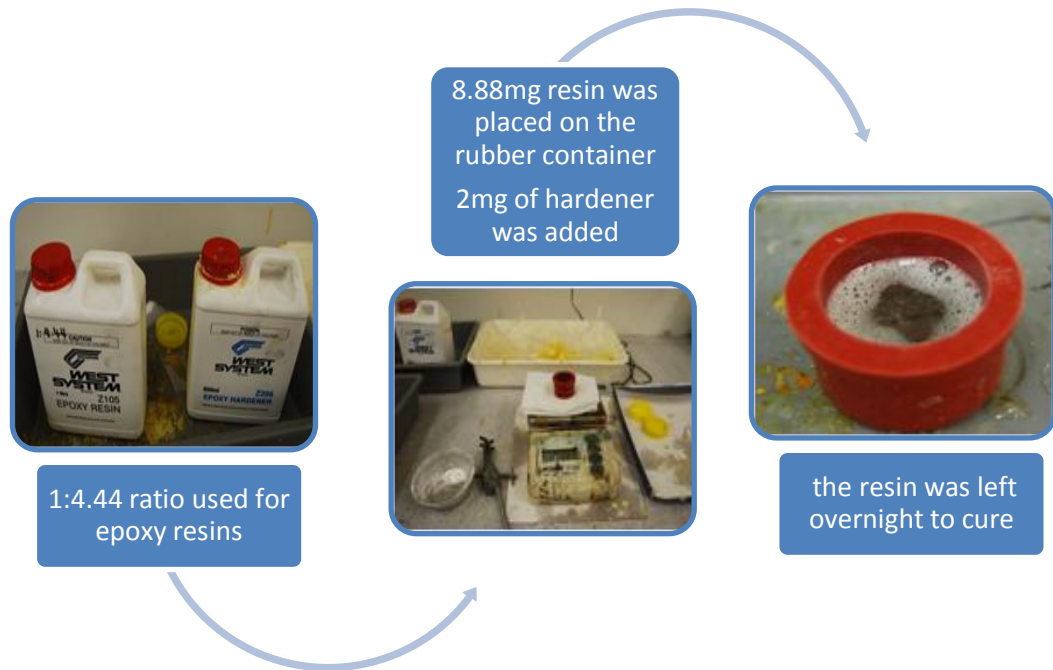


Figure 4.2: Preparation of 10ml Epoxy resins mounting

4.1.4 Grinding and polishing specimens

The procedure for grinding titanium specimens is similar to that for grinding steel specimens. The specimens are ground on successive grades of silicon carbide paper, using water to flush away loose particles of metal and abrasive. All specimens were ground and polished to produce flat and unscratched surfaces for better metallographic analysis. The specimens were ground using wet SiC papers of 600, 1000, and 2000 and 4000 mesh, 300mm wheel, 300 rpm, counter-revolving the specimen. Initial fine polishing consisted of 10min on a short nap cloth impregnated with a $3\mu\text{m}$ diamond paste using moderate hand pressure on each specimen at 150rpm on a 300mm wheel. Final polishing was done for 4min using $1\mu\text{m}$ Alumina on a felt cloth at 300rpm with moderate hand pressure. This opens and slightly enlarges the pores.

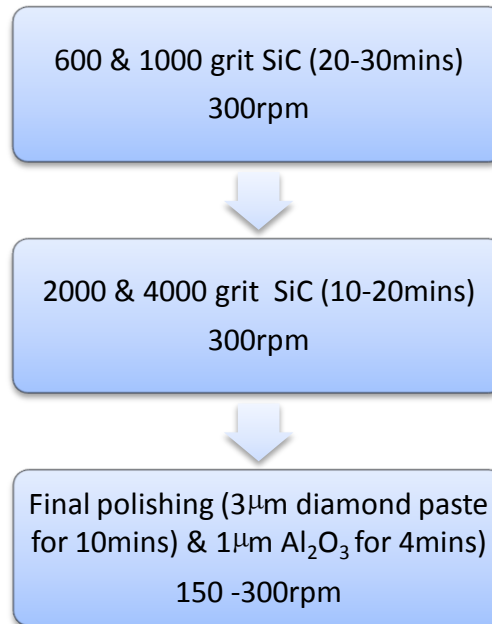


Figure 4.3: Steps for grinding and polishing

4.1.5 Kroll's Etchant

There are several etchants used for macro-etching and micro-etching (M. Donachie, 2000). In this work, Kroll's etchant was prepared for metallographic analysis. The solution was prepared in order to make the microstructure visible during optical microscopy. Kroll's reagent, a dilute aqueous solution containing HF and HNO₃, is the most widely used for commercial titanium alloys. The Kroll's etchant consists of

- a. 5ml of HNO₃
- b. 10ml of HF (48% concentration)
- c. 85ml H₂O

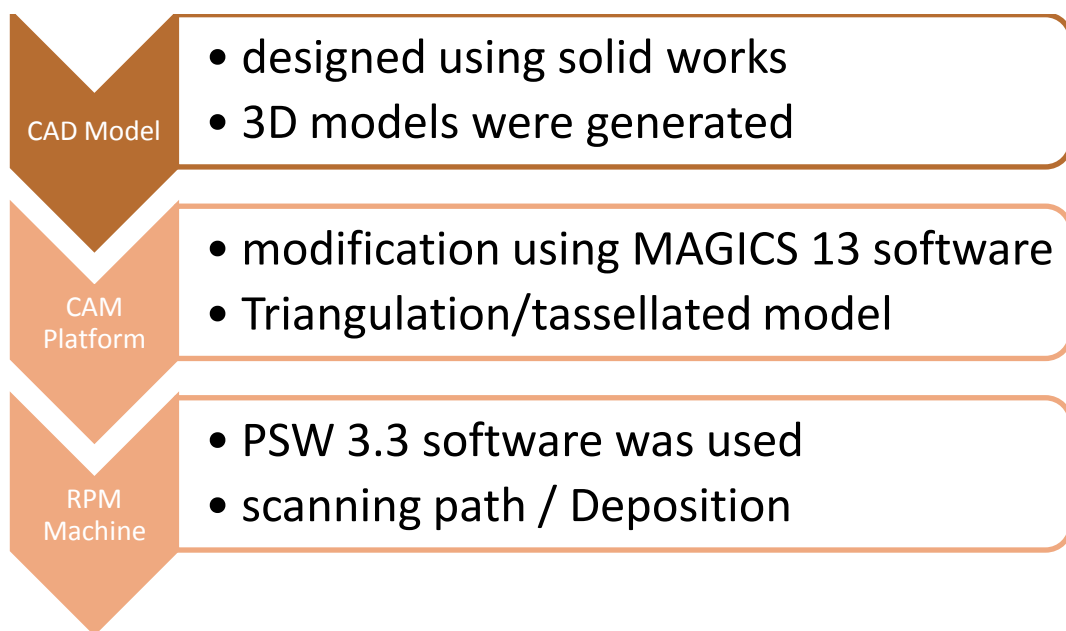
All specimens were immersed in the solution for 10s and 15s followed by washing with distilled water and drying. Finally, ethanol was used to ensure that specimens were completely dry. The specimens were examined after light etching to avoid over-etching. 100 ml of the Kroll's etchant was prepared during this experiment and placed on the plastic bottle. The bottle was labelled appropriately.

4.2 Fabrication Process

4.2.1 Specimens Design Format

All specimens were designed using Solid Works CAD software version 2008. The files were saved in the solid works format which is *.sld. The detailed dimensions were shown through the drawing files. Once the designs were confirmed, they were then converted to *.stl and *.igs format. The files in standard data transfer format were then sent to the manufacturer at the University of Wolverhampton, United Kingdom by email.

Figure 4-4: Data transfer platform



4.2.2 Specimen fabrication

The files received were converted to a readable RPM's machine format. The basic rule of data transfer is to get better data quality which will contribute to smooth parts fabrication. Therefore, it is necessary to remove all superfluous information from the STL data generation. The files were cleaned to ensure that all planes were equivocally intersected and trimmed. Each line was connected and there were no missing lines or geometries. The possible file formats are *.STL, *.IGES, *.VDA. The sensible CAD settings for STL export were a 10 mm maximum triangle size and a chord error of 0.01mm. The file conversion from

the CAD format to *STL format was important because the finer mesh generation than necessary in *.STL format would lead to very large file sizes and take longer to fabricate. To speed up the data transfer, the files were zipped and sent as attachment through an email.

Below shows the contact person;

Mark Stanford

School of Engineering and Built Environment

Telford Campus,

University of Wolverhampton

M.stanford@wlv.ac.uk

4.2.3 Machine Parameters

The EOSINT M 270 directly produces metal parts additively layer by layer. The process involved intricate interaction between the laser and the metal powders. For this research, all specimens were made based on the EOS standard setting parameter. The Ti6Al4V metal powders were fully melted. A 200W fibre laser with continuous mode was used and pure titanium was used as a base plate during the fabrication. A thin layer of powders were deposited using the high speed steel blade.

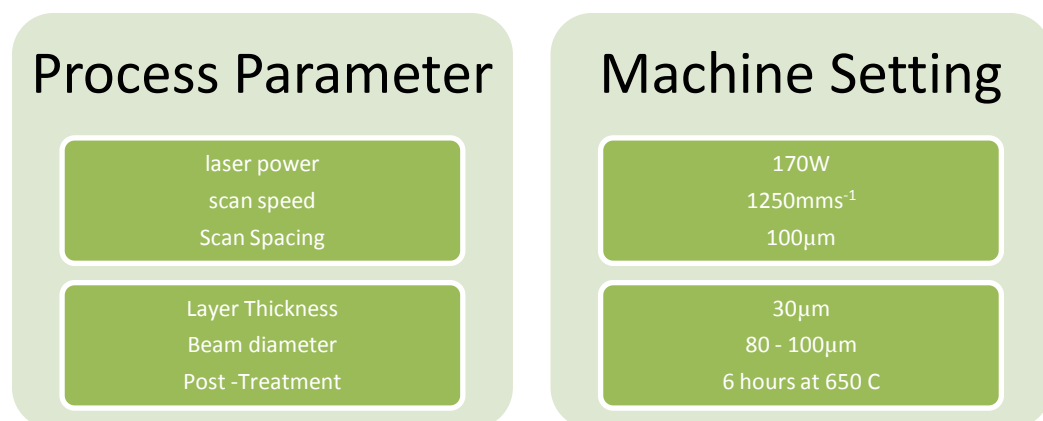


Figure 4.5: EOS GmbH Standard Parameters for M270 machine

The cross-section which corresponded to the CAD data is melted using a fibre laser. A scanning strategy was used during the specimens' fabrication in order to optimize the processing time. Each specimen was divided into two regions with

different scanning strategy. The material was first contoured around the cross-section using a focused beam at 0.1mm diameter at a speed of 1250mm/s at 150watts. The cross-section was then raster scanned at 1250mm/s at 170watts with a step over of 0.09mm.

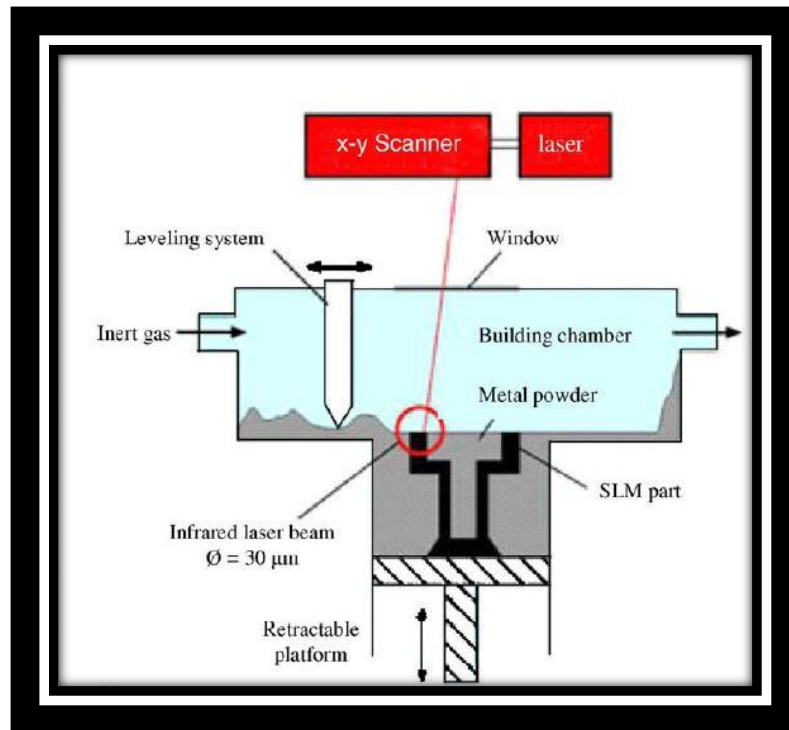


Figure 4.6: Schematic representation of SLM processes, source; E.C Santos et al (2006)

The parts were built flat in the platform and the build height was the thickness of the parts which is approximately 5mm. Once completed, the parts were wire cut from the platform leaving 1mm on the platform so no contamination from the platform would be in the samples. The software used on the machine was EOS GmbH proprietary software called PSW 3.3. The parts were drawn in a solid modeller (Delcam Powershape) and then exported as a stereolithographic file (triangulation *.stl file) into Materialise Ltd software called Magics 13. The positioned parts then were sliced using EOS software into 20 micron layers using EOS RP Tools. This software generates a file called a .sli file (slice file) .This file is imported onto the sintering machine and is used to make the parts.

Specimen Post treatments after fabrication

The parts were shot-peened whilst on the platform just after the removal from the machine. The parts were also stress relieved whilst on the platform before removal. The stress relieving was done at 650°C for 2 hours. If this is not done then the internal build stresses will cause the part to distort.

4.2.4 Energy Density Calculation

Four main parameters were used for the energy density calculation. These were laser power, scan speed, scan spacing and layer thickness. These parameters were chosen because they have a large influence on density. These parameters also determine the energy supplied by the laser beam to a volumetric unit of powder material. This is defined as energy density and has large influence on density

$$\text{energy density} = \frac{P \text{ laser power}}{\text{scan speed hatch spacing layer thickness}}$$

Build speeds vary from around 2mm³/s to more than 20mm³/s, depending on the material being processed and the selected layer thickness and build style. This is because some materials require more energy to melt than others.

4.2.5 Processing Environment

The M270 machine has a sealed process chamber which enables a high purity of protective gas to be maintained, thereby making it able to process a wide range of materials including reactive metals (www.mcadonline.com). In this work, an argon gas was used to control the oxygen levels inside the chamber and acts as a protective gas. The Oxygen concentration was controlled between 0.01 % to 0.13%. The machine fills at 40 litres /min and drives the O₂ down to 0.03% and then goes into hold mode where the chamber is fed with argon at 10 litres/min. The argon enters the chamber around the theta lens assembly to keep the lens glass free from products generated by the sintering. The argon that is in the chamber is driven through a filter and returned to the chamber again around the lens cover.

4.2.6 Scanning Strategy

The EOS GmbH M270 machine has huge advantages by offering a controllable scanning strategy, which means the scanning of the part can be divided into different regions or areas with a different scanning parameter. The machine's process software can split the model into two types of build areas, Skin (outer shell) and Core (inner). This can speed up the fabrication times by defining different laser scan speeds and layer thickness

As for this research, the scanning strategy was divided into two categories;

- Contour scan* – The material is first contoured around the cross-section using a focused beam at 0.1mm diameter at a speed of 1250mm/s at 150watts.
- Raster scan* - The cross-section is then raster scanned at 1250mm/s at 170watts with a stepover of 0.09mm

The energy density for the raster scan is;

$$\begin{aligned} \text{energy density} &= \frac{170}{1250 \times 0.1 \times 0.3} \\ &= 4.5 \text{ J/mm}^3 \end{aligned}$$

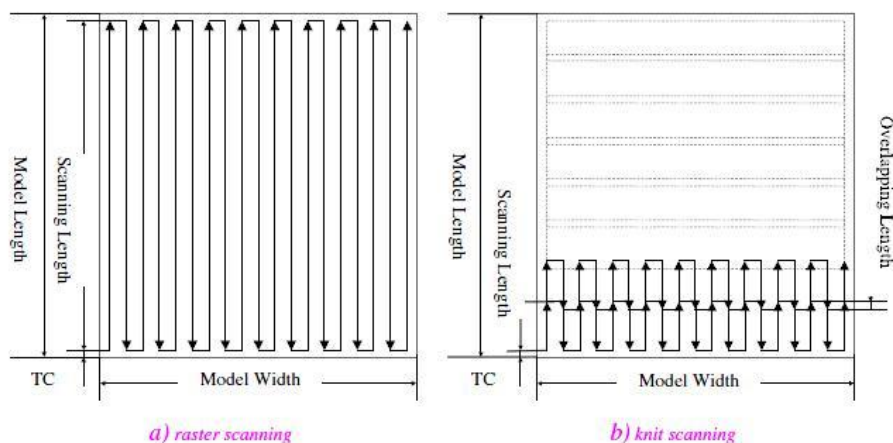


Figure 4.7: Type of scanning strategy, source; J.Zhoa et al (2009)

4.2.7 Parts Orientation and Scanning Layout

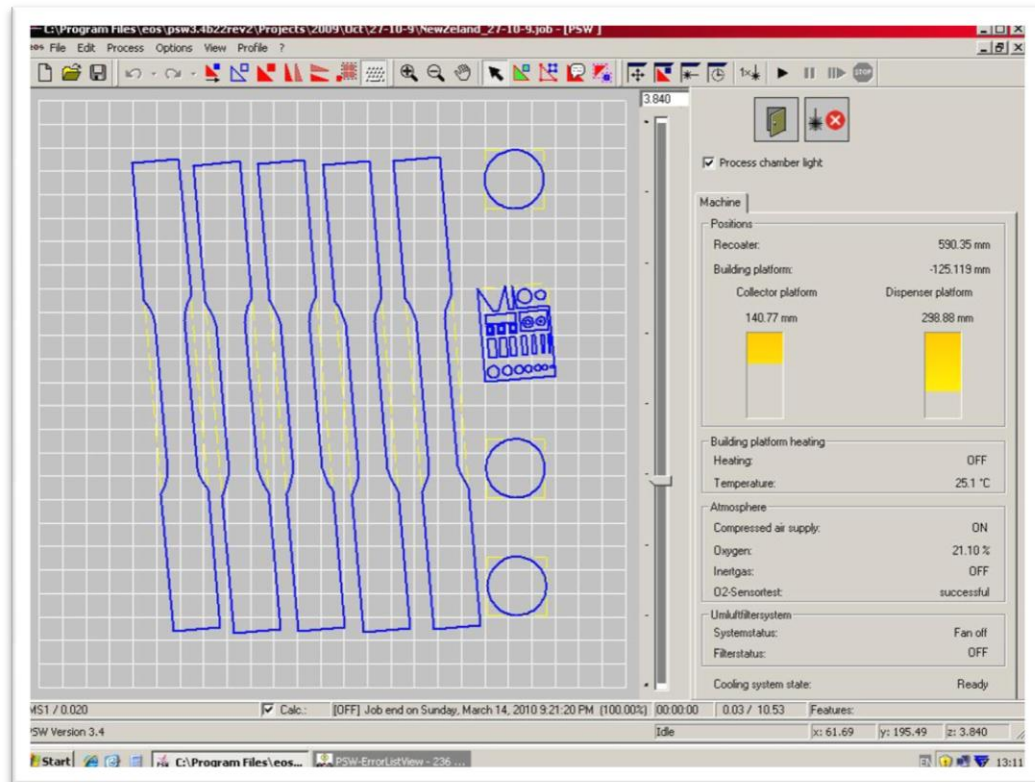


Figure 4.8: Scanning layout for specimen's fabrication

The orientation and packing in RP processing are considered to be the most important factors to maximize the utilization of space in the build vat and reduce build time (Sung Min Hur, 2001). All specimens were built in one run and arranged accordingly for full optimization of build time. This orientation also has minimal fabrication on the z- axis relative to the x and y axis. The specific software was used to automatically calculate the best orientation prior to the build time and surface quality. Notably, the orientation has the minimum build height. The factors considered during parts orientation were;

- a. The minimum build height
- b. The minimum ratio of x-length to y-length at the cross-section of prototypes

4.3 Powder Characterizations

4.3.1 Particle Size and Distribution

Titanium pre-alloy powders, Ti6Al4V (6% of aluminium, 4% of Vanadium) was used for laser sintering. This titanium alloy powder was produced through a gas atomization technique and theoretically would be more spherical and small in size. Typically, surface energy is assessed by the surface area. Smaller particles have high surface areas and more energy per unit volume, which promotes faster sintering. There is a close relationship between the densification, the processing parameters and the powder characteristics. A.Simchi (2006) concluded that the densification coefficient is related to powder characteristics such as chemical composition, particle size and distribution. The sintering rate increases as the densification coefficient value decreases.

Malvern Particle Sizer

The powder particles size and distribution was determined using a laser diffraction method or more accurately known as Low Angle Laser Light Scattering (LALLS). This method is used in many industries for particle characterisation and quality control. The method relies on the fact that the diffraction angle is inversely proportional to the particle size. The machine is a Malvern MasterSizer machine.



Figure 4.9: Melvern MasterSizer Machine

Test procedure;

1. The powder sample of Ti6Al4V in a plastic container is shaken and a small portion is extracted with a scoop or spatula.
2. An obscuration of 12.83% was used for this experiment. A working range of 10% - 30% is required to ensure that there is a sufficient amount of noise for good measurements with the elimination of multiple scattering
3. The reflective index of the particle was set. The Ti6Al4V has a reflective index of 2.220.
4. The powders were introduced into the tank till the obscuration value reached the working range.
5. A dispersant, generally water was poured into the tank. The dispersant reflective index was 1.33
6. A volume distribution was generated directly. A reading was taken and printed for the analysis.

Explaining the MasterSizer Report

Below shows the definition of the terms used for the Particle size and distribution report.

Obscuration:

A measure of the amount of sample added to the tank. Unscattered light is focused onto the obscuration detector. If there is no sample present then the obscuration is zero. When the sample is introduced some of the light is absorbed, reflected, diffracted, scattered, etc. The working range of the instrument is with obscuration values between 10% and 30% - this ensures sufficient signal to noise for good measurements, but eliminates the possibility of multiple scattering. The obscuration value is also used to calculate the volume concentration.

Particle Reflective Index (RI):

The reflective index of the particle was measured. If it is unknown a default reflective index will be entered. The reflective index for Ti6Al4V is 2.22

4.3.2 Particle Shape Characterisation

The simplest way to characterize the shape of profiles is to evaluate what is known as geometric shape factors. The British standard institute has prepared the standard glossary of terms used in the description of the appearance of powder grains;

- a. Acicular – needle shaped
- b. Angular – sharp edge or roughly polyhedral derives from poly, meaning many and hedra meaning a base; therefore polyhedral is understood to be a geometric shape having many faces each of which can act as a base
- c. Crystalline – a geometric shape freely developed in a liquid
- d. Dendritic – a branched crystalline shape
- e. Fibrous – regularly or irregularly threadlike
- f. Flacky – no formal definition in the standard
- g. Lamellar – platelike
- h. Granular – approximately equidimensional but irregular shape
- i. Modular – rounded, irregular shaped
- j. Irregular – lacking any symmetry
- k. Spherical – globular shaped

Sampling Techniques

Scoop sampling – this is the technique used for particle size and distribution analysis. It is the least precise technique but the most frequently used sampling technique. A plastic container with the powder sample of Ti6Al4V is shaken and a small portion is extracted with a scoop or spatula. It also known that if the intermediate handling has caused vibration of the sample, coarse material tends to collect near the surface. Therefore the powder was extracted from the middle portion of the container.

4.3.3 Morphology and Chemical Compounds

A morphology and Chemical Analysis were done in order to verify the size, shape and the chemical compounds of the Ti6Al4V powders used for the laser sintering machine. The shape of the individual powder particles was evaluated based on the standard shapes such as spherical, cylindrical, and acicular. A Hitachi S-4700 Scanning Electron Microscope was used to run the analysis. A portion of the Ti6Al4V powders used for the specimen fabrication was requested. The analysis was done through

- a. Scanning Electron Microscope (SEM)
- b. Electron Dispersive Spectroscopy (EDX)

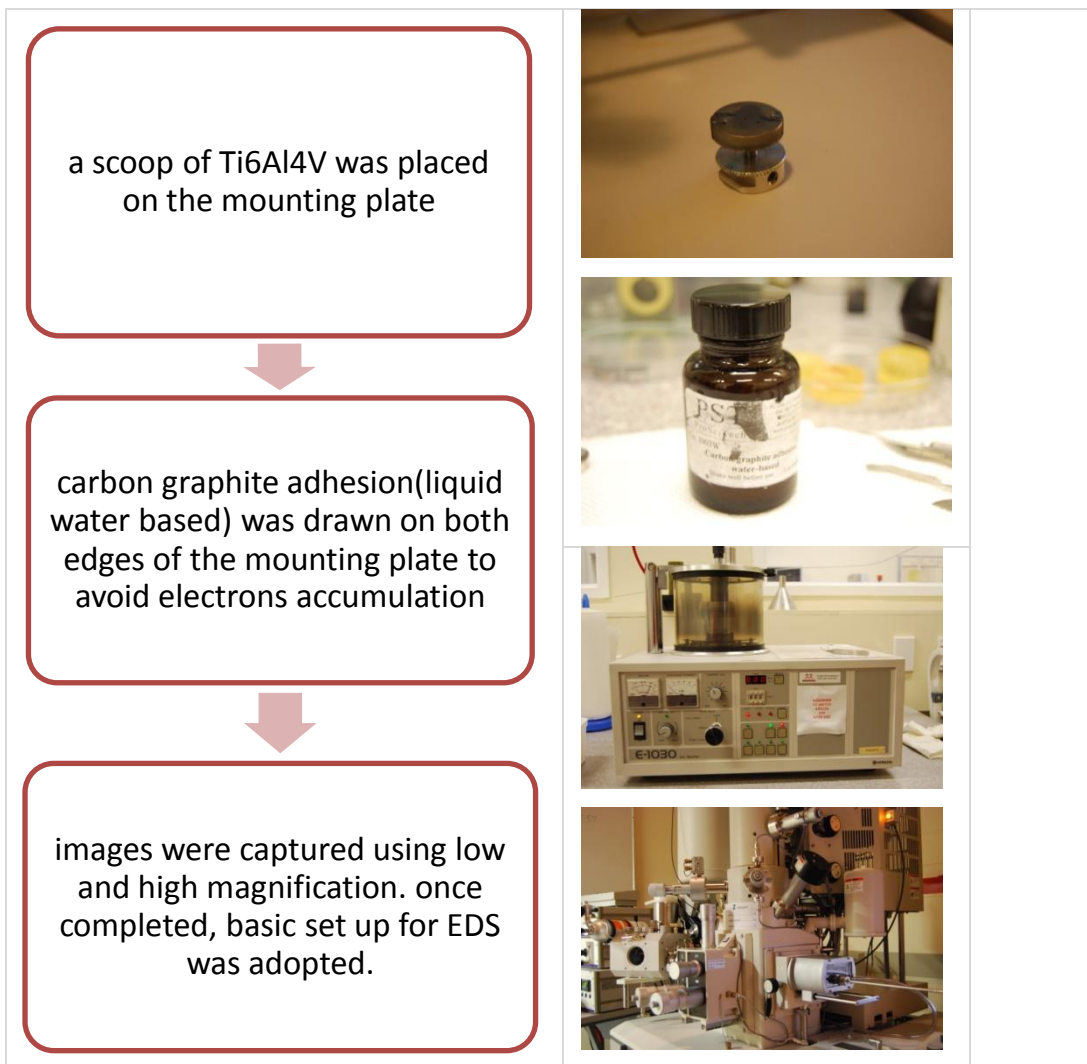


Figure 4.10: Specimen preparation for SEM

4.3.4 Powder Density

Gas Pycnometry

A Quantachrome Instrument, Ultrapycnometry 1000 was used to calculate the density of the laser sintered part. The operation of this instrument is based on Archimedes principle which is a gas displacement and volume pressure relationship known as Boyle's Law. Nitrogen gas was used instead of Helium which can penetrate the finest pores of the sample near to 0.25nm.



Figure 4.11: Gas Pycnometry Instrument

Test Procedure

1. The sample was weighed using a digital weighing machine. The mass of the sample was recorded onto the gas pycnometry instruments.
2. The sample was placed in the sample chamber and nine intended consecutive runs were performed for the sample.
3. Once completed, the average volume, density and the percentage of volume standard deviation were recorded

4.4 Mechanical Behaviour

The material properties determined were;

- a. Yield strength – the strength of a material in tension is measured by its yield strength (the stress at which irreversible plastic deformation begins)
- b. Ultimate Tensile strength (UTS) – the stress at maximum load
- c. Fracture Strength - The stress coordinate on the stress-strain curve at the point of rupture
- d. Elongation to fracture – deformation at fracture
- e. 0.2% Yield Strength – Yield strength at 0.2% strain offset
- f. Young’s Modulus – stress and strain ratio during elastic deformation

4.4.1 Tensile Testing

Tensile testing was carried out with an Instron 4204 machine following the ASTM E8M standard and according to the ISO 6892 standard indication. A 0.2 mm/min cross head speed was applied. An axial extensometer was employed for measuring the elongation. In particular, the ASTM E8M standard for the tensile specimen’s geometry was followed. The specimens had a rectangular shape with an overall length of 200mm and a reduced section length of 50mm with the thickness of 4mm

Table 4.3: machine’s parameter used for the tensile testing;

Tensile machine	Setting
<ul style="list-style-type: none"> • Interface type • Machine parameters • sample rate (points/secs) • cross head speed (mm/min) • Extensometer switch value 	<ul style="list-style-type: none"> • 4200/4300/4400 • standard • 100 • 0.25 • 50mm

Estimated load calculation

Estimated maximum load was calculated based on the load-stress relationships.

An average estimated stress of 1000MPa was used for this calculation

The cross sectional area:

$$\begin{aligned}
 A &= \text{length} \times \text{thickness} & F &= \text{stress} \times \text{cross - section} \\
 &= 12.5 \times 3.3 & &= 1000\text{MPa} \times 41.75 \text{ mm}^2 \\
 &= 41.75 \text{ mm}^2 & &= 41750 \text{ N}
 \end{aligned}$$

The estimated load was 41.8KN. This value was used for setting up the machine.

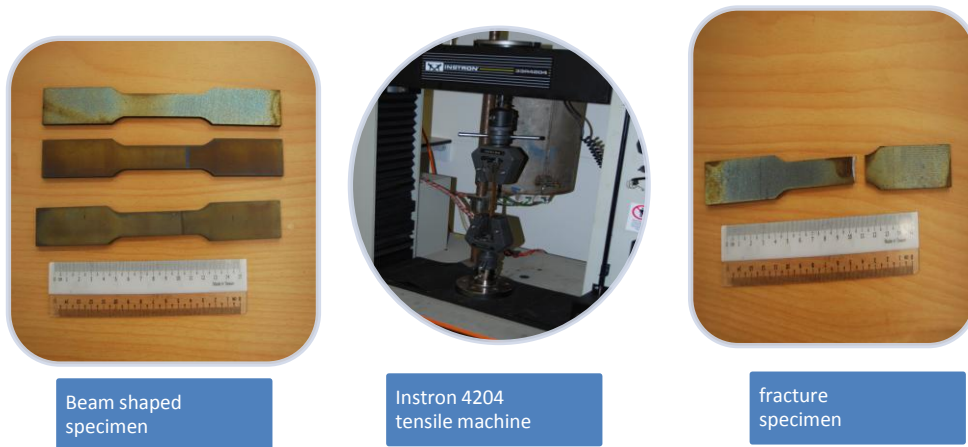


Figure 4.12: Tensile specimen, machine and fractured specimen

4.4.2 Fracture surface morphology

The fracture surfaces of the tensile specimens were analysed in a Hitachi S-4700 Scanning electron.



Figure 4.13: Fracture surface for SEM

4.4.3 Vicker's Hardness Test

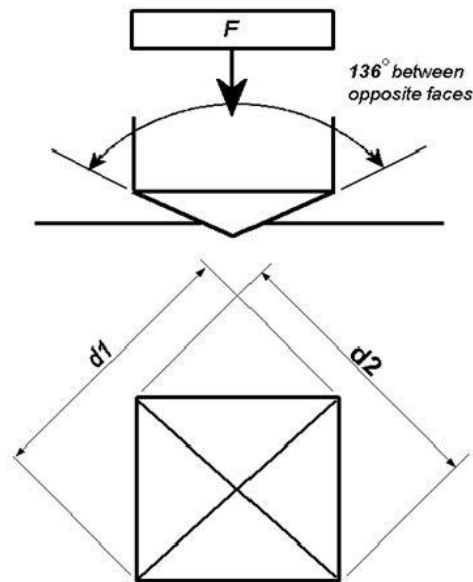


Figure 4.14: indenter for Vicker's hardness Test, source; (www.wikipedia.com)

The Vickers hardness test method consists of indenting the test material with a diamond indenter, in the form of a right pyramid with a square base and an angle of 136 degrees between opposite faces subjected to a load of 1 to 100 kgf. The full load is normally applied for 10 to 15 seconds. The two diagonals of the indentation left in the surface of the material after removal of the load are measured using a microscope and their average calculated. The area of the sloping surface of the indentation is calculated. The Vickers hardness is the quotient obtained by dividing the kgf load by the square mm area of indentation.

Experimental Procedure

1. A disc shaped specimen was used for the Vickers hardness Testing.
2. The specimen's surface was polished properly for better visualisation.
3. Load and the holding time for each indentation was placed as shown below;
 - a. Load = 50kgf
 - b. Holding time = 15s
 - c. Reading = 15
4. The Vickers hardness number was recorded and average value was calculated.

4.4.4 Density Measurements

The density of laser sintered parts was measured according to the Archimedes principle by weighing the sample in air and subsequently in water to measure the volume.

Archimedes Principle - *“When an object is immersed in a liquid, the liquid exerts an upward buoyant force that is equal to the object volume and the density of the liquid. The difference in weight between an object weighed in air and its weight when suspended in water is equal to the object volume in cubic centimetres times the density of the water”.*

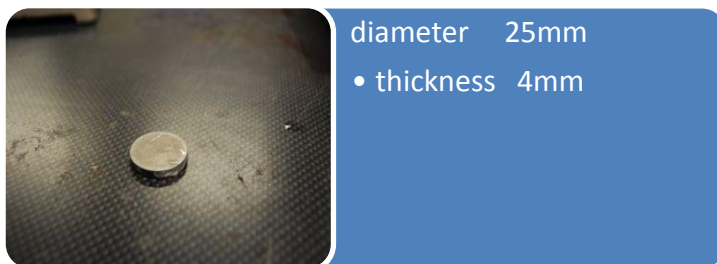


Figure 4.15: Disc shaped specimen used for density measurement

1. The sample was weighed using a digital balance. A reading of the mass of the sample was recorded and marked as M_1 . The sample was removed from the machine
2. A sample holder (a bottle with a long tube) was used to suspend the sample during the process. A bottle was placed on the digital weight machine and the reading was reset to zero.
3. The disc sample was coated with a porcelain film properly. A sufficient amount of film was used just to enclose the sample with the film thus avoiding any penetration of water into the sample
4. A coated sample was hung at the tip of the bottle tube and the reading of the coated sample was taken and marked as M_2 .
5. A beaker with 200ml of water was used and the coated sample was placed inside the beaker properly. A new reading of the sample was taken and marked as M_3 .

6. The relative density and theoretical density were calculated and recorded. Pure titanium has a 4.51 g cm^{-3} density and Ti6Al4V has a density of 4.46 g cm^{-3}

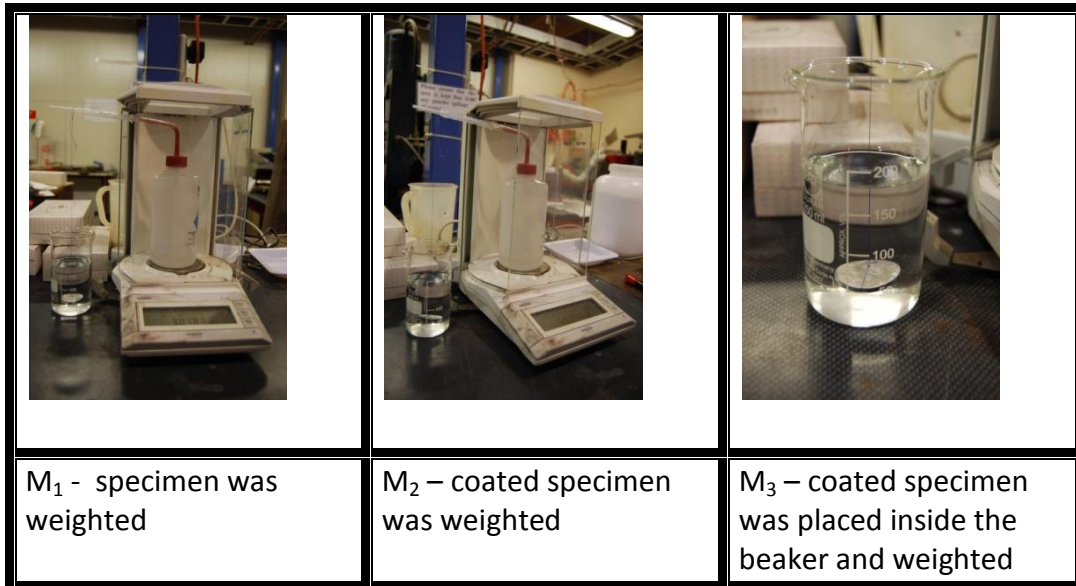


Figure 4.16: Archimedes Technique for part's density

The calculation was based on the density formula

$$\rho = \frac{m}{V}$$

ρ (rho) is the density,
m is the mass,
V is the volume.

$$\text{density of the part} = \frac{\text{weight}}{\text{displaced weight}} (\text{density of fluid})$$

Therefore;

1. Apparent density = $\frac{M_1 \times \rho_{\text{water}}}{(M_2 - M_3)}$
2. Relative density = $\frac{\rho_{\text{specimen}}}{\rho_{\text{Ti6Al4V}}} \times 100\%$
3. Theoretical Density = mass / volume

4.5 Heat Treatment

The disc shaped specimens were heat treated using a tubular Vacuum furnace. Solution treatment was performed under an atmosphere of welding grade argon gas (purity >99.995%) at a flow rate of 10L/min. The details of the specific heat treatment are summarized below;



Figure 4.17: Tubular Vacuum Furnace used for the heat treatment

1. The sample was placed on a cylindrically shaped ceramic crucible. This eases the handling during deposition and during completion of heat treatment
2. A long tube was used to measure the middle portion of the vacuum furnace chamber. The distance was marked and the tube was used to push the sample inside the vacuum furnace chamber.
3. The surface between the tubular pipe and pressure gauge was cleaned and grease was applied.
4. Both ends of the furnace were closed tightly and the vacuum valve opened. The pressure gauge dropped to -100kPa and this was held for 3 minutes.

5. The chamber was flushed with argon gas till the pressure dropped to zero. This process was repeated three times.
6. The process parameter was set accordingly. Once finished, both ends were opened at the same time and the sample was pushed into the water bath.
7. For air cooling, the furnace was turned off and the specimen was ejected out and allowed cool to room temperature.

4.5.2 Designated Heat treatment

For this research, different heat treatments were performed in order to modify the laser sintered microstructure. The same disc specimen was used for each designated heat treatment. Microstructure and micro hardness were carried out to investigate the mechanical behaviour of the specimen.

Specimen	Cooling	Abbreviation	Solution Treatment	Aging
D3	Water Quenching	ABST - Q	925C for 2 hour	None
D3	Air cool	BST - AC	1055C for 2 hour	None
D3	Air Cool	BST -AC	1055C for 2 hour	540C for 8 hour

Table 4.4: Designated Heat Treatment

The first solution treatment was to look at the effect of rapid cooling of the as built microstructure via water quenching. A Beta solution treatment was applied in order to form a fully lamellar microstructure.

4.6 Metallographic analysis

The metallographic analysis was performed using;

- An Olympus BX 60 Digital Optical Microscopy
- X-ray Diffraction Analysis
- A Philips EM30 Transmission Electron Microscopy

Specimen preparation for Optical Microscopy (OM)

Firstly, the disc shaped specimen (D1) was sectioned so that the cross-section and surface area could be examined. The two specimens were mounted using the epoxy resins and labelled as D1LSCS and D1LSSA. Finally, the specimens were polished to remove scratches. The same procedures were repeated for the heat treated specimens but without the epoxy resin applied. All specimens were recorded before and after etching.

Specimen preparation for X-ray Diffraction Analysis

There is no specific preparation for XRD since the size of the as built specimen was suitable and fitted onto the available mounting plate. The 2θ was 20° to 80° and the setting was $\text{CuK}\alpha_1$ with 1.54064\AA

Specimen preparation for Transmission Electron Microscopy (TEM)

Specimen preparation is a crucial aspect of Transmission Electron Microscopy (TEM). TEM requires ultra thin specimens in which the electron transparent regions are a few microns thick.

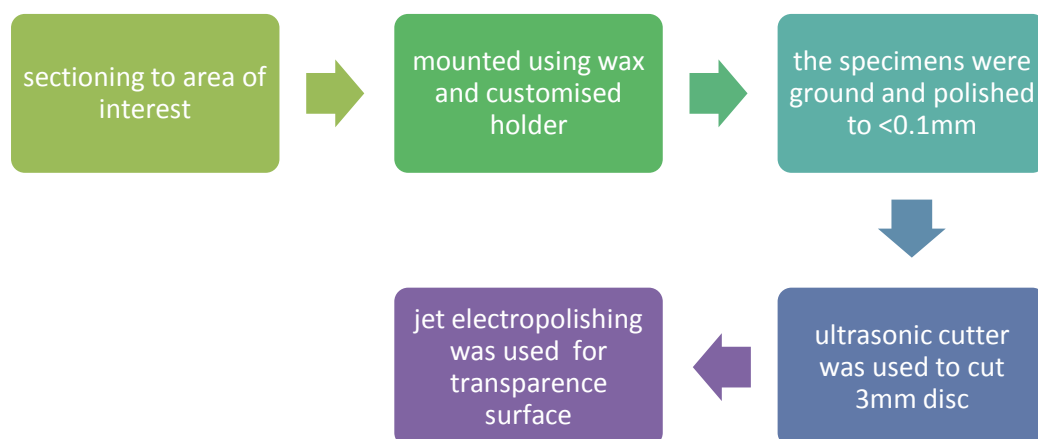


Figure 4.18a: TEM specimen's preparation

TEM specimen preparation is material dependant. Therefore, appropriate techniques must be selected initially for the intended specimen. A Common sequence of TEM specimen preparation is ultrasonic cutting, dimpling and jet electro-polishing. An important aspect of preparing a specimen from a bulk state to a 3mm disc is to preserve it in unaltered state. Thus proper steps need to be taken for good specimen quality;

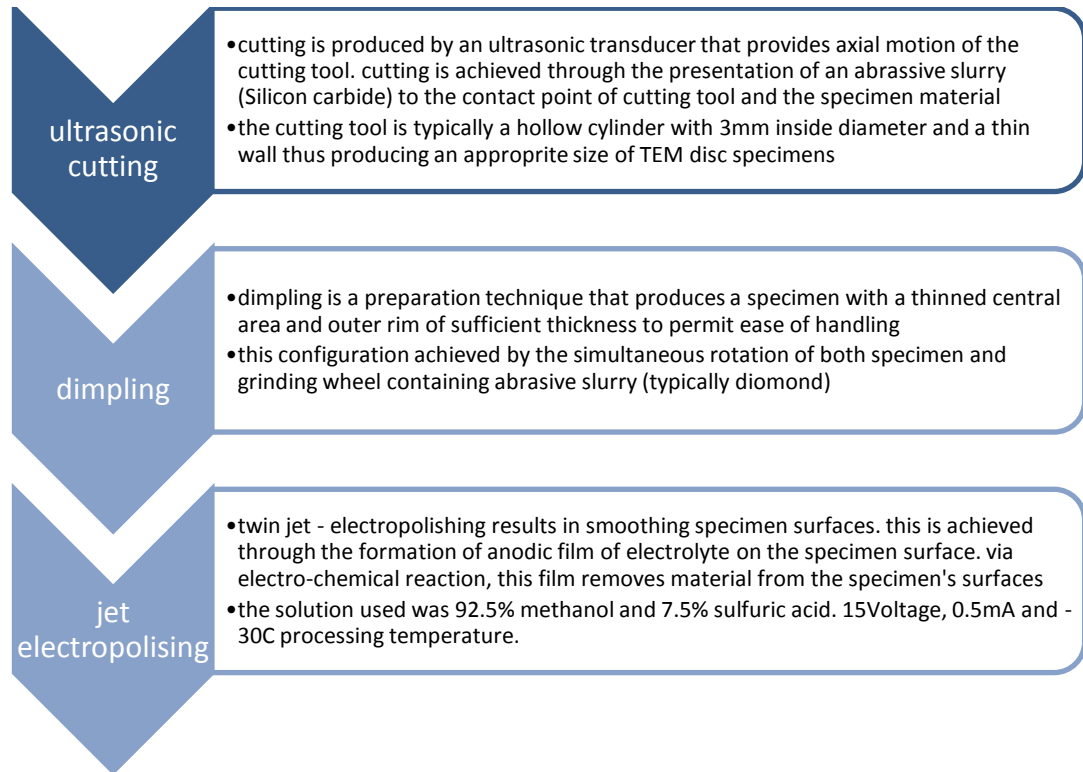


Figure 4.18b: Instruments used for TEM specimen's preparation

4.7 Process Accuracy and Feasibility

A block of Ti6Al4V titanium alloy was manufactured with a variety of different features via direct metal laser sintering. The block was designed with rectangular shapes; holes, various cylindrical shapes, sharp angles and sharp edges. The holes in spherical and rectangular shapes were different in size in order to measure the process repeatability. The block was analysed and measured using;

- Visual observation – for certain specific features such as top and bottom surfaces, sharp angle, depth.
- Digital calliper – linear dimension.
- Micrometer – linear dimension and small features.

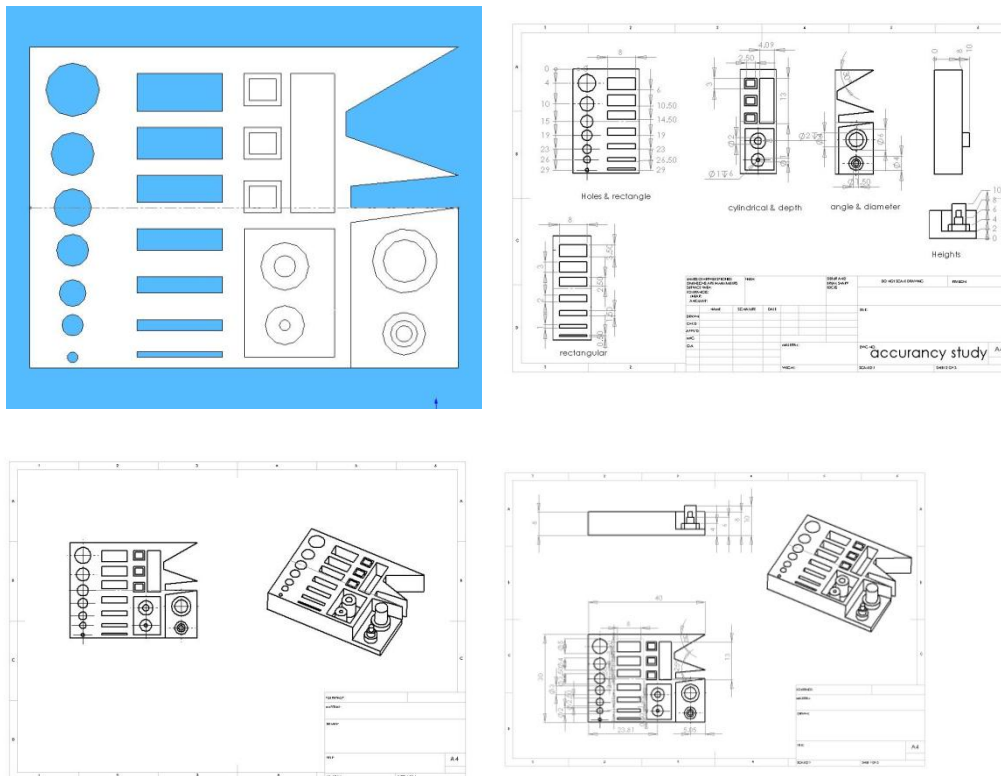


Figure 4.19: Benchmark used for Process Accuracy and Feasibility Study

Chapter 5: Results

5.1.1 Visual Observation & Evaluation

A visual observation was made to describe the surface, geometrical output with direct comparison with the CAD files. Immediately after receiving the specimens from the manufacturer, the parts were visually examined and photographically recorded. All specimens were similar and had geometric features according to the design. The beam and disc shaped specimens were accurately manufactured with acceptable surface quality. The top and bottom surfaces cannot be evaluated since the bottom surface was sectioned to 1mm from the substrate after the sintering process. A small block with distinct features was successfully built and showed the capability of this RPM process to build tiny and complex parts. Table 5.1 shows the summarized evaluation;



Figure 5.1: a. Beam shaped, Disc Shaped, A Block specimen

Property	Beam	Disc	Block
As built surface	rough	Rough	rough
Total Shape	complete	complete	Complete
Dimension	Thickness slightly lower	Thickness slightly lower	Thickness slightly lower
Holes	NA	NA	good
Fine details	good	Good	good
Edges	sharp	Sharp	Not smooth
Corners	sharp	Sharp	sharp
Cracks	No cracking	No cracking	No cracking

Table 5.1: Visual Observation and Evaluation results

5.2.1 Particle Size, Shape and Distribution

The powder particles were in a range of 10 to 100 micron. The analysis shows that the average of the particle size was $37.93 \mu\text{m}$ with the lowest percentile (0.1) reported at $24.45 \mu\text{m}$ and highest percentile (0.9) at $58.05 \mu\text{m}$. The specific area of the powder particles was $0.168 \text{m}^2/\text{g}$. The results also showed that the size distribution of the powder particles produced by a gas atomisation technique is generally small and below than $100 \mu\text{m}$. The powder particles also have a tighter range of size distribution which is mainly around $40 \mu\text{m}$.

Parameter	
Powder Particle	Ti6Al4V
Particle Reflective index (RI)	2.22
Dispersant Name	Water
Dispersant Reflective Index (RI)	1.33
Obscuration	12.83
d(0.1)	24.48 μm
d(0.5)	37.93 μm
d(0.9)	58.05 μm
Mean	39.82 μm
Standard deviation	13.04 μm

Table 5.2: Particles Size distribution

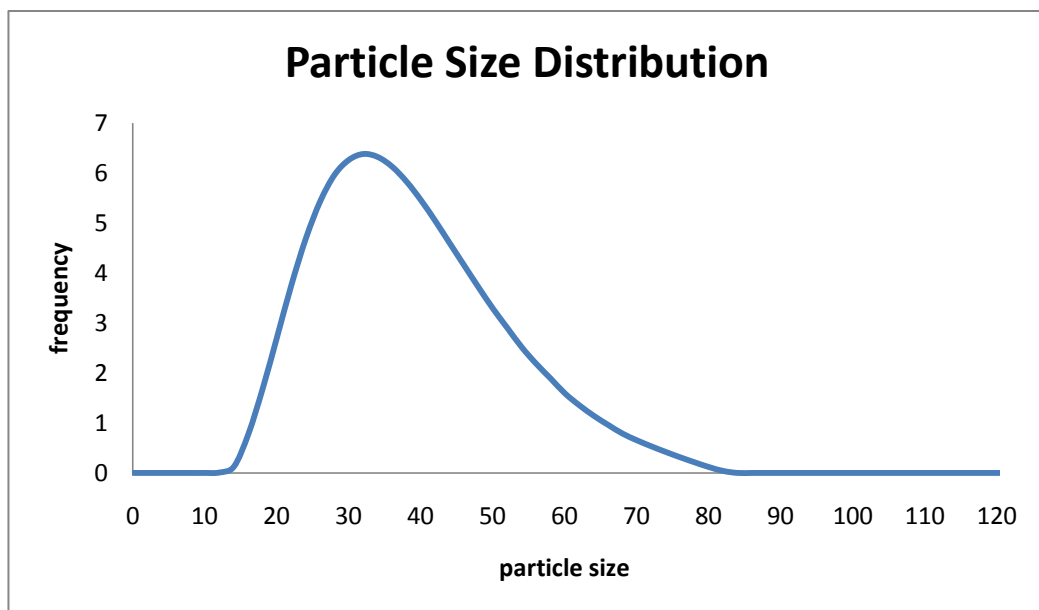


Figure 5.1: Graph of the particle size distribution

5.2.2 Morphology and Chemical compounds

The morphology of the Ti6Al4V gas atomized powder was examined through the optical microscope and the scanning electron microscope. The chemical compounds were investigated using Electron Dispersive Spectroscopy (EDS).

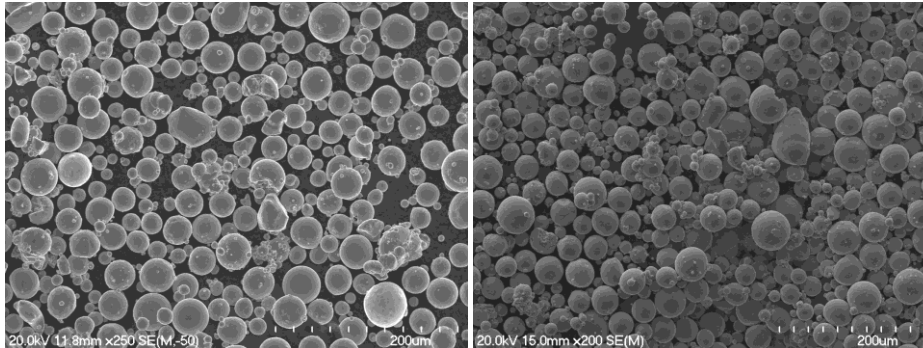


Figure 5.2: Ti6Al4V powder particles via SEM

Generally, all the powder particles were spherical. A few irregular particle shapes were seen in the powder sample due to vibration and rough handling. It was also noted that the powder particles were of a small size with an average of 50microns.

5.2.3 Compositional analysis

From the elemental analysis, no other elements were detected besides the titanium, aluminium and vanadium, confirming a lack of chemical contamination on the surface.

Ti6Al4V	Raw powder	mounted with epoxy resins
<ul style="list-style-type: none"> Aluminium Vanadium Titanium 	<ul style="list-style-type: none"> 5.76 4.66 balance 	<ul style="list-style-type: none"> 4.91 4.84 balance

Table 5.3: Compositional analysis of Ti6Al4V powder

The interstitial elements were not investigated since the sample powder received from the fabricator was not carefully sealed. Contaminations were expected.

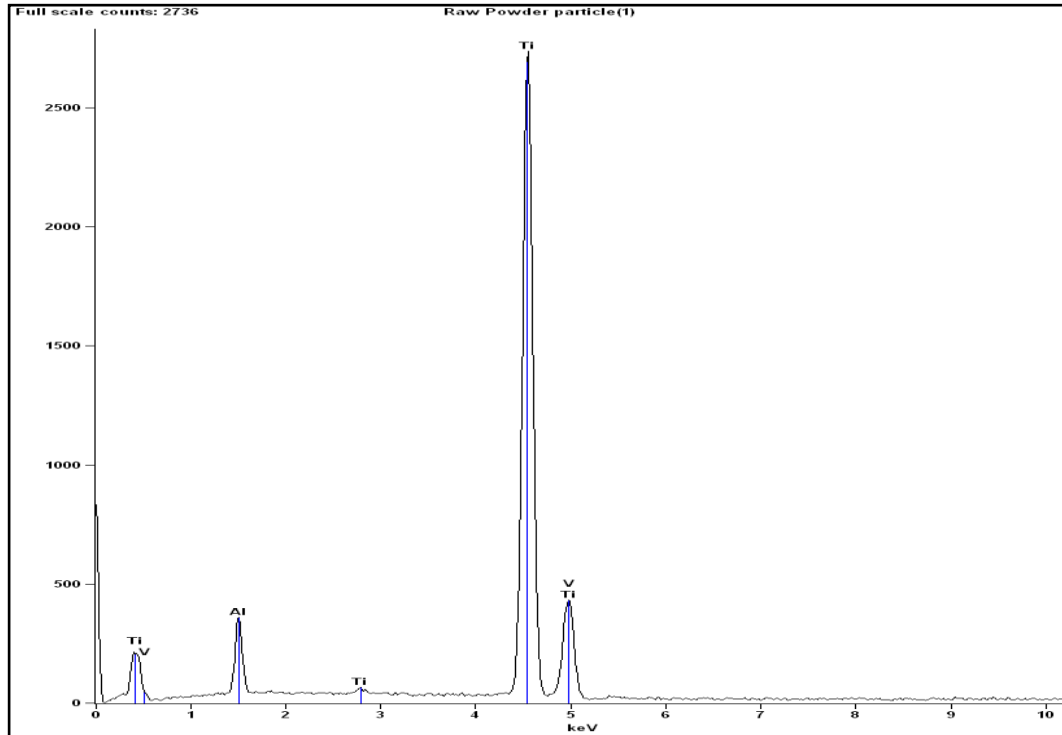


Figure 5.3: EDS of the Ti6Al4V powder particles confirming elements of Titanium, Aluminium and Vanadium

The results shown in figure 5.3 indicate that the composition of the Aluminium and Vanadium elements were within the ISO and ASTM standards.

Ti6Al4V	Wt %	Error	ISO 5832-3	ASTM F1472(%)
Ti	89.57	±0.67	balance	balance
Al	5.76	±0.15	5.50/6.75	5.50/6.75
V	4.66	±0.43	3.50/4.50	3.50/4.50

Table 5.4: EDX compositional test results compare to ISO & ASTM standards

Table 5.3 shows that the composition of the mounted Ti6Al4V gas atomised has a lower aluminium percentage (4.91%) compared to the ISO and ASM standards, but has an acceptable vanadium content (4.84%). The unmounted Ti6Al4V

powder showed a good percentage of the aluminium and vanadium elements of 5.76% and 4.66% respectively.

Table 5.4 confirmed that the percentage of Aluminium and Vanadium is within the range of the ASM and ISO Standards. The gas atomized powder used for the laser sintering process has 5.76% of Aluminium and 4.66% of Vanadium elements respectively. The percentage set by the standard is 5.50 to 6.75 % for Aluminium and 3.5 to 4.5% for Vanadium.

5.2.4 Powder Particle Density

The powder density was calculated via the gas pycnometry apparatus. Three consecutive readings were performed to calculate the mean and standard deviation. The result as shown below;

	Ti6Al4V
Powder Mass	89.21g
Average Volume	20.26cc
Average Density	4.4025 g/cc
Volume SD %	0.0047

Table 5.5: Ti6Al4V titanium alloys powder's density

$$\text{Relative density} = \frac{4.40}{4.46} \times 100$$

$$= 98.65\%$$

Based on the Ti6Al4V reference density of 4.46gcm^{-3} (M.Donachie, 2000). The laser sintered of Ti6Al4V has 98.65% relative density which is considered as near to full density.

5.3 Mechanical Testing

All specimens were prepared by selective laser sintering. Ti6Al4V alloy powder produced via gas atomisation with a particle size of 10-100um was used as the starting material. Processing was carried out in an argon atmosphere using a powerful Yb(ytterbium) fiber laser system (EOS GmbH M270, Munchen, Germany) with the capacity to build a volume up to 250mm x 250mm x 215mm. The tensile machine used for the testing was an INSTRON 4204 servo-hydraulic machine.

Table 5.6: Results recorded from the Tensile's machine

	Specimen 1	Specimen 2
Maximum load(kN)	46.29	46.29
Maximum stress (MPa)	1120.00	1141.00
Young Modulus(MPa)	111500	111500
Force at Break (kN)	44.78	44.80
Stress at Break (MPa)	1086.00	1103.0
Break display (mm)	2.0220	2.2250

As shown above, the maximum load of the laser sintered parts is 46.29KN and the Young's Modulus is 112GPa for both specimen 1 and 2. The tensile stress-strain curves of the as built specimens 1 and 2 are shown in figure 5-4 (a-d). They display the typical behaviour of Ti6Al4V, characterized by low strain hardening. Specimen 1 has 0.2% proof stress of 1080MPa, Ultimate Tensile strength of 1122MPa and elongation of 4.04%. Specimen 2 has 0.2% proof stress of 1075MPa, Ultimate Tensile Strength of 1144MPa and elongation of 4.44%. Table 5.7 summarises the calculated value of both specimens.

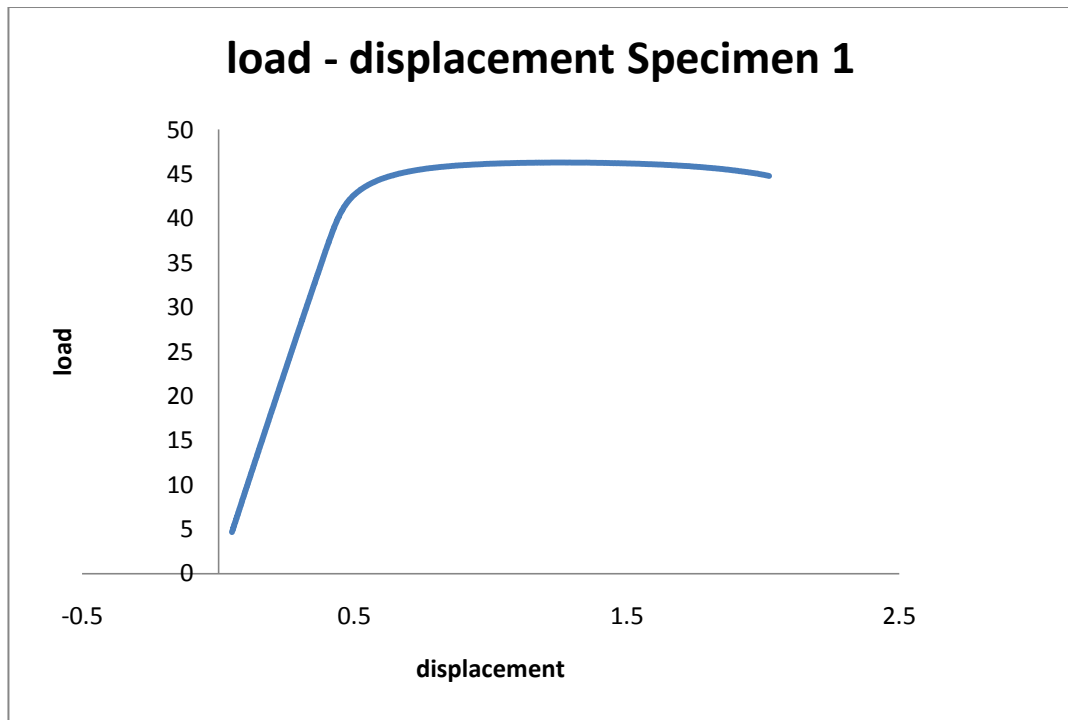


Figure 5.4a: Load-Displacement Graphs for tensile test 1

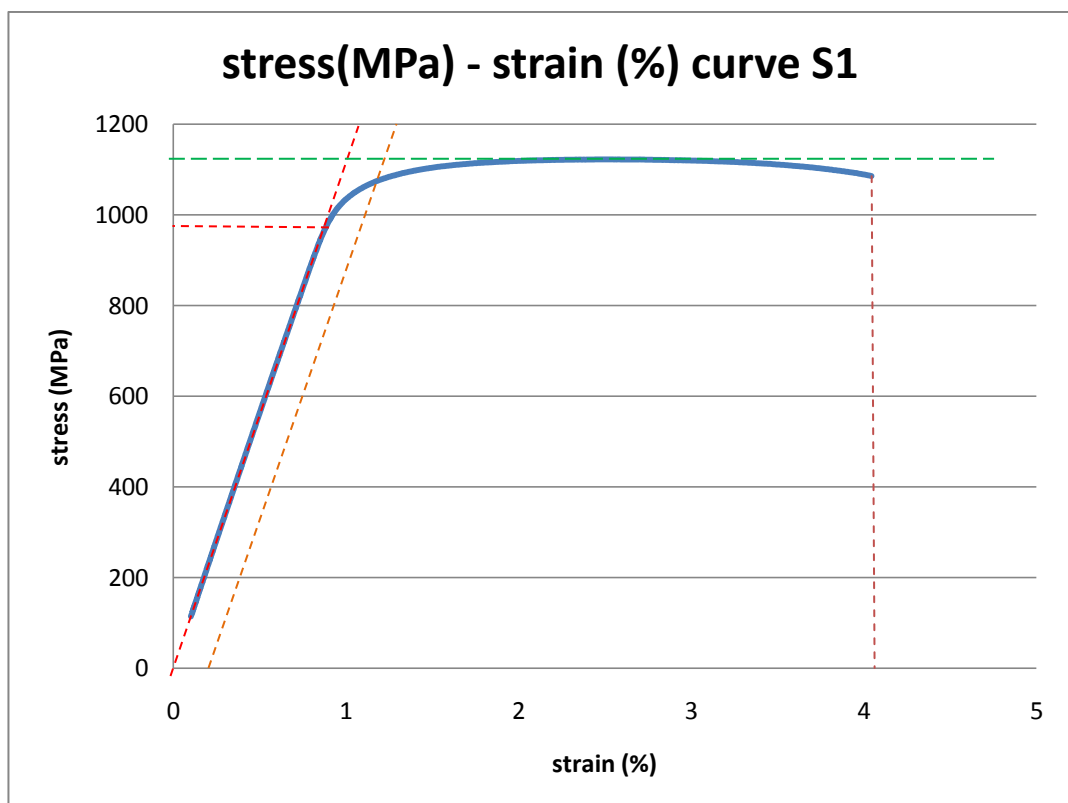


Figure 5.4b: Stress- Strain Graphs for tensile test 1

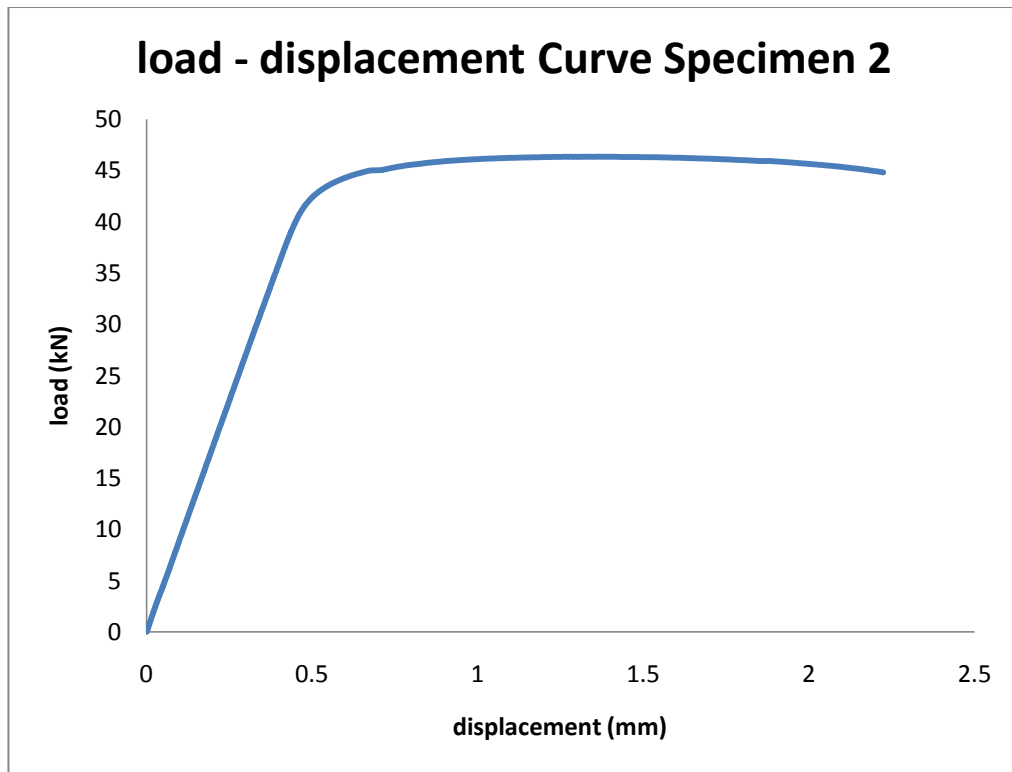


Figure 5.4c: Load-Displacement Graphs for Tensile Test 2

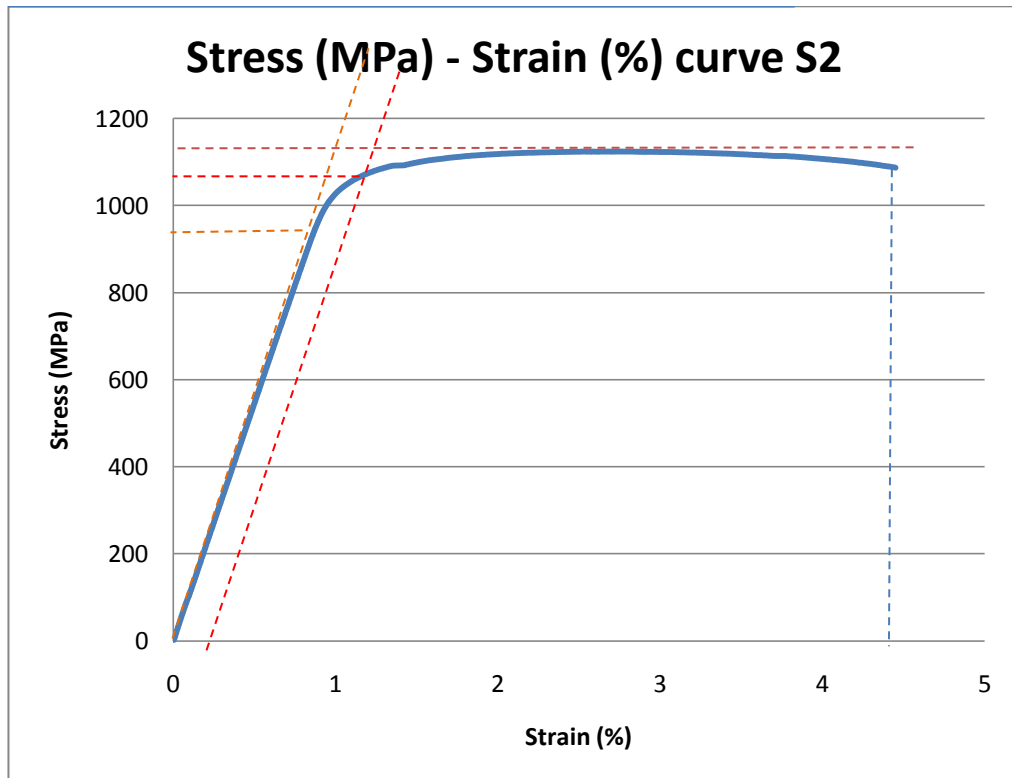


Figure 5.4d: Stress-Strain Graphs for Tensile Test 2

	Specimen 1	Specimen 2
Ultimate tensile strength	1122 MPa	1141 MPa
Young Modulus	112GPa	112GPa
Yield Strength	970MPa	965MPa
0.2% Yield Strength	1080MPa	1075MPa
Breaking Strength	1085MPa	1086MPa
Elongation at break	4.04%	4.45%

Table 5.7: Tensile testing results of as built specimen

5.3.2 Vickers Hardness Test

Microhardness was measured using a LECO LM700 tester. The applied load was 50gf for 15secs dwelling time. 15 readings were recorded and an average value was calculated.

Specimen	Hardness Value
D2 – as built	320HV
D3 – ABST – Q	723HV
D3 – BST – AC	677HV
D3 – BST – Ageing	606HV

Table 5.8: Microhardness results

Table 5-8 shows the Vicker's Microhardness value of the laser sintered and heat treated parts. The as built specimen shows the lowest hardness value which is 320HV. The second heat treatment cycle, which is an alpha-beta solution treatment with water quenching, shows the highest value of 723HV follows by the beta solution treated parts which is 677HV. The last solution treated parts have a hardness of 606HV.

5.3.3 Fracture Surface Topology

Figure 5.5: (A) –(F) Scanning Electron Microscope micrograph for fracture surface 1 deformed at maximum tensile stress of 1122MPa

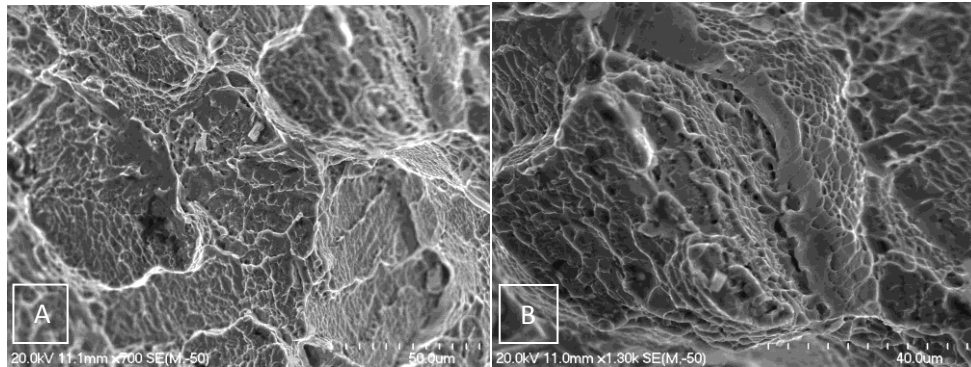


Figure 5.5 (A) shows the dimple rupture mode of fracture. (B) Large and small dimples on the fracture surface of laser sintered parts

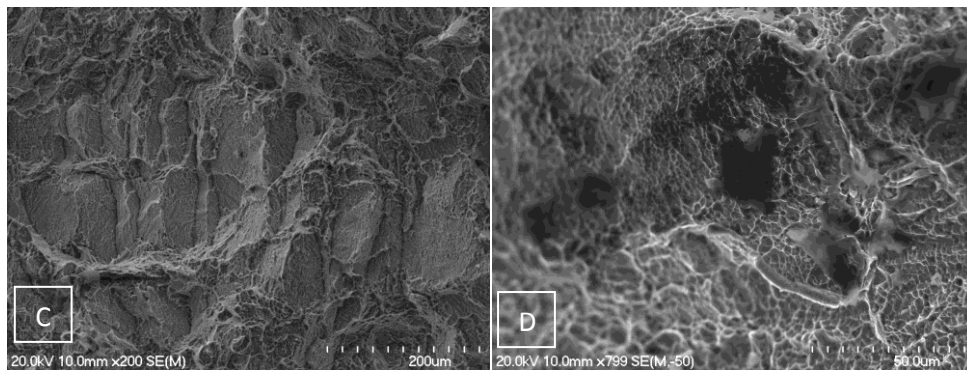


Figure 5.5 (C) fracture surface of the powder particles having average size of 40µm. (D) exhibits the microvoid distribution on the fracture surface

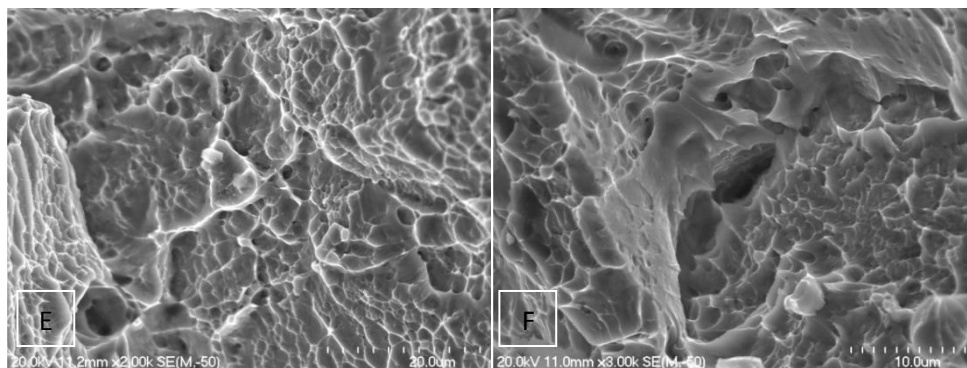


Figure 5.5 (E-F) Conical and shallow types of dimples formed during microvoid coalescence.

The fracture images showed a largely ductile fracture with ductile dimple. The images clearly show the presence of microvoids and porosity. The tensile specimen has an elongation of 4.04% which is less than the 10-12% expected in Ti6Al4V alloy.

Figure 5.4(a) and (c) shows particle boundaries suggesting incomplete powder bonding. The particle boundary size is about 40 - 50 μm confirming that the features on the fracture surface are most likely caused by particle pull-out.

5.3.4 Part Density

As mentioned before, the density of the sintered parts was measured manually using Archimedes principle and using the gas pycnometry equipment. Both gave different results but these were considered acceptable to indicate that the solid parts fabricated through a laser sintering process are not fully dense in this case.

	Archimedes	Gas Pycnometry
Part's density	4.211 gcm ⁻³	4.3194 gcm ⁻³
Relative density	94.42%	96.84%

Table 5.9: Gas Pycnometry density results

Calculated density for the disc shaped specimen;

$$\begin{aligned} \text{Specimen surface area } A &= \pi r^2, \text{ where } r = 24.9 \text{ mm} \\ &= 3.142 \times (12.45)^2 \\ &= 487.02 \text{ mm}^2 \end{aligned}$$

$$\begin{aligned} \text{Volume} &= 487.02 \text{ mm}^2 \times 3.05 \text{ mm} \\ &= 1485.4 \text{ mm}^3 \end{aligned}$$

$$\text{Density} = \frac{\text{mass}}{\text{volume}} = \frac{6.4915}{1485.4}$$

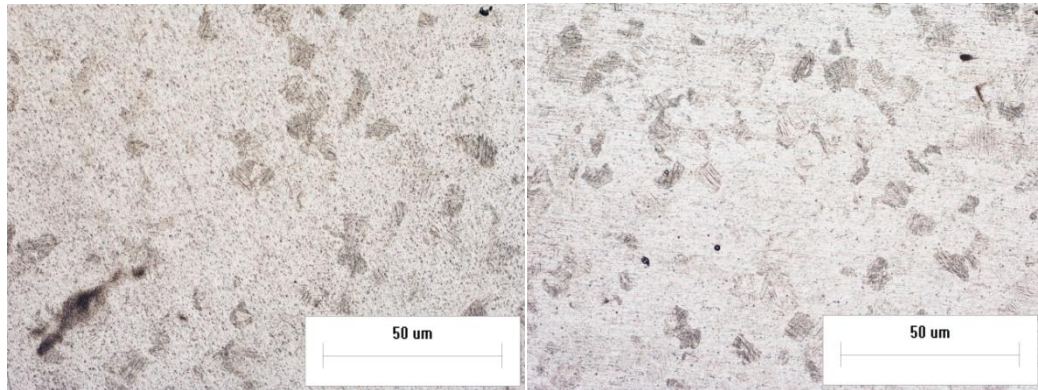
$$= 4.37 \text{ g cm}^{-3}$$

$$\text{Relative density} = 4.37/4.46 \times 100$$

$$= 97.98\%$$

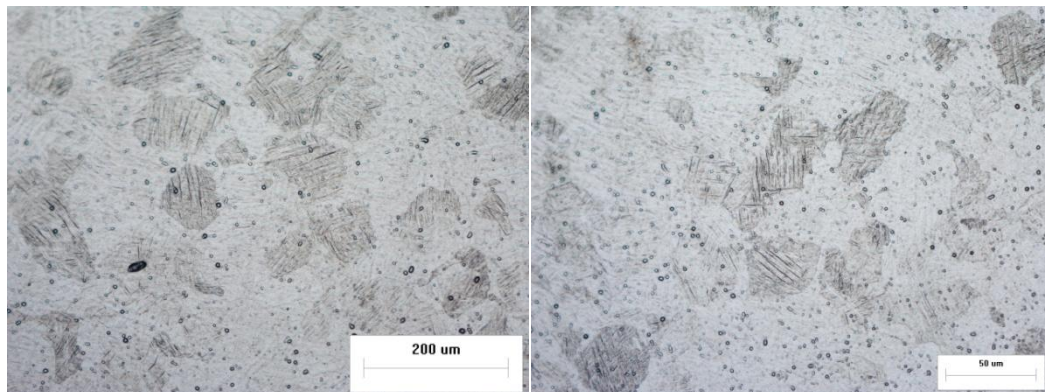
5.4. Metallographic Analysis

Figure 5.6 (a-f): Optical micrographs of the as built specimens (15s Kroll's etching) with different magnifications. The structure is lamellar and has a fine morphology consisting of some primary α and an acicular phase probably α' and retained β . Pores can be observed. Higher magnification shows very fine needle like colonies of martensitic α' .



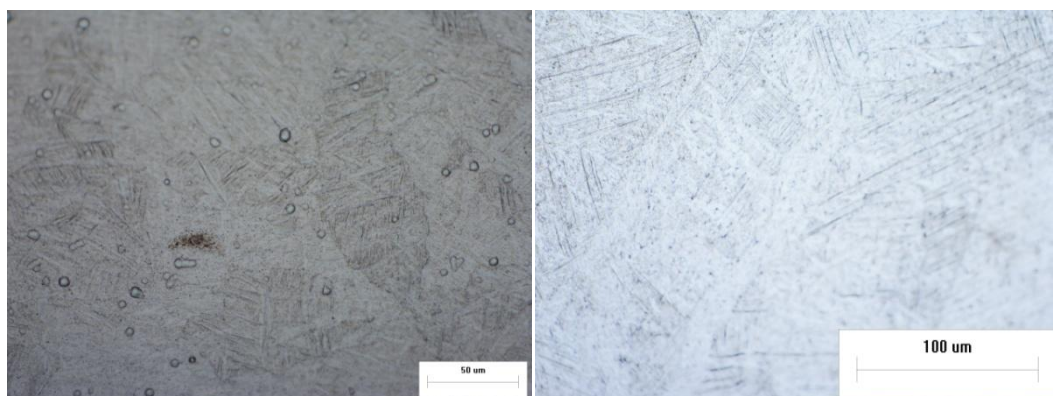
A (50x)

B (100x)



C (100x)

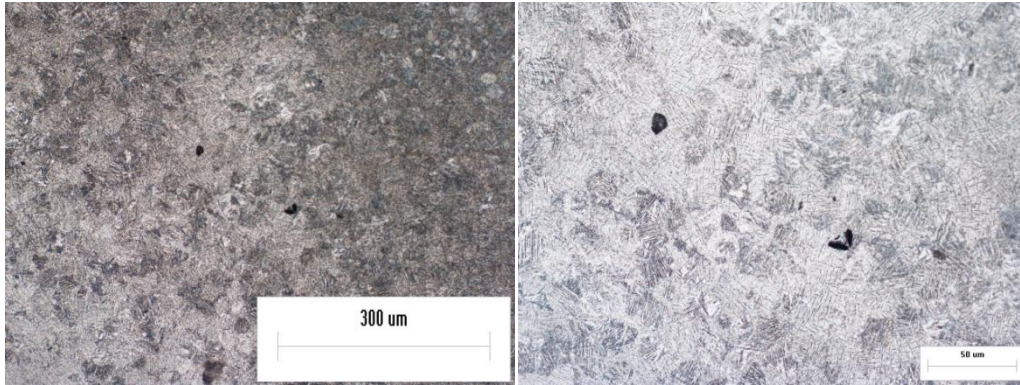
D (200x)



E (500x)

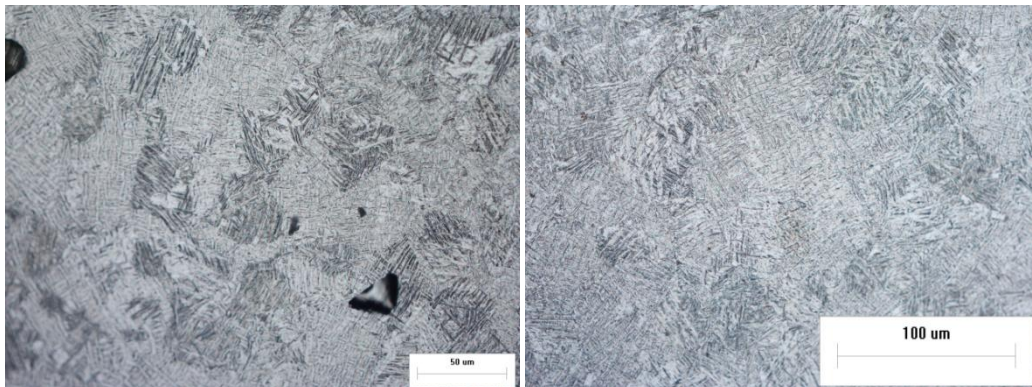
F (1000x)

Figure 5.7: Optical micrograph of laser sintered parts after holding at 925°C, 2h, water quench. Consists of a very fine lamellar structure but coarser than the laser sintered parts (Kroll's etching). There are numerous α colonies within prior beta grains which is known as a basket-weave structures. The optical micrograph also depicts the α' regions.



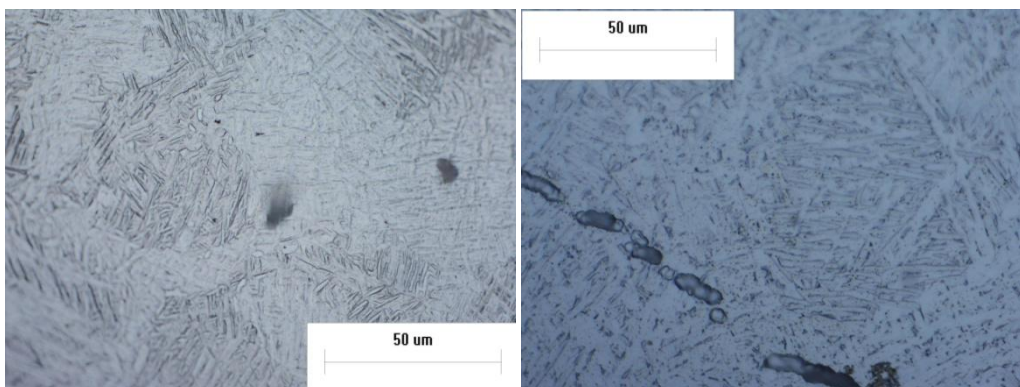
A (50x)

B (100x)



C (200x)

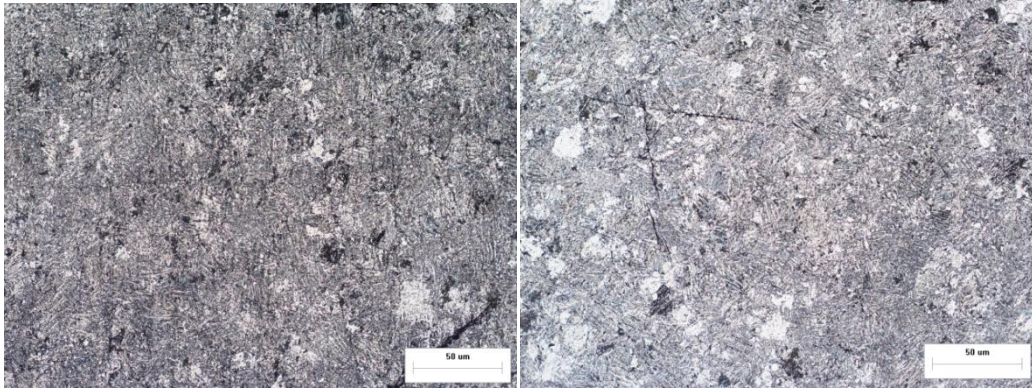
D (200x)



E (500x)

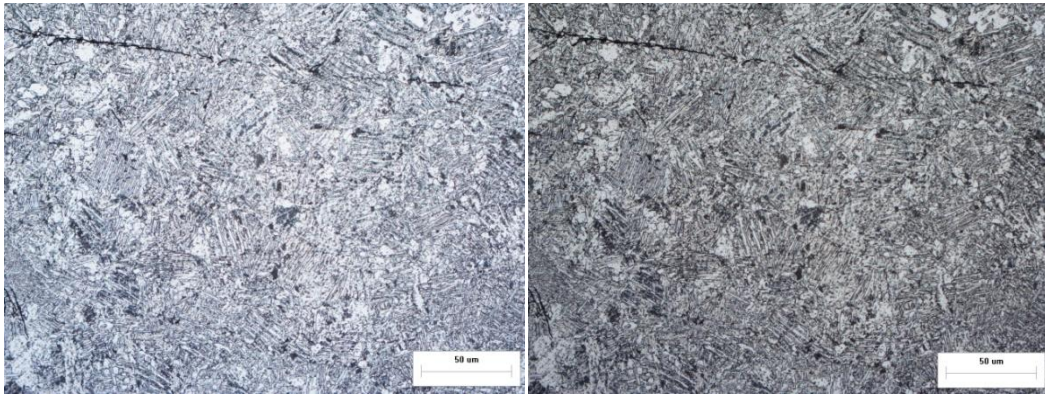
F (1000x)

Figure 5.8: Optical micrograph of laser sintered parts after holding at 1055°C, 2h, and air cooled (15s etching). Consists of a fully lamellar structure of transformed acicular α in a retained β matrix. It has thicker morphology compared to the as received specimens.



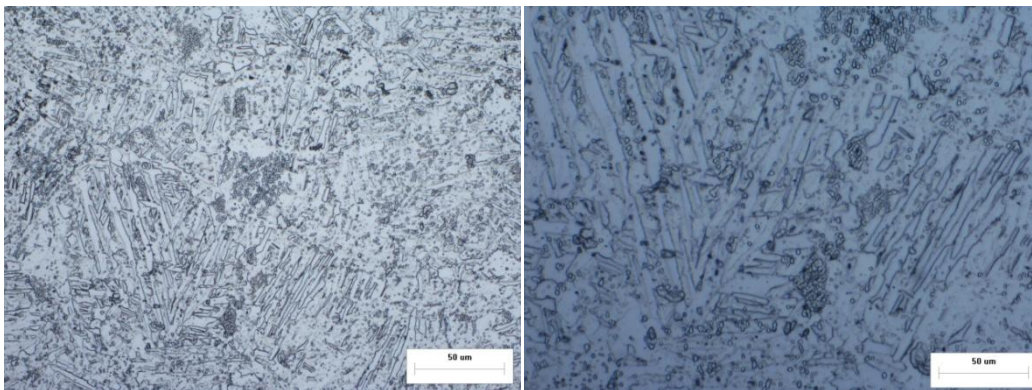
A (50x)

B (50x)



C (100x)

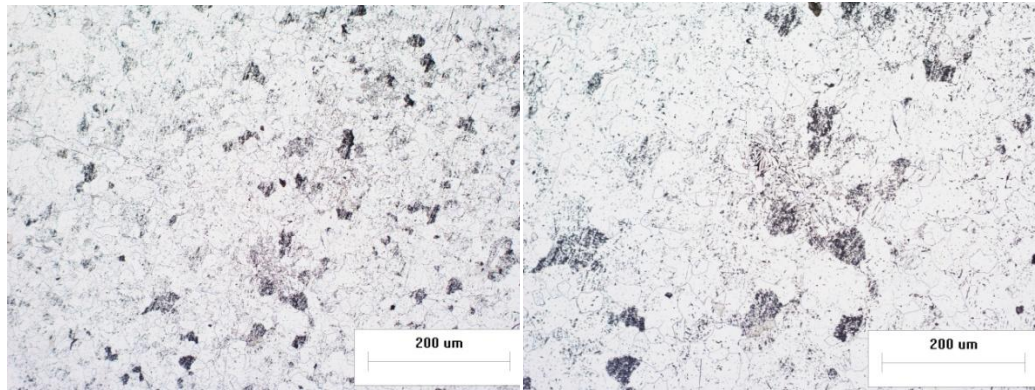
D (100x)



E (200x)

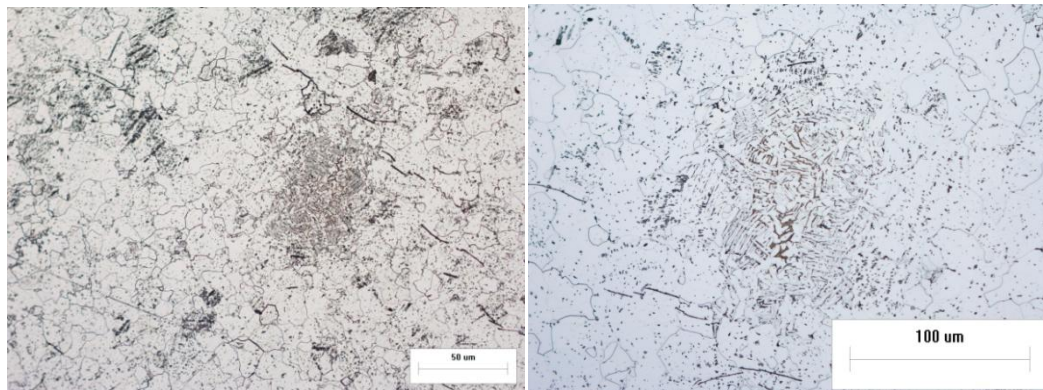
F (500x)

Figure 5.9: Optical micrograph of the laser sintered parts held at 1055°C, 2h, air cooled and aged at 540C for 7h, air cooled (10ml HF, 5ml HNO₃, 85ml H₂O). Consists of equiaxed α (recrystallized grains of primary α) and transformed β containing acicular α .



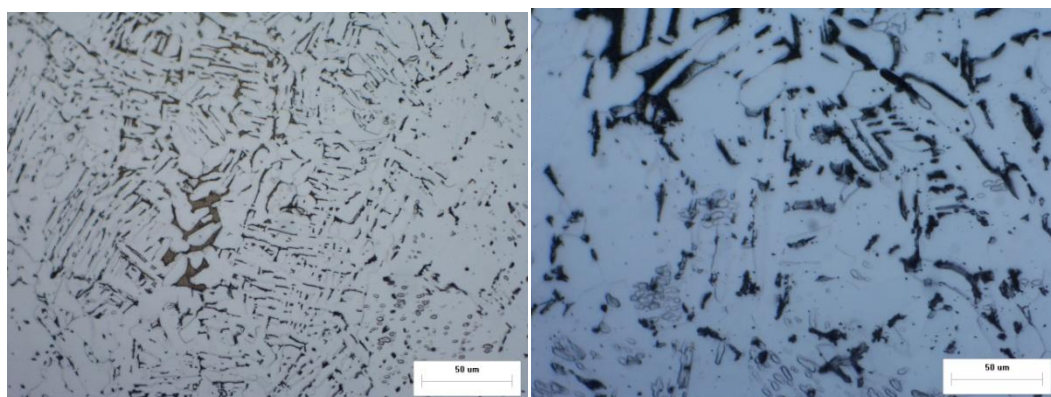
A (50x)

B (50x)



C (100x)

D (200x)



E (500x)

F (1000x)

5.4.5 X-Ray Diffraction and d-spacing analysis

Figure 5.10a: Diffraction pattern of Ti6Al4V powder (Gas Atomization Process)

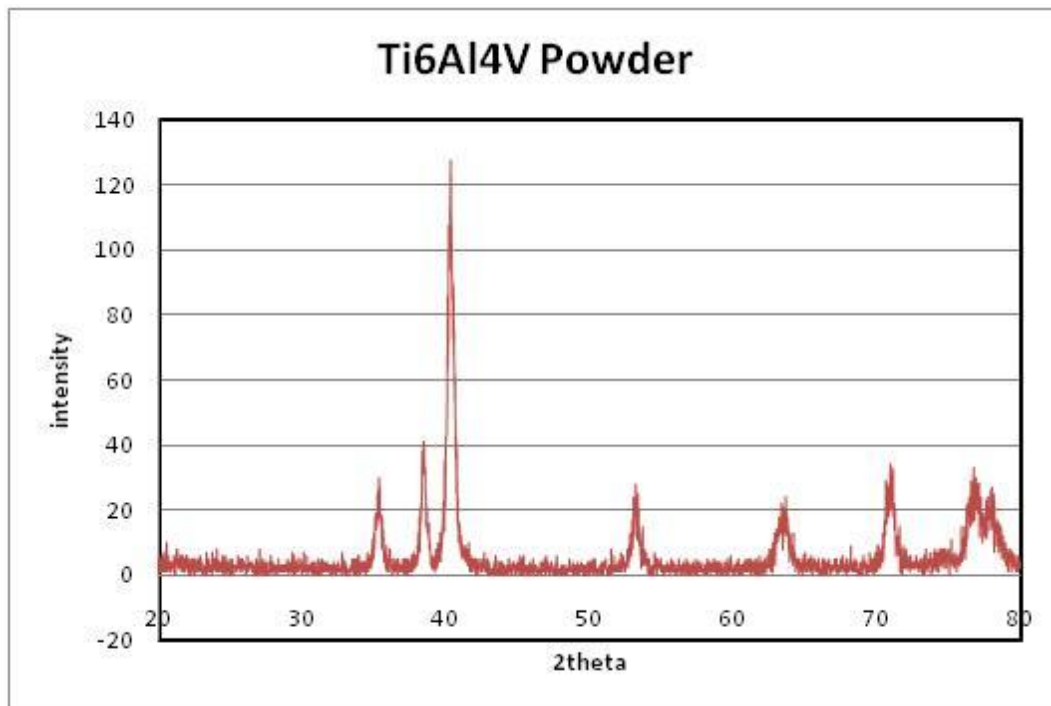


Figure 5.10b: d- spacing value of Ti6Al4V Powder (gas Atomization Process)

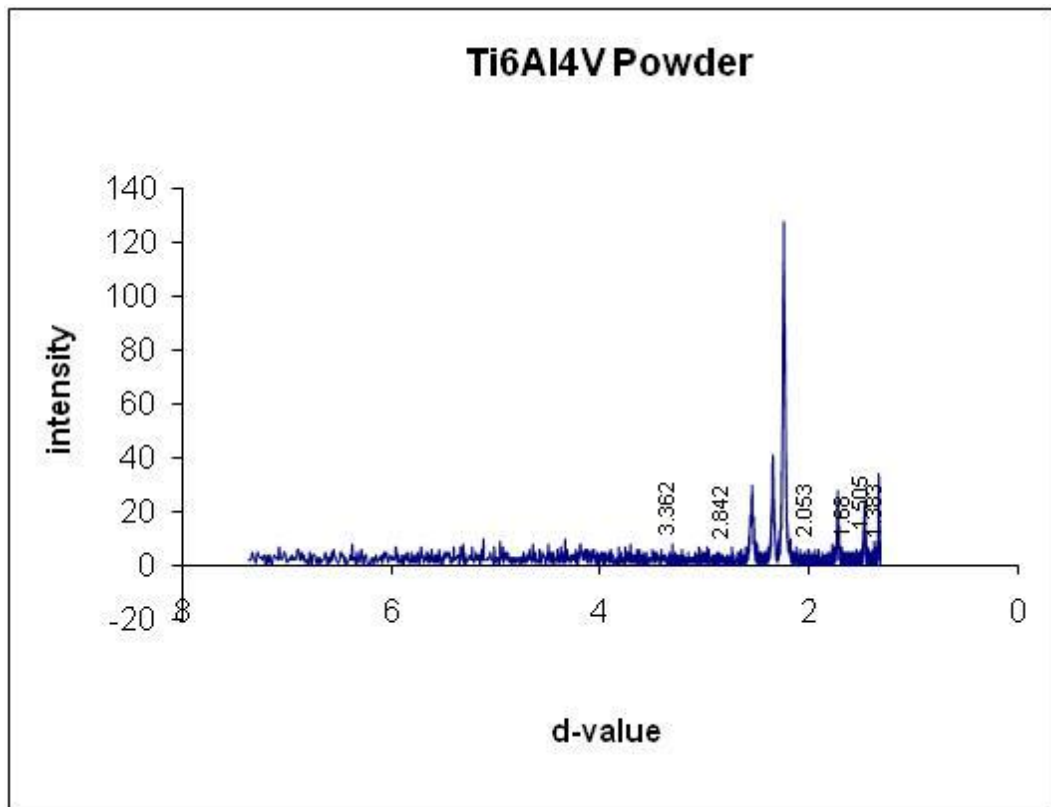


Figure 5.11a: Diffraction pattern of laser sintered parts (as built specimen)

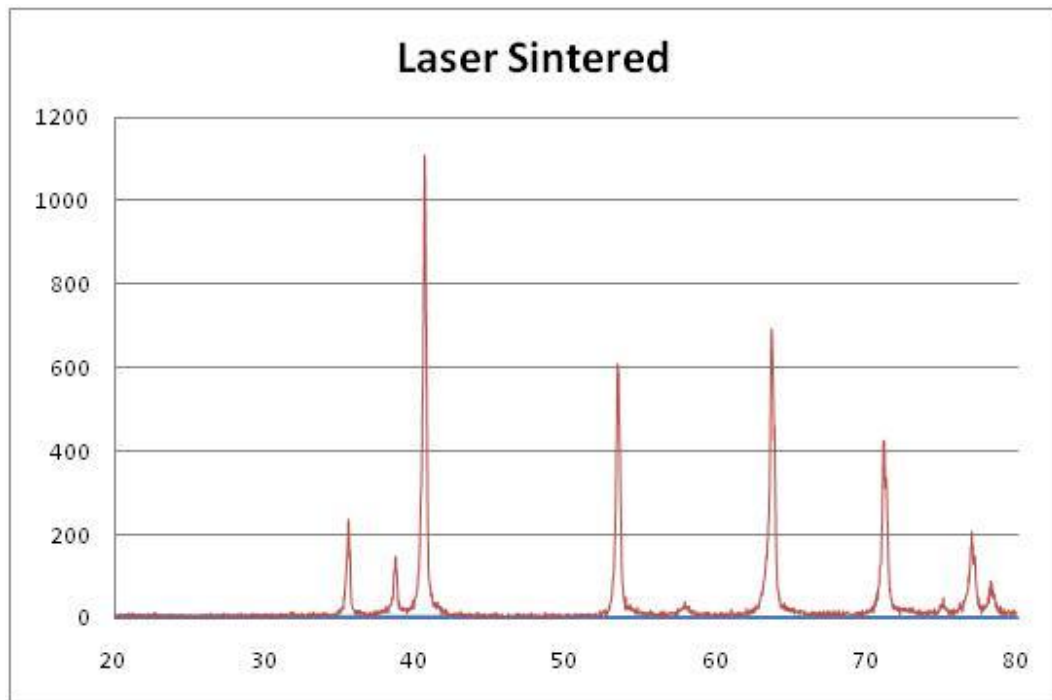


Figure 5.11b: d-spacing value of laser sintered parts

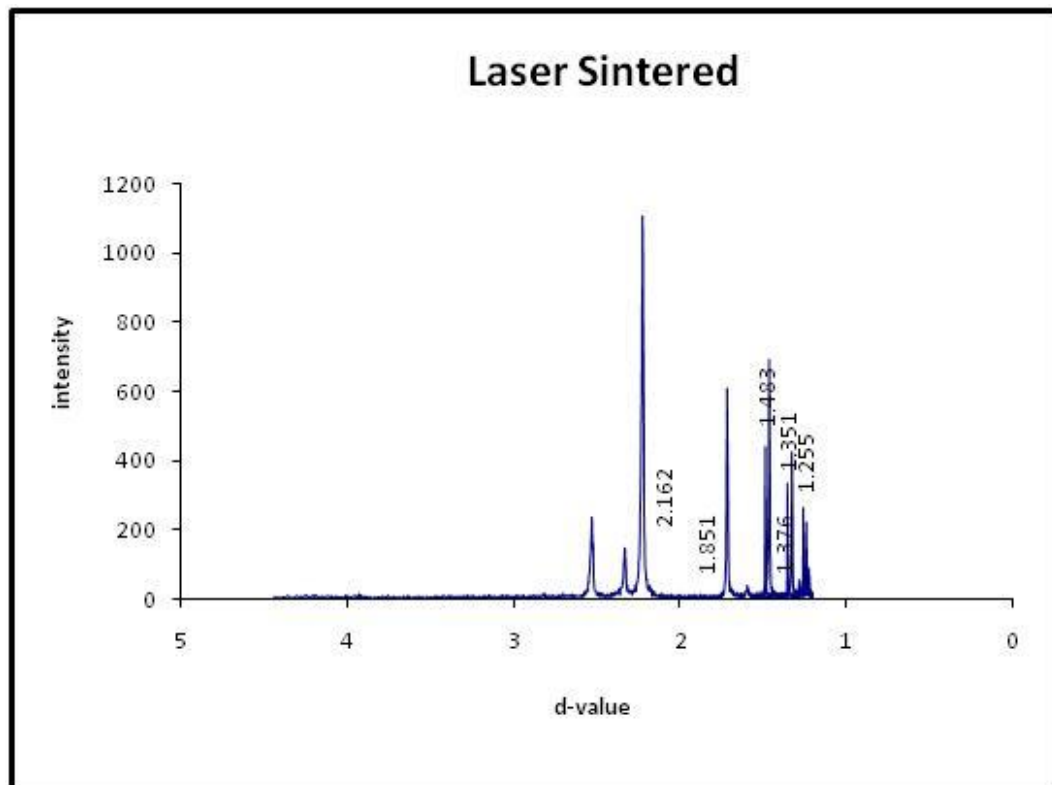


Figure 5.12a: Diffraction pattern after Solution treated (held at 1055°C, 2hr, air cooled, Aged for 7hr at 540°C and air cooled)

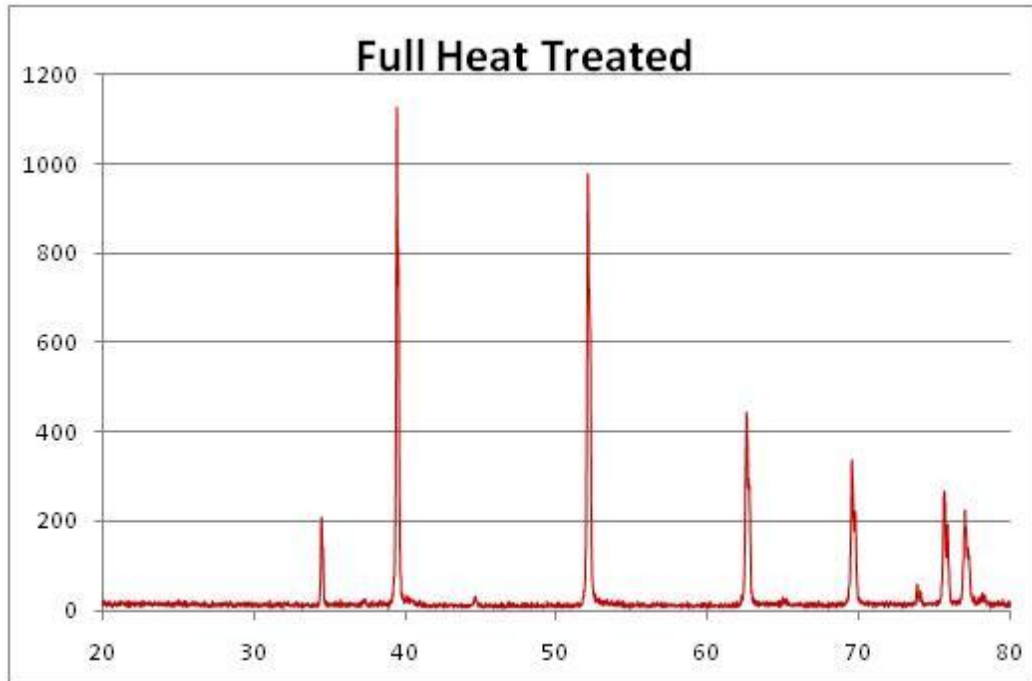
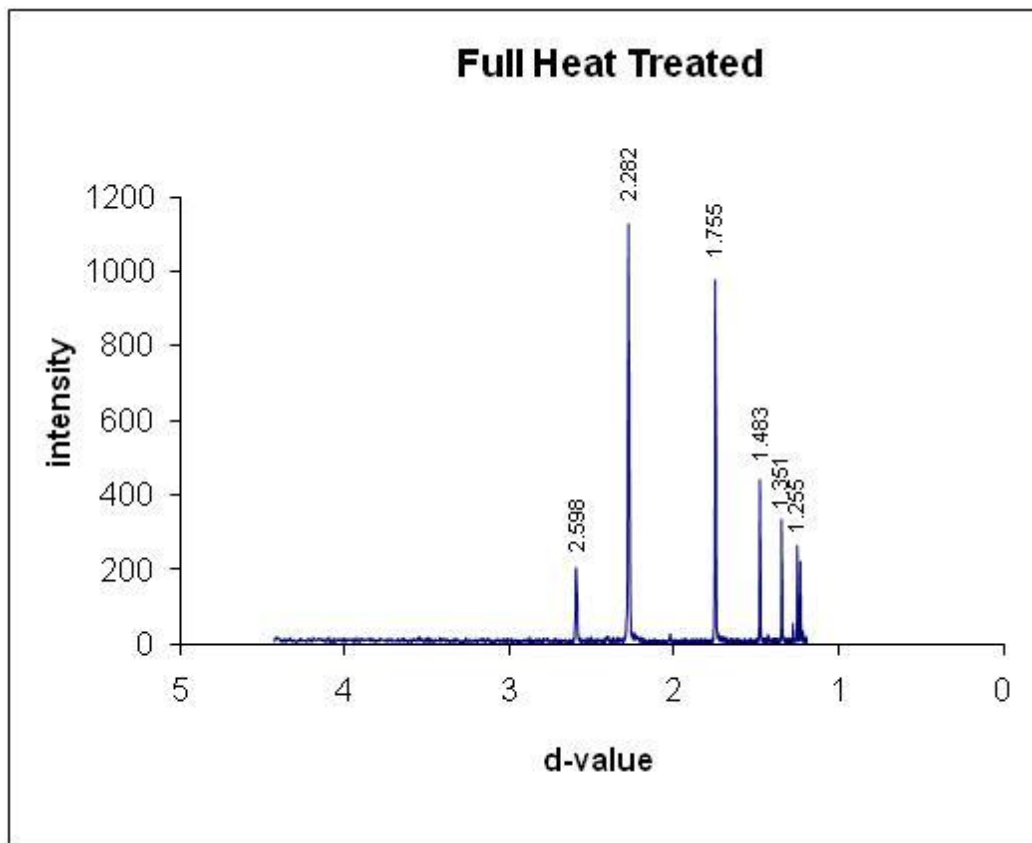


Figure 5.12b: d-spacing values of D3BST-AC-Ageing specimens (held at 1055°C, 2hr, air cooled, Aged for 7hr at 540°C, air cooled)



XRD patterns and d-spacing analysis of the as built specimen and heat treated specimen compared with d-spacing for hexagonal α -titanium.

d-Å for Ti	Laser sintered	<i>hkl</i>	d-Å for Ti	Full heat treated	<i>hkl</i>
2.555	2.548	1010	2.555	2.598	10 $\bar{1}$ 0
2.341	2.351	0002	2.341	-	0002
2.243	2.243	1011	2.243	2.282	10 $\bar{1}$ 1
1.726	1.729	1012	1.726	1.755	10 $\bar{1}$ 2
1.475	1.473	1120	1.475	1.483	1120
1.332	1.336	1013	1.332	1.351	10 $\bar{1}$ 3
1.278	1.281	2020	1.278	1.255	2020

Table 5.10: XRD pattern and d-spacing analysis

Calculation for c: a ratio based on the reference value of Titanium (c:a 1.5871)

- a. As laser sintered c: a ratio with

$$a = 1.473 \times 2 = 2.946 \text{ d}\text{\AA} \text{ and } c = 2.351 \times 2 = 4.702 \text{ d}\text{\AA}$$

$$\mathbf{c/a = 1.5960}$$

- b. As for full heat treated specimen the c:a ratio is

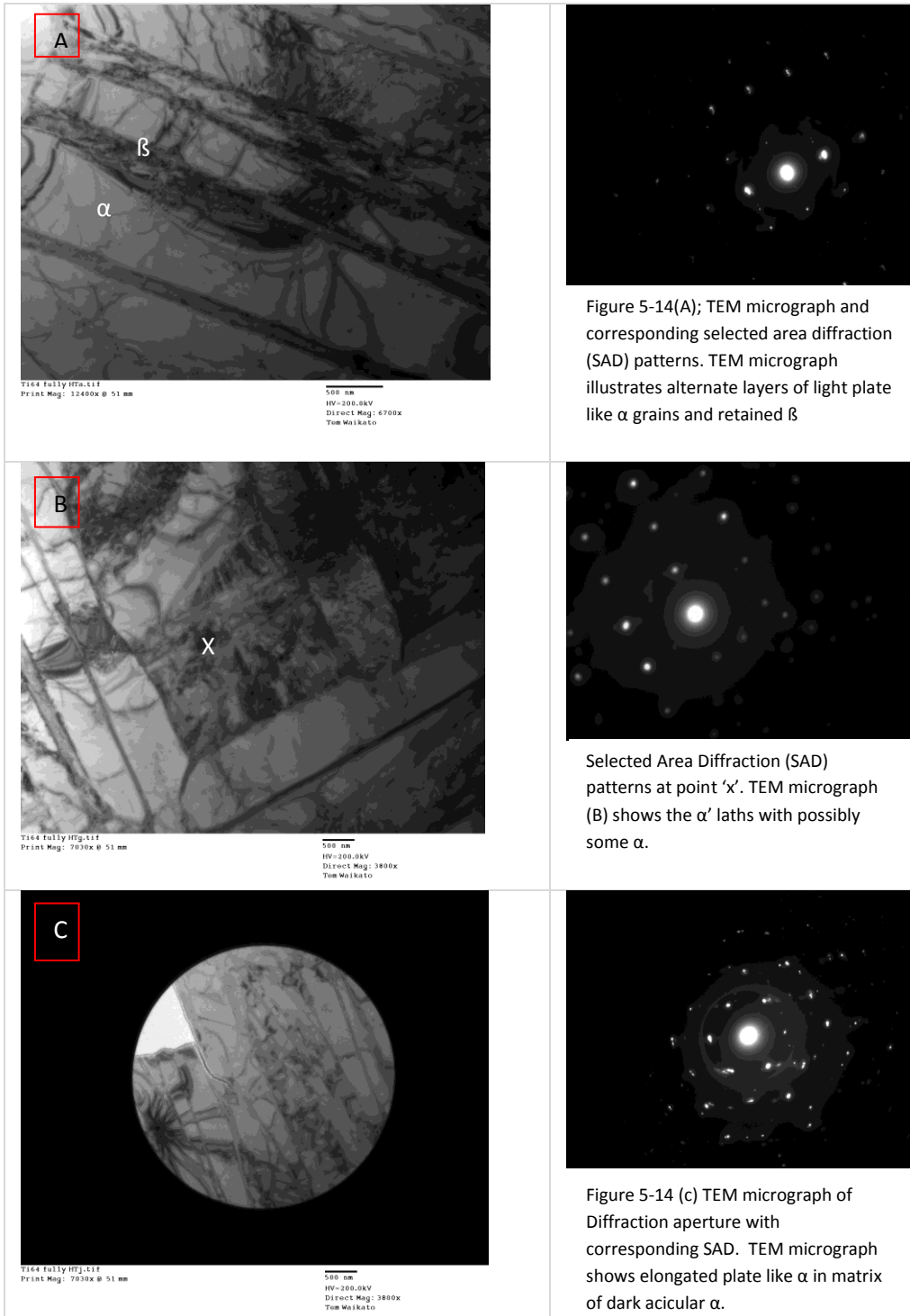
$$a = 1.475 \times 2 = 2.95 \text{ d}\text{\AA} \text{ and } c = 2.345 \times 2 = 4.69 \text{ d}\text{\AA}$$

$$\mathbf{c/a = 1.5898}$$

The XRD data and associated d-spacing in table 5.10 for the laser sintered material are in good agreement with accepted values for α - titanium. The d-spacing for fully heat treated material vary from the accepted values. This is probably because the α' phase has not fully reverted to α .

5.4.6 Transmission Electron Microscope and corresponding Selected Area Diffraction (SAD)

Figure 5.14: TEM micrograph of fully heat treated specimens and the selected area pattern (SAD). The specimen was annealed at 1055°C for 2 hour and air cooled. Further annealed at 540°C for 7hour and air cooled. The TEM sample was jet polished using a solution 92.5% methanol, 7.5% H₂SO₄.



Indexing Diffraction Patterns

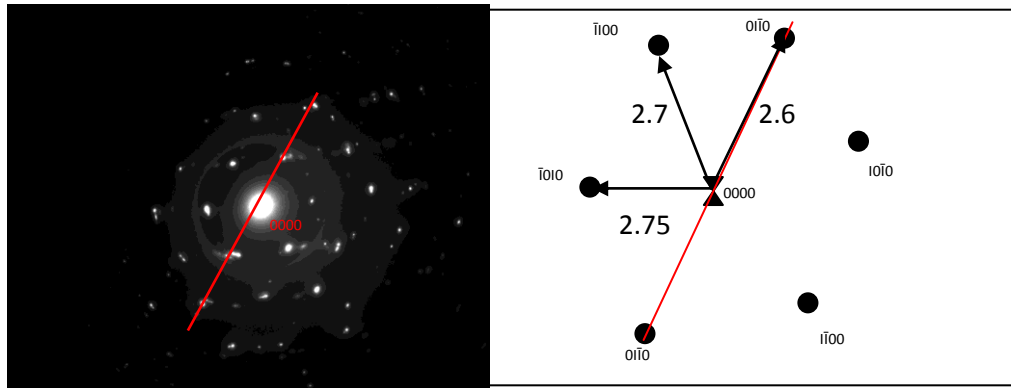


Figure 5.15: Indexing diffraction patterns based on the Selected Area Diffraction (SAD).

The SAD in fig. 5.14 (c) derives from the corresponding bright field image. Indexing of this Selected Area Diffraction (SAD) pattern is given in figure 5-15 for a $[0001]$ zone axis and a foil plane of (0001) . This indicates that the lath structure is α -titanium, formed by decomposition from α' .

5.5.0 Benchmark measurement and analysis

Table 5.12 shows the results of the dimensional analysis performed on the benchmark part. The process accuracy in the x, y and z- direction was evaluated and the precision of the RM process to build different features of holes and cylinders was measured. In Table 5.11 mean and maximum deviation between measured and CAD data are stated absolutely (μm) and relatively (%) to the nominal dimension.

	X direction		Y direction		Z direction		Diameters	
	mean	Max	Mean	Max	Mean	Max	Mean	Max
abs(mm)	0.05	0.08	0.02	0.03	0.45	0.58	0.06	0.16
rel (%)	62%		66.7%		77.5%		37.5%	

Table 5.11: Dimension tolerances for benchmark accuracy study

Dimension analysis shows that the deviation values along the x, y and z axis. The z-direction shows a bigger deviation which is 0.45mm followed by the y direction and the x direction.

Feature	Actual (mm)	Measures			Avg	SD	Difference
		1	2	3			
Length (x)	40	40.03	40.14	40.07	40.08	0.06	0.08
Width (y)	30	29.98	29.96	29.98	29.97	0.01	0.03
Thickness (z)	8	7.43	7.41	7.43	7.42	0.01	0.58
Holes (Φ)	5	4.98	4.99	4.97	4.98	0.01	0.02
	4	3.91	3.97	3.97	3.95	0.03	0.05
	3.5	3.31	3.3	3.42	3.34	0.07	0.16
	3	2.99	2.98	2.95	2.97	0.02	0.03
	2.5	2.45	2.49	2.42	2.45	0.04	0.05
	2	1.9	1.94	1.91	1.92	0.02	0.08
Rectangular							
Length (x)	8	7.97	7.99	7.99	7.98	0.01	0.02
Width (y)	3.5	3.52	3.5	3.51	3.51	0.01	-0.01
	3	3.04	3.02	3.03	3.03	0.01	-0.03
	2.5	2.52	2.5	2.52	2.51	0.01	-0.01
	2	2.03	1.98	2.04	2.02	0.03	-0.02
	1.5	1.52	1.54	1.52	1.53	0.01	-0.03
	1	1.01	1.03	0.99	1.01	0.02	-0.01
Height (z)	10	9.51	9.55	9.58	9.55	0.04	0.45
	8	7.51	7.55	7.48	7.51	0.04	0.49
	6	5.45	5.47	5.48	5.47	0.02	0.53
	4	3.46	3.48	3.51	3.48	0.03	0.52
Cylindrical (Φ)	6	5.99	6.01	5.93	5.98	0.04	0.02
	4	3.99	3.98	3.94	3.97	0.03	0.03
	4	3.94	3.93	3.94	3.94	0.01	0.06
	2.5	2.43	2.42	2.43	2.43	0.01	0.07
	1.5	1.41	1.42	1.46	1.43	0.03	0.07

Table 5.12: Dimension measurement of the customised benchmark

Chapter 6: Discussion & Conclusion

Rapid Manufacturing is a relatively new manufacturing process which is under development. It is an emerging technology that functions through material addition, in contrast to the established traditional cutting, forming and casting methods (P. Fisher et al, 2003). Formerly known as Rapid Prototyping, this technology has developed from producing models and prototypes for evaluation to actual manufacturing of the parts. A few of the commercially available RP systems are Selective laser sintering, Fused Deposition Modelling (P.A Kobryn & S.L Semiatin, 2001), 3D Printing and Laminated Object Manufacturing (S.M Hur et al, 2001). There are two appealing factors associated with these RM systems; firstly the capability of processing metallic powders and secondly the capability of the machine to fabricate geometrical complexity in a relatively lower time at lower cost with minimum technical expertise required.

The direct metal laser sintering techniques used in this study successfully built the metal parts with defined structure and shape on the basis of 3D virtual data. This technique offers the advantage of using Ti6Al4V titanium alloy powder that is completely melted and fused in the laser focus resulting in high mechanical strength. The parts were fabricated using the standard EOS process parameters with the powder density of 98.96%. The substrate used was pure titanium and argon gas was flushed through the chamber to maintain the gas purity inside the fabrication chamber. Ti6Al4V powder was provided by the University of Wolverhampton, manufacturing group with the spherical powder particles in a range of 10 to 100 μ m. The chemical composition of Ti6Al4V powder is reported in Table 5.3. The contents of the substitutional elements are in agreement with the ISO and ASTM prescriptions.

Visual observations confirmed that as received specimens were in accordance with the CAD data. The simple benchmark studies on the parts fabricated using this technique showed dimensional variations along the x, y and z axes of orientation. The DMLS benchmark showed dimensional variations of 0.45mm on the z-axis, 0.05mm and 0.02mm on the x-axis and y-axis respectively. Sharp edges and corners were blunt and the benchmark's surface was smooth. Cracks and

layer coherence were not visible. Results showed that dimensional tolerances parallel to the build bed (X and Y directions) can be considered together as they exhibit similarities in behaviour. However, results from the z-direction, which is dictated by the increment of the layer thickness, indicates greater tolerances. Studies highlighted that the dimensional accuracy of the SLS parts is controlled by few factors and is mainly due to a highly focussed laser beam and the rapid solidification process; the built parts are facing high residual stresses which leads to distortion, shrinkage and warpage (P. Fisher et al, 2004; P. Mercelis et al, 2006). Manufacturers normally employ pre-defined offset value during fabrication of metal parts to minimize this effect.

	As built	Hipped	STA	Annealed
Density (kg/m ³)	4319	-	4430	4430
Hardness (HV)	320	312	395	350
Young's Modulus (GPa)	117	117	110	110
Tensile Yield Strength (MPa)	970	795	920	920
Ultimate Tensile Strength (MPa)	1122	870	1000	1000
Elongation at Rupture (%)	4	-	10	12

Table 6.1: Mechanical Properties of Ti6Al4V parts, Source: Ben Vandenbroucke and J.P Kruth (2007), Luca facchini et al (2009)

Research efforts have demonstrated the great potential available with direct laser metal sintering to achieve a microstructure and mechanical properties equivalent or superior to bulk material after a post-processing treatment (M.Makesh et al, 2004; S. Storch et al, 2003). Table 6.1 gives an overview of the results of all the mechanical tests. The tensile stress-strain curves of the as built specimens display typical behaviour of Ti6Al4V characterized by low strain hardening. The obtained mechanical properties of the DMLS specimens are compared with those bulk materials from literature reviews. The as built specimen shows slightly lower density and hardness compared to solution treated and annealed samples. It has the highest tensile strength and ultimate tensile strength and the lowest elongation to fracture. The tensile properties of the as built Ti6Al4V has satisfied the ISO 5832-3 standard requirements (TS >780MPa, UTS >860MPa) but the elongation at fracture is below the limit

accepted by the standards (>10%). The microhardness of the as built specimen is 320HV. It is noteworthy that the as built specimens fabricated via a M270 laser sintering machine have good mechanical properties.

The fracture surface of the as built specimen shows ductile dimples, typical of ductile fracture. The stress-strain curves display low elongation to fracture significantly lower than that in cast/wrought Ti6Al4V. Several microvoids were seen on the fracture surface. In some areas, the particle boundaries are still visible and suggest that particles have been pulled out. This is a clear indication that the surface melting on some powder particles during laser sintering process was incomplete.

The microstructure obtained as a result of rapid solidification after selective laser sintering reveals a very fine lamellar morphology with dark particles of precipitated α in β boundaries. The presence of martensitic or α' is also visible and which is expected due to the high solidification rate of the liquid pool and the evidence that the material has undergone rapid cooling from a temperature above the β -transus during the laser sintering process. Some heat treatments were carried out to evaluate the possibility of modifying the microstructure. After solution treating in the $\alpha+\beta$ regions (925°C) and water quenching, the microstructure had a basket weave structure.

The second solution treatment was placed slightly above the β -transus temperature (1055°C) and air cooled. This produced a fully lamellar structure but had a thicker morphology compared to that of as built specimen. Beta solution treatment was done in an attempt to produce a fully lamellar structure and a different cooling rate was adopted in order to evaluate the α - β - α transformation. With greater time for diffusion and growth as the cooling rate is reduced the morphology of transformed α increases in thickness and length and contained larger and fewer α colonies. In order to check the completeness of the phase transformation, the last solution treatment was held at 1055°C, air cooled and re-annealed at 540°C for 7 hour. This produced mostly equiaxed α , which confirms the complete recrystallization of the α grains and with transformed β

containing acicular α . Microhardness testing was performed in order to investigate and correlate the microstructural evolution with the mechanical behaviour. However, the results illustrate that oxidation occurred on the specimens during heat treatment. This in return produced very high hardness values.

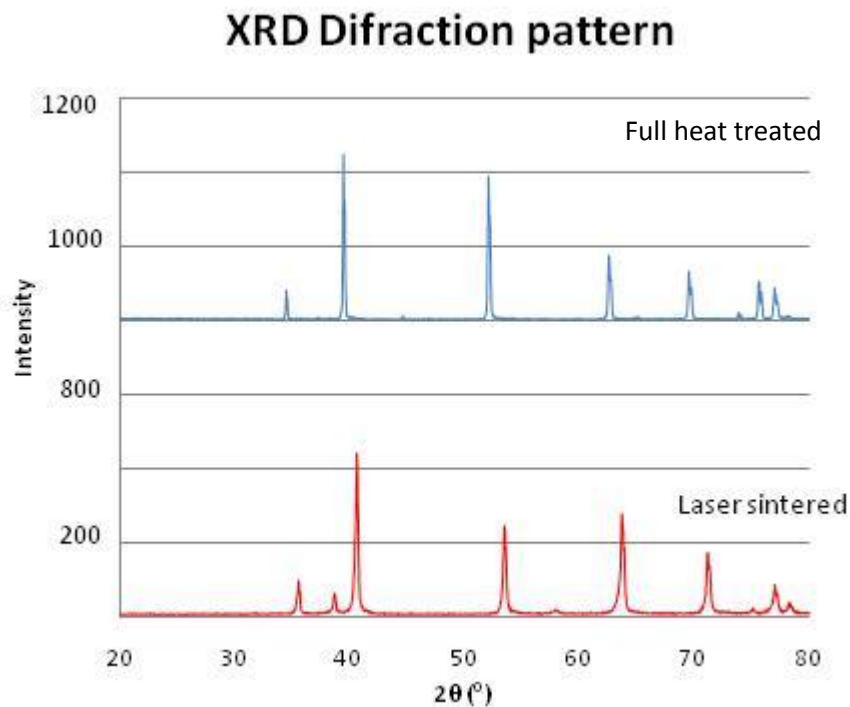


Figure 6.2: XRD pattern for Ti6Al4V laser sintered part with different heat treatments. The intensities are given relative to the maximum. For clarity, the diffraction patterns are shifted with respect to each other along the vertical axis.

The fully heat treated specimen was further analysed using XRD diffraction pattern and Transmission Electron Microscopy (TEM). The analysis was performed, not to determine the fractions of alpha and beta but purposely to investigate the diffraction pattern after full heat treatment of the as built specimen. The graph shows that the diffraction pattern of the fully heat treated specimen is shifted to the left. On the other hand, the as built specimen has wider α -reflections which possibly indicates the formation of α' or martensite. Transmission electron bright field micrograph showed the presence of α' laths and the elongated plate-like α on the heat treated specimen.

Conclusion

Additive principle used in the selective laser sintering has proved to be a new and promising method to directly fabricate metal parts. In this work, a direct metal laser sintering technique was characterized as the Rapid Manufacturing technique to build metal parts from Ti6Al4V gas atomized powder. The relative density of the Ti6Al4V titanium alloy powder is 98.65% with an average particles size of 37.93 μm . EOS standard process parameters were applied to minimize porosity and this led to part densities of up to 96.84% with a very fine $\alpha+\beta$ microstructure. Different mechanical tests proved that SLS metal parts fulfil the mechanical property requirement such as tensile, strength and hardness. Because of a very fine as built microstructure, the yield stress and ultimate tensile stress are quite high whilst elongation to fracture is low. Dimensional analyses were performed on the customised benchmark sample showing process accuracy below 0.5mm.

In this research, heat treatments were used to modify the microstructure of the as built Ti6Al4V produced by SLS. Evaluation of the microstructure indicates that the as built specimen with a very fine lamellar morphology was changed by beta solution treating. Water quenching from slightly below the beta transus temperature formed a martensite structure and slow cooling from slightly above the beta transus allowed the recrystallization of α grains. Future work will include a quantitative analysis of the α and β phases after each heat treatment process and evaluate these in the context of material's application. The results are expected to ascertain the effect of the designated heat treatments and confirm the hypothesis proposed here.

Chapter 7: Future Recommendations

The preliminary investigation of Rapid Manufacturing systems has shown promising results. However, the direct metal laser sintering process require more in depth studies in order to understand the correlation between the process parameters and the material properties especially in the area of metallographic analysis. Detailed and careful TEM is the best tool to further evaluate the α and β phases but requires vast metallographic experience and is time consuming. More effort in this area is suggested for PhD studies. The future recommendations are related to several areas;

- a. Producing metal parts for biomedical applications – further research will be focused on the biomedical requirements and standards. The mechanical properties of laser sintered parts will be thoroughly investigated to suit the high physical requirements and unique geometrical complexity of biomedical applications. The new design and manufacturing frameworks will be established. Fabrication cost will be analysed and compared with other methods
- b. Understanding of the process parameters; there are five crucial process parameters which contribute to different part densities. The effects of laser power, scan speed, scan spacing, scan strategy and layer thickness. A deep understanding of these process parameters would assist users to optimise the fabrication process and produce metal parts that can fulfil intended applications.
- c. Powder technologies properties; production, powder particle size, shape and distribution. Instead of gas atomized powder, there are other ways of producing powder particles such as PREP, Hydride Dehydride process and mechanical alloying. Different type of raw materials might have a different influence on the process parameters and deposition systems. The powder deposition system of the direct metal laser sintering machine will be investigated.
- d. Post treatment process to increase part densities; study on the effect of post treatment such as Hot Isostatic Pressing (HIP), Cold Isostatic Pressing

- (CIP). Phase compositions and fraction of α and β phases after various designated heat treatments via XRD analysis and TEM micrograph
- e. Numerical analysis and phase transformation modelling ; the numerical analysis and the mathematical modelling of the intrinsic relationship between the process parameters and the microstructure evolution will tremendously reduce fabrication errors thus avoiding having defective metal parts. A quantitative analysis of heat treatments on the laser sintered specimen will lead to greater understanding of β to α transformation and more accurate prediction of desired microstructure.
 - f. Process Accuracy & Feasibility; the process accuracy of direct metal laser sintering process is partly influenced by the fabrication orientation and direction whether parallel or perpendicular to the build direction. Taking into account these parameters will perhaps contribute to sound mechanical properties.

List of References

1. A. Simchi, H. Pohl : Effects of laser sintering processing parameters on the microstructure and densification of iron powder ; *Materials and Engineering A* 359 (2003), pp 119 – 128
2. A.Simchi, F. Petzoldt, H.Pohl: On the development of direct metal laser sintering for Rapid Tooling;*Journal of Materials Processing Technology* 141(2003), 319-328
3. A.Simchi: Direct Laser sintering of metal powders: Mechanism, Kinetics and microstructural features; *Materials Science and Engineering, A* 428(2006), pp 148 – 158
4. Anna Bellini and Selcuk Guceri: Mechanical Characterization of parts fabricated using fused deposition modelling; *Rapid Prototyping Journal*, Volume 9, Number 4, 2003, pp 252 – 264
5. Anna Kochan : Rapid Prototyping Takes on Manufacturing; *Design News*, Julai 22, 2002, 57,14, Academic Research Library, pg 15
6. ASM : *Metal Handbook: Powder Metal Technologies and Applications* Volume 7
7. B. D Engel, L Bourell : Titanium alloy powder preparation for selective laser sintering; *Rapid Prototyping Journal*, Volume 6, Number 2 (2000), pp 97 -106
8. B.Van der Schueren, J.P. Kruth: Powder Deposition in Selective Metal Powder Sintering; *Rapid Prototyping Journal*, Volume 1, Number 3 (1995), pp 23 - 31
9. Ben Vandembroucke, Jean Pierre Kruth : Selective laser melting of biocompatible metals for rapid manufacturing of medical parts; *Rapid Prototyping Journal*, 13/4 (2007), pp 196 - 203
10. Brian K.Paul, Vinay Voorakarnam: effect of layer thickness and orientation angle on surface roughness in laminated object manufacturing; *Journal of Manufacturing Processes*; 2001, 3, 2;ABI/INFORM Global
11. Christoph Leyens, Manfred, Peters: *Titanium and Its Alloy : Fundamental and Applications*; John Wiley c 2003

12. Direct Rapid Manufacturing of Metallic Parts – A UK Industry Overview – February 2008, (www.econolyst.com)
13. Edson Costa Santos, Masanari Shiomi, Kozo Osakada, Tahar Laoui; Rapid Manufacturing of metal components by laser forming, *International Journal of Machine Tools & Manufacture* 46(2006)1459-1468
14. Farid Fouchal, Phill Dickens; Adaptive Screen Printing for Rapid Manufacturing; *Rapid Prototyping Journal*,13/5 (2007), 284 -290
15. Fude Wang, J.Mei, Xinhua Wu; Microstructure study of direct laser fabricated Ti alloys using powder and wire; *Applied Surface Science*, 253(2006) 1424 -1430; www.sciencedirect.com
16. G. Giannatsis, V dedaassis; Additive Manufacturing Technologies applied to medicine and healthcare : A review; *Int. Journal of Advanced Manufacturing Technology* (2009), 40: 116-127
17. G.D Kim, Y. T Oh: A benchmark study of Rapid Prototyping process and machine: Qualitative comparisons of mechanical properties, accuracy, roughness , speed and material cost; *Proc. IMechE 2008 Volume 222 Part B, Journal of Engineering Manufacture*
18. Gideon N Levy, Ralf Schindel, J.P Kruth: Rapid Manufacturing and Rapid Tooling with Layer Manufacturing technologies, state of the art and Future Perspective: *Annals of the CIRP* 52/2, (2003), 589-609
19. H.H. Zhu, J.Y.H Fuh and L.Lu: Microstructural Evolution in direct laser sintering of Cu-based metal powder: *Rapid Prototyping Journal*, 11/2 (2005), 74 – 71.
20. I J Palmer : *Light Alloys : Titanium and its Alloys (metallurgy of the Light Metals)* 3rd Edition, London, Arnold (1995)
21. I.Gibson, L.K Cheung, S.P Chow, W.L Cheung, S.L. Beh : The Use of Rapid Prototyping for medical applications; *Rapid Prototyping Journal*, 12/1 (2006), pp 53 - 58
22. J.H. Liu, Y.S Shi, Z.L. Lu, Y.Xu, K.H. Chen, S.H. Huang: Manufacturing of metal parts via indirect SLS of composite elemental powders; *Materials Science and Engineering, A* 444 (2007), 146 - 152

23. J.P Kruth, G. Levy, F.Clock, T.H.C Childs; Consolidation phenomena in laser and powder –bed based layered manufacturing, *Annals of CIRP*, volume 56/2/, (2007)
24. J.P Kruth, X. Wang, T.Laoui, F. Froyen: Lasers and Materials in selective laser sintering; *Assembly Automation*, Volume 23, Number 4 (2003), pp 357 – 371
25. Javier Munguia, Joaquin de Ciurana, Charles Riba; Pursuing Successful Rapid Manufacturing: a users’ best practices approach: *Rapid Prototyping Journal*, Volume 14 number 3, 2008, pp 173-179
26. Jialin Yang, Hongwu Ouyang and Yang Wang; Direct Meta I laser fabrication: Machine development and experimental work; *International Journal of Manufacturing Technology* (2010), 46, 1133-1143
27. Jing Zhao, Wenbin Cao, Changchun Ge: Research on laser engineered net shaping of thick-wall nickel-based alloy parts, *Rapid Prototyping Journal*, 15/1, (2009), pp 24-28
28. John D Williams and Carl R. Deckard: Advances in modelling the effects of selecting parameters on the SLS process, *Rapid Prototyping Journal*, Volume 4, number 2 (1998), pp 90 - 100
29. Jose Calvalho ferriera, Eduardo Santos, Hugo Madureira, Joao Castro : Intergration of VP/RP/RT/RE/RM for rapid product and process development, *Rapid Prototyping Journal* 12/1, (2006), pp 18 - 25
30. K Abdel Ghany, S.F Moustafa: RPM systems for metals, *Rapid Prototyping Journal*, Volume 12, (2006), number 2, page 84-86
31. K.Dai and L.Shaw: Distortion Minimization of laser processed components through control of laser scanning patterns: *Rapid Prototyping Journal*, Volume 8, Number 5, 2002, pp 270 – 276
32. Kamran Mumtaz and Neil Hopkinson: Top Surface and side roughness of Inconel 625 parts processed using Selective laser melting, *Rapid Prototyping Journal*, 15/2 (2009), pp 96 – 103
33. L.Dong, A. Makradi, S.Ahzi, Y. Remond: Three Dimensional transient finite element analysis of the selective laser sintering process, *Journal of Materials Processing Technology* 209, (2009), 700 - 706

34. Lino Costa: Laser Powder Deposition, *Rapid Prototyping Journal*, 15/4, (2009), pp 264 – 279
35. Luca Facchine ;Microstructure and mechanical properties of Ti6Al-4V produced by electron beam melting of pre-alloyed powders, *Rapid Prototyping Journal*,15/3, 2009 pp 171-178
36. M. Ruffo, R. Hague; Cost estimation for Rapid Manufacturing-Simultaneous production of mixed components using laser sintering, *Proc. IMechE Volume 221 Part B, J. Engineering Manufacture*, IMechE 2007
37. M.Makesh, Y.S. Wong, J.Y.H Fuh, H.T Loh; Benchmarking for comparative evaluation of RP systems and processes, *Rapid Prototyping Journal*, Volume 10, Number 2, 2004, pp 123-135
38. M.Ruffo, C. Tuck and R. Hague; Cost Estimation for Rapid Manufacture: *Proceedings of the Institution of Mechanical Engineers*, Sep 2006, 220B9, ProQuest science Journals, Pg 1417
39. M.Ruffo, C. Tuck and R. Hague; Make or buy analysis for Rapid Manufacturing; *Rapid Prototyping Journal*, 13/1 (2007), pp 23-29
40. M.Shellabear, O.Nyrhila: Advances in Materials and Properties of Direct Metal Laser-Sintered Parts, Paper Presented in LANE Conference 2007
41. Maarten Van Elsen, Farid Al Bender, Jean Pierre Kruth: Application of dimensional analysis to selective laser melting, *Rapid Prototyping Journal*, 14/1 (2008), pp 15 – 22
42. Maria Grazia Violante, Luca Iuliano,Paolo Minetola: Design and Production of fixtures for freeform components using selective laser sintering, *Rapid Prototyping Journal*, 13/1 (2007), pp 30-37
43. Mark A. Evans, R.Ian Campbell: A Comparative analysis of Industrial Design models produced using rapid prototyping and workshop based fabrication technique, *Rapid Prototyping Journal*, Volume 9 (2003),Number 5, pp 344 -351
44. Matthew J. Donachie, Jr: *Titanium: A technical guide*, Second edition, ASM International, (2000) The Materials Information Society

45. Matthew Wong, Sozon Tsopanos, Chris J. Sutcliffe and Ieuan Owen: Selective laser melting of heat transfer devices, *Rapid prototyping Journal*, 13/5 (2007), pp 291-297
46. Mukesh Agarwala, David Bourell, Joseph Beaman, Harris Marcus, Joel Barlow : Direct Selective laser sintering of metals, *Rapid Prototyping Journal*, Volume, Number 2.1995, pp 26-36
47. N.Ragunath, Pulak M. Pandey : Improving accuracy through shrinkage modelling by using Taguchi method in selective laser sintering, *International Journal of Machine Tools and Manufacture* 47 (2007), 985 - 995
48. Neil Hopkinson, Phill Dickens; *Rapid Prototyping for Direct Manufacture*, *Rapid Prototyping Journal*, Volume 7 ,Number 4, 2001, pp 197 – 202
49. Neil Hopkinson: Process repeatability and sources of error in indirect SLS of Aluminium, *Rapid Prototyping Journal*;,14/2, (2008), pp 108-113
50. Nikolay K.Tolochko,Tahar Laoui,Yurii V. Khlopkov, Sergei E.Mozzharov,Victor I.Titov and Michail B Ignatiev: Absorbance of powder materials suitable for laser sintering, *Rapid Prototyping Journal*, Volume 6, Number 3(2000),pp 155 - 160
51. Nikolay T. Tolochko, Maxim K. Arshinov, Andrey V. Gusarov, Victor I. Titov, Tahar Laoui, Ludo Froyen, 2003; Mechanism of SLS and heat transfer of Ti Powder, *Rapid Prototyping Journal*, volume 9, pp 314-326
52. Nikolay Tolochko, Sergei Mozzharov, Tahar Laoui and Ludo Froyen: Selective Laser Sintering of single and two component metal powders, *Rapid Prototyping Journal*, Volume 9, Number 3 (2003), pp 68-78
53. Nikolay K. Tolochko, Sergei E. Mozzharov, Igor A. Yadroitsev, Tahar Laoui, Ludo Froyen. Victor I.Titov, Michail B. Ignatiev: Balling processes during selective laser treatment of powders, *Rapid Prototyping Journal*, Volume 10, Number 2, 2004, pp 78-87
54. Ola L.A. Harrysson, Omar Cansizoglu, Dennis J. Marcellin-Little, Dennis R. Cormier, Harvey A. West H: Direct Metal Fabrication of Titanium Implants with Tailored materials and mechanical properties using electron beam melting, *Materials Science and Engineering C* 28 (2008), 366 - 373

55. P.A Kobryn and S.L Semiatin; The laser Additive Manufacture of Ti6Al4V, Journal of Manufacturing, Sept 2001:53,9: ABM/INFORM Trade and Industry
56. P.Fischer, V.Romano, A. Blatter, and H.P.Weber: Highly precise pulsed selective laser sintering of metallic powders, Laser Physics Letter, 2, No 1, 48-55 (2005)
57. P.Fischer, V.Romano, H.P. Weber, N.P. Karapatis, E. Boillat, R.Glardon : Sintering of commercially pure titanium powder with Nd:YAG laser source, Acta Materialia 51 (2003), 1651 – 1662
58. P.Fisher, M.Locher, V Romano, H.P Weber, S. Kolossov, R. Glardon : Temperature measurements during selective laser sintering of titanium powder, International Journal of Machine Tools and Manufacture 44 (2004), 1293 - 1296
59. P.Mognol, M Rivette, L.Fegou and T. Lesprier: A first Approach to choose between HSM, EDM and DMLS processes in Hybrid Rapid Tooling, Int Journal of Manufacturing Technology, 2006, 29, 35-40
60. Peter Mercelis, Jean Pierre Kruth: Residual Stresses in Selective laser sintering and Selective laser melting, Rapid Prototyping Journal 12/5 (2006) pp 254 - 265
61. Prashant Kulkarni, Anne marson, Debasish Duta; A review of Process planning techniques in Layered Manufacturing, Rapid Prototyping Journal, Volume 6, Number 1, 2000, pp 18-35
62. R Morgan, C J Sutcliffe, W O'Neill; Experimental Investigation of nanosecond pulsed Nd:YAG laser re-melted pre-placed powder beds, Rapid Prototyping Journal 2001, 7/3, pp159
63. Randall M. German : Sintering Theory and Practice , New York, Wiley (1996)
64. S.R. Pogson, P. Fox, C.J Sutcliffe and W.O'Neill: The Production of Copper Parts using DMLS, Rapid Prototyping Journal, Volume 9, Number 5, 2003, pp 334 - 343

65. S.S. Dimov, D.T. Pham, F.Lacan, K.D. Dotchev: Rapid Tooling applications of the selective laser sintering process, *Assembly Automation*, Volume 21, Number 4 (2001), pp 296 - 302
66. Sebastian Storch, Detmar Nellesen, Guenther Schaefer and Rolf Reiter: Selective laser sintering: Qualifying analysis of metal based powder systems for automotive application, *Rapid Prototyping Journal*, Volume 9, Number 4, 2003, pp 240-241
67. Suman Das, Joseph J. Beaman, Martin Wohlert, David L. Bourell: Direct Metal Laser Sintering for High Performance Metal Components, *Rapid Prototyping Journal*, volume 4, no 7, pp 112-117 (1998)
68. Sung Min Hur, Kyung Hyun Choi, Seok Hee Lee, Pok Keun Chang : Determination of fabricating orientation and packing in SLS process, *Journals of Materials Processing Technology* 112 (2001), 236 – 243
69. T.Laoui, E. Santos, K.Osakada, M.Shiomi, M. Morita, S.K. Shaik, N.K. Tolochko, F.Abe: Properties of Titanium Implant Models made by Laser Sintering Processing, *Laser Assisted Net Shape Engineering* 4, Proc of the LANE 2004
70. T.Traini, C. Mangano, R.L. Sammons, F. Mangano, A. Macchi, A. Piatelli : Direct laser metal sintering as new approach to fabrication of an isoelastic functionally graded material for manufacture of porous titanium dental implants, *Dental Materials* 24 (2008), 1525 - 1533
71. Thomas Himmer, Anja Techel, Steffen Nowotny, Ekhard beyer: Recent Developments in metal laminated tooling by multiple laser processing, *Rapid Prototyping Journal*, volume 9, Number 1, 2003, pp 24-29
72. Tim Sercombe, Noel Jones, Rob Day, Alan Kop: Heat Treatment of Ti-6Al-7Nb components produced by Selective laser sintering, *Rapid Prototyping Journal*, 14/5 (2008), pp 300 – 304
73. Todd Grimm: RP A True Tool for Change, *Manufacturing Engineering*, April 2004;132,4: ABI/INFORM Global, pg 16
74. Vito R. Gervasi, Adam Scheinder and Joshua Rocholl: Geometry and procedure for benchmarking SFF and Hybrid fabrication process resolution, *Rapid Prototyping Journal*, 11/1 (2005), pp 4 - 8

75. Wei Sha and Savko Malinov: Titanium alloys: modelling of microstructure, properties and application, Woodhead Publishing in Material, 2009
76. Xiang Li, Chengtoa Wang, Wenguang Zhang, Yuanchao Li; Fabrication of porous Ti6Al4V parts for biomedical applications using electron beam melting, Material Letters 63 (2009), 403 -405